

Introduction to particle physics: experimental part

Making predictions for hadron colliders

- **From Feynman diagrams to cross-sections**
- **From cross-sections to events**

First data at LHC

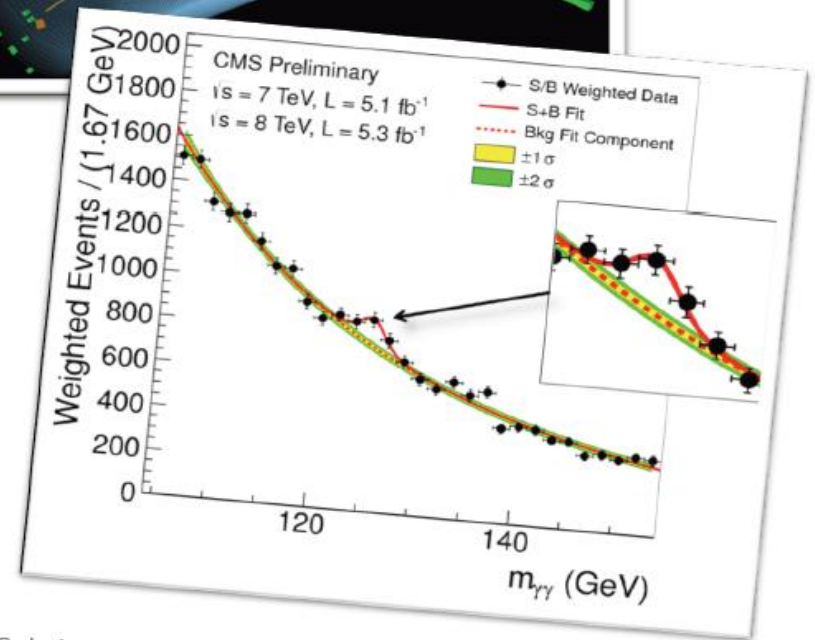
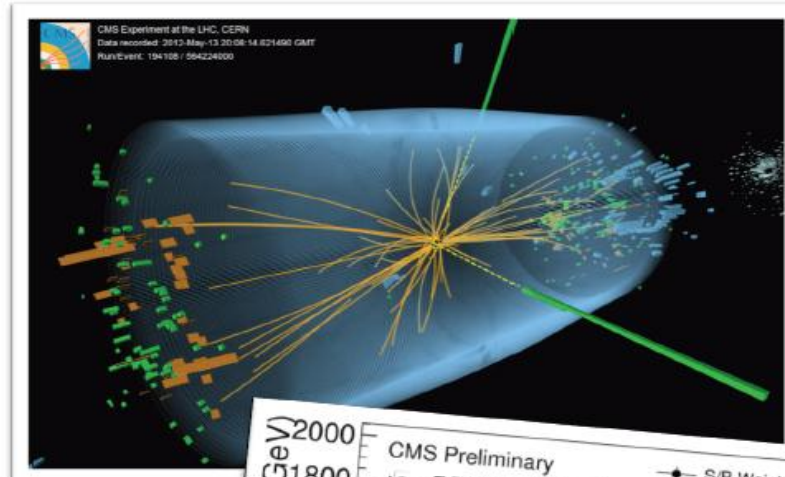
Standard Model measurements

- **Soft and hard QCD**
- **W and Z bosons**
- **Prompt photons**
- **b-jets**
- **Top quarks**

Parts based in part on M. Seymour lecture at CERN Summer School, 2018

Experiment = probing theories with data

$$\begin{aligned}
 & -\frac{1}{2}\partial_\mu g_\nu^\rho \partial_\rho g_\mu^\nu - g_s f^{abc} \partial_\mu g_\nu^\rho g_\rho^\sigma g_\sigma^\mu - \frac{1}{2}g_s^2 f^{abc} f^{ade} g_\mu^\nu g_\nu^\rho g_\rho^\sigma g_\sigma^\mu + \\
 & \frac{1}{2}g_s^2 (\bar{q}^i \gamma^\mu q_j^i) g_\mu^\nu + G^a \partial^\mu G^a + g_s f^{abc} \partial_\mu G^a G^b G^c - \partial_\mu W_\nu^+ \partial_\mu W_\nu^- - \\
 & M^2 W_\mu^+ W_\mu^- - \frac{1}{2}\partial_\mu Z_\nu^0 Z_\nu^0 - \frac{1}{2}M^2 Z_\mu^0 Z_\mu^0 - \frac{1}{2}\partial_\mu A_\nu \partial_\mu A_\nu - \frac{1}{2}\partial_\mu H \partial_\mu H - \\
 & \frac{1}{2}m_h^2 H^2 - \partial_\mu \phi^+ \partial_\mu \phi^- - M^2 \phi^+ \phi^- - \frac{1}{2}\partial_\mu \phi^0 \partial_\mu \phi^0 - \frac{1}{2}M^2 \phi^0 \phi^0 - \beta_h \frac{2M^2}{\Lambda^2} + \\
 & \frac{2M}{\Lambda} H + \frac{1}{2}(H^2 + \phi^0 \phi^0 + 2\phi^+ \phi^-) + \frac{2M^4}{\Lambda^4} \alpha_h - ig_{c_w} [\partial_\mu Z_\nu^0 (W_\mu^+ W_\nu^- - \\
 & W_\mu^- W_\nu^+) - Z_\nu^0 (W_\mu^+ \partial_\mu W_\nu^- - W_\mu^- \partial_\mu W_\nu^+) + Z_\nu^0 (W_\mu^+ \partial_\mu W_\nu^- - \\
 & W_\mu^- \partial_\mu W_\nu^+) - ig_{s_w} [\partial_\mu A_\nu (W_\mu^+ W_\nu^- - W_\mu^- W_\nu^+) - A_\nu (W_\mu^+ \partial_\mu W_\nu^- - \\
 & W_\mu^- \partial_\mu W_\nu^+) + A_\nu (W_\mu^+ \partial_\mu W_\nu^- - W_\mu^- \partial_\mu W_\nu^+) - \frac{1}{2}g^2 W_\mu^+ W_\nu^- W_\nu^+ W_\mu^- + \\
 & \frac{1}{2}g^2 W_\mu^- W_\nu^+ W_\nu^- W_\mu^+ + g^2 c_w^2 (Z_\mu^0 W_\nu^+ Z_\nu^0 W_\mu^- - Z_\mu^0 Z_\nu^0 W_\nu^+ W_\mu^-) + \\
 & g^2 s_w^2 (A_\mu W_\nu^+ A_\nu W_\mu^- - A_\mu A_\nu W_\nu^+ W_\mu^-) + g^2 s_w c_w [A_\mu Z_\nu^0 (W_\mu^+ W_\nu^- - \\
 & W_\mu^- W_\nu^+) - 2A_\mu Z_\nu^0 W_\nu^+ W_\mu^-] - g\alpha [H^2 + H\phi^0 \phi^0 + 2H\phi^+ \phi^-] - \\
 & \frac{1}{8}g^2 \alpha_h [H^4 + (\phi^0)^4 + 4(\phi^0)^2 \phi^+ \phi^- + 4H^2 \phi^+ \phi^- + 2(\phi^0)^2 H^2] - \\
 & g M W_\mu^+ W_\nu^- H - \frac{1}{2}g \frac{M}{\Lambda^2} Z_\mu^0 Z_\nu^0 H - \frac{1}{2}ig W_\mu^+ (\partial_\mu \phi^0 \phi^- - \phi^- \partial_\mu \phi^0) - \\
 & W_\mu^- (\partial_\mu \phi^0 \phi^+ - \phi^+ \partial_\mu \phi^0) + \frac{1}{2}ig [W_\mu^+ (H\partial_\mu \phi^- - \phi^- \partial_\mu H) - W_\mu^- (H\partial_\mu \phi^+ - \\
 & \phi^+ \partial_\mu H)] + \frac{1}{2}g \frac{1}{c_w} (Z_\mu^0 (H\partial_\mu \phi^0 - \phi^0 \partial_\mu H) - ig_{c_w}^2 M Z_\mu^0 (W_\mu^+ \phi^- - W_\mu^- \phi^+) + \\
 & ig_{s_w} M A_\mu (W_\mu^+ \phi^- - W_\mu^- \phi^+) - ig \frac{1-2c_w^2}{2c_w} Z_\mu^0 (\phi^+ \partial_\mu \phi^- - \phi^- \partial_\mu \phi^+) - \\
 & ig_{s_w} A_\mu (\phi^+ \partial_\mu \phi^- - \phi^- \partial_\mu \phi^+) - \frac{1}{2}g^2 W_\mu^+ W_\nu^- [H^2 + (\phi^0)^2 + 2\phi^+ \phi^-] - \\
 & \frac{1}{4}g^2 \frac{1}{\Lambda^2} Z_\mu^0 Z_\nu^0 [H^2 + (\phi^0)^2 + 2(2s_w^2 - 1)^2 \phi^+ \phi^-] - \frac{1}{2}g^2 \frac{2c_w}{c_w} Z_\mu^0 \phi^0 (W_\mu^+ \phi^- + \\
 & W_\mu^- \phi^+) - \frac{1}{2}ig^2 \frac{2c_w}{c_w} Z_\mu^0 H (W_\mu^+ \phi^- - W_\mu^- \phi^+) + \frac{1}{2}g^2 s_w A_\mu \phi^0 (W_\mu^+ \phi^- + \\
 & W_\mu^- \phi^+) + \frac{1}{2}ig^2 s_w A_\mu H (W_\mu^+ \phi^- - W_\mu^- \phi^+) - g^2 \frac{2c_w}{c_w} (2c_w^2 - 1) Z_\mu^0 A_\mu \phi^+ \phi^- - \\
 & g^1 s_w^2 A_\mu A_\nu \phi^+ \phi^- - e^\lambda (\gamma^\partial + m_\nu^2) e^\lambda - \rho^\lambda \gamma^\partial \nu^\lambda - \bar{u}_j^2 (\gamma^\partial + m_\nu^2) d_j^2 + \\
 & g^1 s_w^2 (\gamma^\partial + m_\nu^2) d_j^2 + ig_{s_w} A_\mu [-(e^\lambda \gamma^\mu e^\lambda) + \frac{2}{3}(\bar{u}_j^2 \gamma^\mu d_j^2)] + \\
 & \frac{ig}{4c_w} Z_\mu^0 [(\bar{\nu}^\lambda \gamma^\mu (1 + \gamma^5) \nu^\lambda) + (e^\lambda \gamma^\mu (4s_w^2 - 1 - \gamma^5) e^\lambda) + (\bar{u}_j^2 \gamma^\mu (\frac{2}{3}s_w^2 - \\
 & 1 - \gamma^5) u_j^2) + (d_j^2 \gamma^\mu (1 - \frac{2}{3}s_w^2 - \gamma^5) d_j^2)] + \frac{ig}{2\sqrt{2}} W_\mu^+ [(\bar{\nu}^\lambda \gamma^\mu (1 + \gamma^5) \nu^\lambda) + \\
 & (\bar{d}_j^2 \gamma^\mu (1 + \gamma^5) C_{\lambda j} d_j^2)] + \frac{ig}{2\sqrt{2}} W_\mu^- [(e^\lambda \gamma^\mu (1 + \gamma^5) \nu^\lambda) + (\bar{d}_j^2 \gamma^\mu (1 + \\
 & \gamma^5) u_j^2)] + \frac{ig}{2\sqrt{2}} \frac{m_\nu^2}{M} [-\phi^+ (\bar{\nu}^\lambda (1 - \gamma^5) e^\lambda) + \phi^- (e^\lambda (1 + \gamma^5) \nu^\lambda)] - \\
 & \frac{ig}{2} \frac{m_\nu^2}{M} [H (e^\lambda e^\lambda) + i\phi^0 (e^\lambda \gamma^5 e^\lambda)] + \frac{ig}{2M\sqrt{2}} \phi^+ [-m_\nu^2 (\bar{u}_j^2 C_{\lambda j} (1 - \gamma^5) d_j^2) + \\
 & m_\nu^2 (\bar{d}_j^2 C_{\lambda j} (1 + \gamma^5) u_j^2)] + \frac{ig}{2M\sqrt{2}} \phi^- [m_\nu^2 (\bar{d}_j^2 C_{\lambda j} (1 + \gamma^5) u_j^2) - \\
 & m_\nu^2 (\bar{u}_j^2 C_{\lambda j} (1 + \gamma^5) d_j^2)] - \frac{ig}{2} \frac{m_\nu^2}{M} H (\bar{d}_j^2 d_j^2) + \frac{ig}{2} \frac{m_\nu^2}{M} \phi^0 (\bar{u}_j^2 \gamma^5 u_j^2) - \\
 & \frac{ig}{2} \frac{m_\nu^2}{M} \phi^0 (\bar{d}_j^2 \gamma^5 d_j^2) + \bar{X}^+ (\partial^\mu - M^2) X^+ + \bar{X}^- (\partial^\mu - M^2) X^- + \bar{X}^0 (\partial^\mu - \\
 & \frac{M^2}{c_w}) X^0 + \bar{Y} \partial^\mu Y + ig_{c_w} W_\mu^+ (\partial_\mu \bar{X}^0 X^- - \partial_\mu \bar{X}^+ X^0) + ig_{s_w} W_\mu^+ (\partial_\mu \bar{Y} X^- - \\
 & \partial_\mu \bar{X}^+ Y) + ig_{c_w} W_\mu^- (\partial_\mu \bar{X}^- X^0 - \partial_\mu \bar{X}^0 X^+) + ig_{s_w} W_\mu^- (\partial_\mu \bar{X}^- Y - \\
 & \partial_\mu \bar{Y} X^+) + ig_{c_w} Z_\mu^0 (\partial_\mu \bar{X}^+ X^- - \partial_\mu \bar{X}^- X^+) + ig_{s_w} A_\mu (\partial_\mu \bar{X}^+ X^- + \\
 & \partial_\mu \bar{X}^- X^+) - \frac{1}{2}ig M [\bar{X}^+ X^+ H + \bar{X}^- X^- H + \frac{1}{c_w} \bar{X}^0 X^0 H] + \\
 & \frac{1-2c_w^2}{2c_w} ig M [\bar{X}^+ X^0 \phi^+ - \bar{X}^- X^0 \phi^-] + \frac{1}{2c_w} ig M [\bar{X}^0 X^- \phi^- - \bar{X}^+ X^+ \phi^+] + \\
 & ig M s_w [\bar{X}^0 X^- \phi^+ - \bar{X}^+ X^+ \phi^-] + \frac{1}{2}ig M [\bar{X}^+ X^+ \phi^0 - \bar{X}^- X^- \phi^0]
 \end{aligned}$$

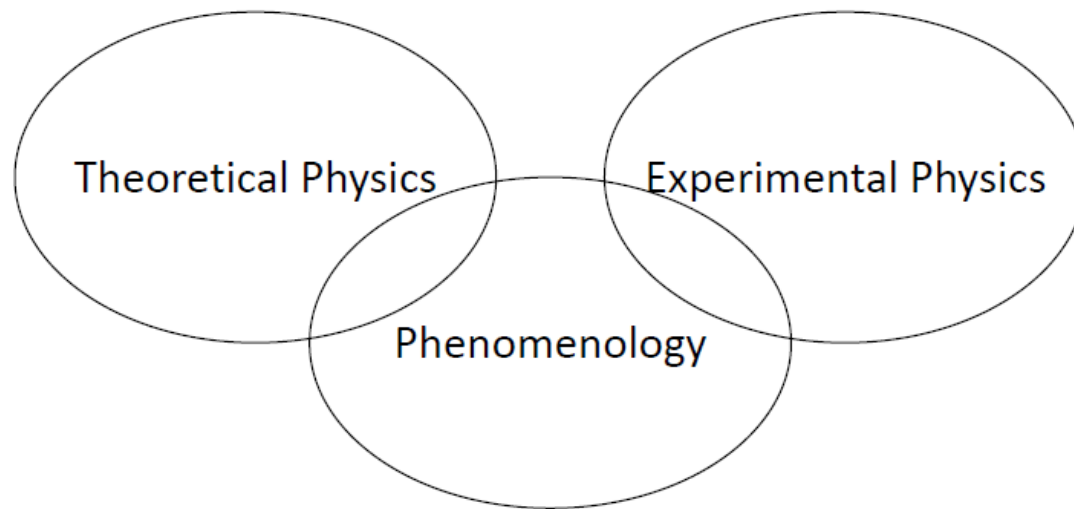


- Delamater

(experimental) LHC physics

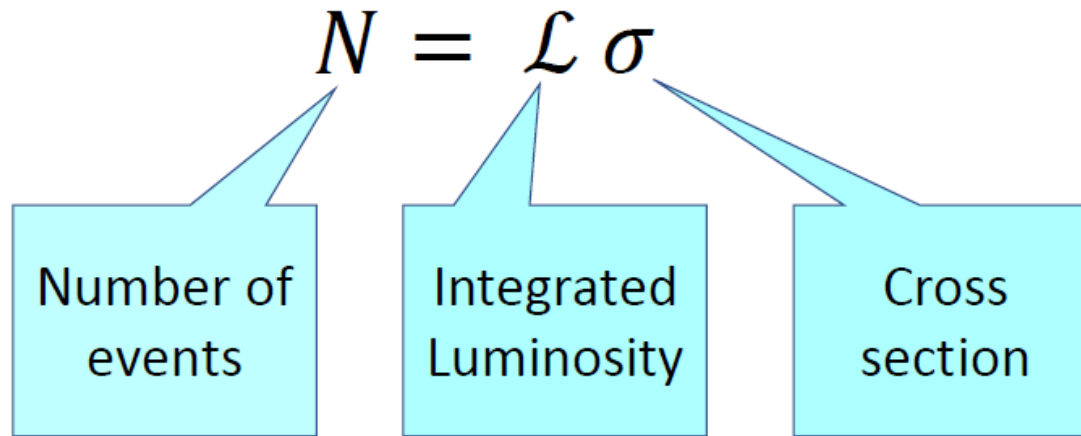
Making predictions for hadron colliders

Phenomenology



Making predictions for hadron colliders

Calculating Event Rates



Making predictions for hadron colliders

Calculating Cross Sections

$$d\sigma = \frac{1}{F} |\mathcal{M}|^2 dLIPS$$

Flux factor

$$= 2s = 4E_1E_2$$

(Quantum
mechanical)
amplitude
squared

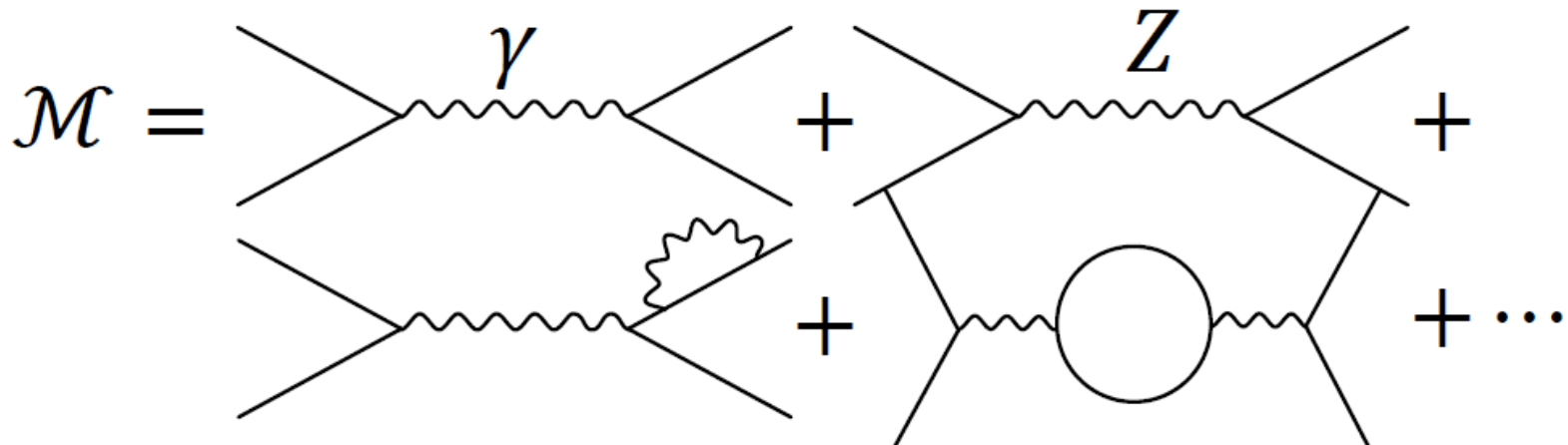
Lorentz
Invariant
Phase
Space

$$= \frac{d^4p_i}{(2\pi)^4} (2\pi)\delta(p_i^2 - m_i^2) \\ \frac{d^4p_j}{(2\pi)^4} (2\pi)\delta(p_j^2 - m_j^2) \dots \\ (2\pi)^4 \delta(p_1 + p_2 - p_i - p_j - \dots)$$

Making predictions for hadron colliders

Calculating Cross Sections

$$d\sigma = \frac{1}{F} |\mathcal{M}|^2 dLIPS$$



Making predictions for hadron colliders

Feynman Rules

$$\alpha \longrightarrow \beta \quad \rightarrow \quad \left(\frac{i}{\not{p} - m + i\epsilon} \right)_{\beta\alpha}$$

$$\mu \text{ wavy line } \nu \quad \rightarrow \quad \frac{-i\eta_{\mu\nu}}{p^2 + i\epsilon}$$

$$\begin{array}{l} \beta \\ \nearrow \\ \alpha \end{array} \text{ wavy line } \mu \quad \rightarrow \quad -ie\gamma_{\beta\alpha}^{\mu} (2\pi)^4 \delta^{(4)}(p_1 + p_2 + p_3).$$

Elementary charge

$$e = \sqrt{4\pi\alpha} \quad \alpha \approx 1/137$$

Making predictions for hadron colliders

Tree Diagrams as Leading Order of Expansion in α

$$\mathcal{M} = \begin{array}{c} \text{Diagram 1: } \gamma \text{ exchange} \\ \text{Diagram 2: } Z \text{ exchange} \\ \text{Diagram 3: } \text{gluon emission} \\ \text{Diagram 4: } \text{gluon loop} \end{array} + \dots \quad \begin{array}{l} \mathcal{O}(\alpha) \\ \mathcal{O}(\alpha^2) \end{array}$$

$$\alpha \approx 1/137 \text{ but } \alpha_s \approx 0.1$$

\Rightarrow QCD corrections important

Making predictions for hadron colliders

Example: The Drell-Yan process ($pp \rightarrow \mu^+ \mu^-$)

$$\mathcal{M} = \begin{array}{c} q \\ \swarrow \\ \gamma \\ \nwarrow \\ \bar{q} \end{array} \begin{array}{c} \mu^- \\ \swarrow \\ \mu^+ \\ \nwarrow \end{array}$$

$$\Rightarrow |\mathcal{M}|^2 \propto e_q^2 \alpha^2 \frac{t^2 + u^2}{s^2} \propto e_q^2 \alpha^2 (1 + \cos^2 \theta)$$

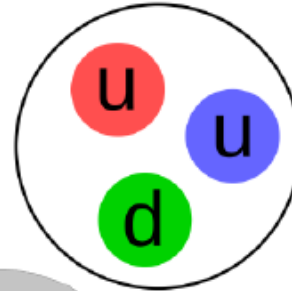
$$\Rightarrow \sigma = \frac{4\pi\alpha^2}{9Q^2} e_q^2$$

$$(s = Q^2 = (p_q + p_{\bar{q}})^2)$$

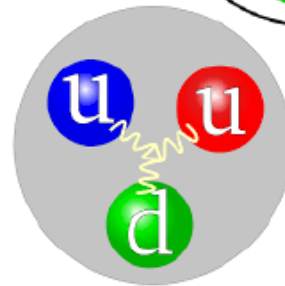
Making predictions for hadron colliders

Proton structure

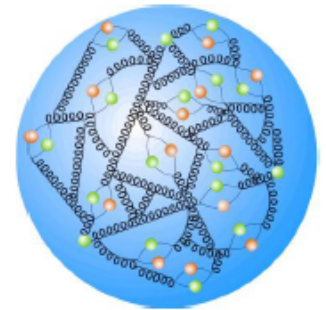
- Proton = uud ?



- Held together by gluons?



- Quantum Field Theory: gluons can create $q\bar{q}$ pairs



- Proton can interact through any of its partons

Making predictions for hadron colliders

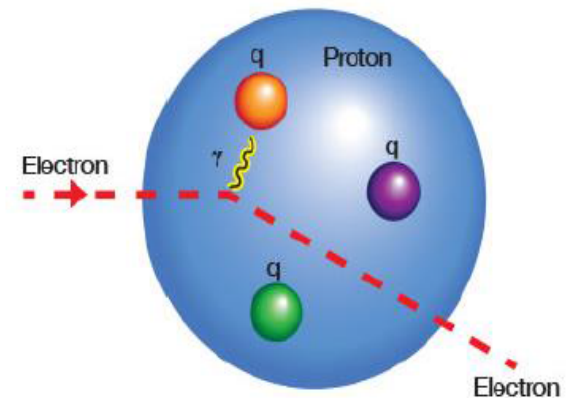
Proton structure: parton distribution functions

- How is the proton's energy shared between its parton constituents?
- Measure in deep inelastic electron scattering
- Quantify by *parton distribution function*

$f_i(x)dx$ = probability that parton of type i is found with fraction of proton's momentum between x and $x + dx$

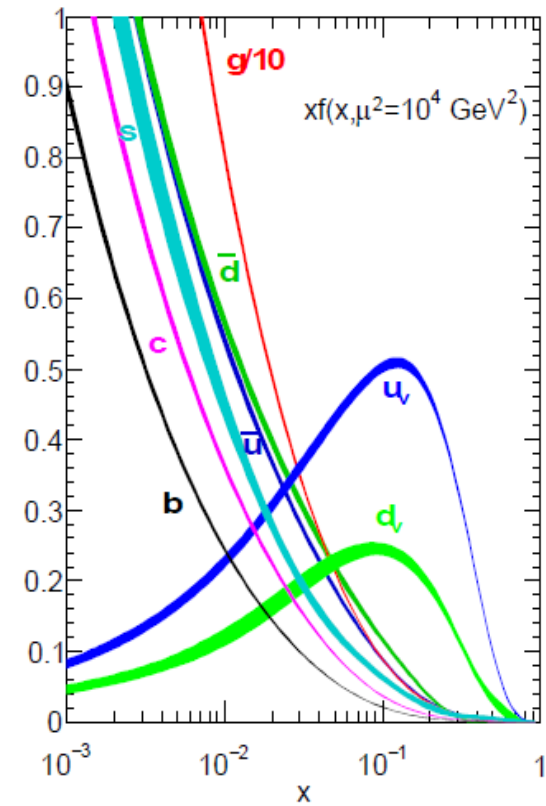
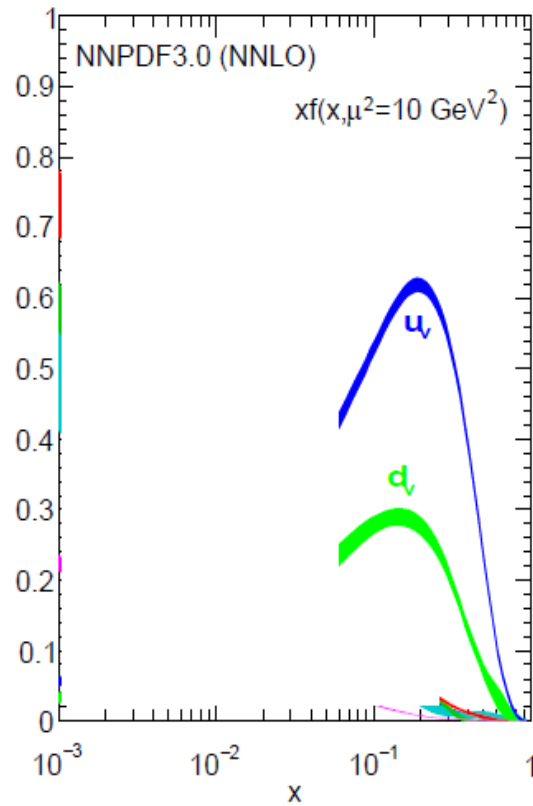
- But how long do those quantum fluctuations live?

⇒ PDFs depend on the momentum scale of the probe $f_i(x, Q^2)dx$



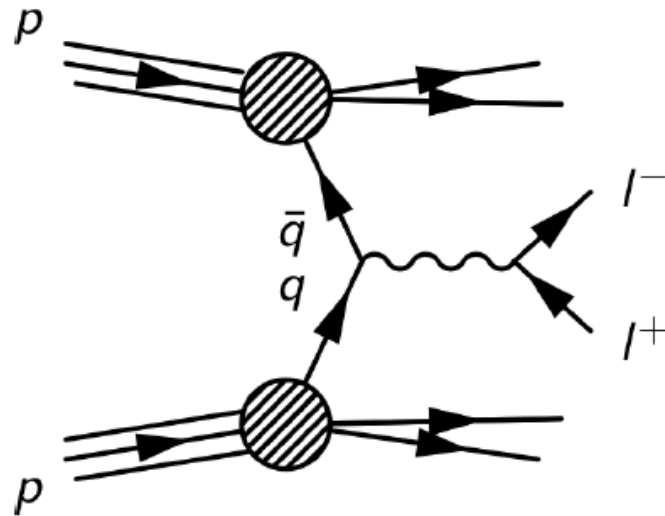
Making predictions for hadron colliders

Proton structure: parton distribution functions



Making predictions for hadron colliders

The Drell-Yan process ($pp \rightarrow \mu^+ \mu^-$)



$$\frac{d\sigma}{dQ^2} = \sum_q \int dx_1 f_q(x_1, Q^2) dx_2 f_{\bar{q}}(x_2, Q^2) \frac{4\pi\alpha^2}{9Q^2} e_q^2 \delta(x_1 x_2 s - Q^2)$$

Making predictions for hadron colliders

Loop Diagrams as Higher Order Corrections

$$\mathcal{M} = \begin{array}{c} \text{tree} \\ \mathcal{O}(\alpha) \end{array} + \begin{array}{c} \text{loop} \\ \mathcal{O}(\alpha\alpha_s) \end{array} + \dots$$

$$|\mathcal{M}|^2 = \begin{array}{c} \mathcal{O}(\alpha^2) \\ |\mathcal{M}_0|^2 \end{array} + \begin{array}{c} \mathcal{O}(\alpha^2\alpha_s) \\ 2\Re(\mathcal{M}_0^* \mathcal{M}_1) \end{array} + \begin{array}{c} |\mathcal{M}_1|^2 \end{array} + \dots$$

- Quantum mechanics: sum over unobserved quantum numbers
= integrate over gluon momenta

Making predictions for hadron colliders

Loop Diagrams as Higher Order Corrections

$$\mathcal{M} = \text{tree} + \text{loop} + \dots$$

The diagram shows the expansion of the amplitude \mathcal{M} . The first term is a tree-level diagram with two incoming lines on the left and two outgoing lines on the right, connected by a wavy line. Below it is the label $\mathcal{O}(\alpha)$. The second term is a loop-level diagram where a triangle loop of three circles is attached to the wavy line. Below it is the label $\mathcal{O}(\alpha\alpha_s)$. The expression ends with a plus sign and three dots.

- Gluon momentum integral is divergent! (= *minus* infinity)
- Divergence comes from:
 - Momentum = 0
 - Momentum = parallel to quark or antiquark

Making predictions for hadron colliders

Glue Emission as Higher Order Correction

$$\mathcal{M} = \text{[Diagram 1]} + \text{[Diagram 2]} \quad \mathcal{O}(\alpha\sqrt{\alpha_s})$$

The diagram shows the mathematical expression for the amplitude \mathcal{M} as the sum of two Feynman diagrams. The first diagram shows a quark and antiquark annihilation into a virtual photon, which then decays into a muon and antimuon pair. A gluon is emitted from the quark line. The second diagram is identical but the gluon is emitted from the antiquark line. The order of the correction is given as $\mathcal{O}(\alpha\sqrt{\alpha_s})$.

- Glue emission describes a different process ($q\bar{q} \rightarrow \mu^+\mu^-g$)
- But if we are only interested in the total cross section for Drell-Yan pairs, must integrate over gluon momenta
- Divergent from momentum = 0 or parallel to quark or antiquark
- Cancels loop divergence

Making predictions for hadron colliders

Next-to-Leading Order (NLO) cross section

- $\sigma_{NLO} = \sigma_{tree} + \sigma_{loop} + \sigma_{emission}$
- σ_{loop} and $\sigma_{emission}$ each divergent
 - must regularize and expose singularities of each
 - *Subtraction algorithms*
- Fully automated,
 - e.g. in Madgraph/aMC@NLO, MCFM, Sherpa, Herwig ...

Making predictions for hadron colliders

From Feynman Diagrams to Cross Sections

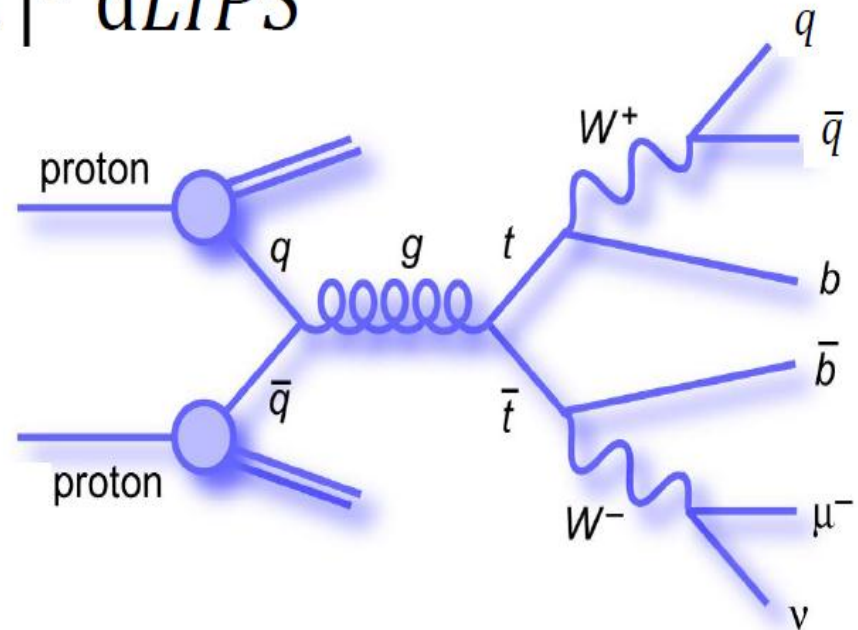
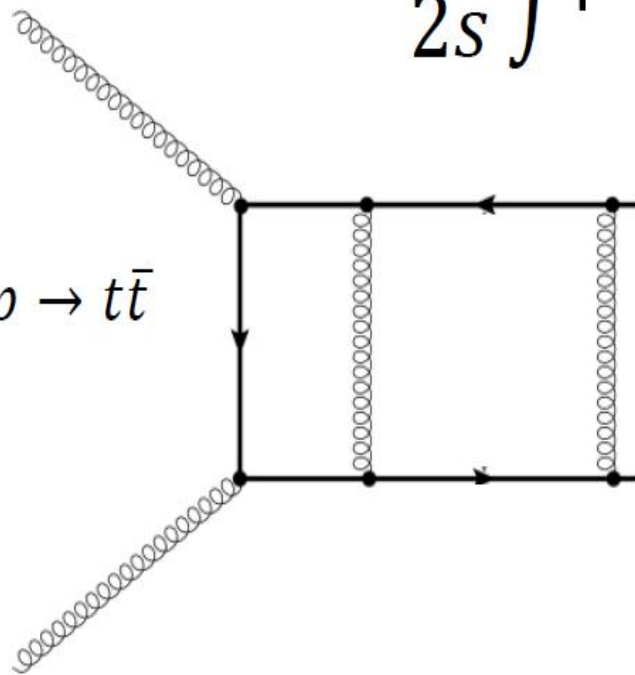
- Major part of phenomenology = calculating cross sections
- LO = write down all tree diagrams, integrate phase space numerically
- Convolute with parton distribution functions (fitted to data)
- NLO = one-loop diagrams, one-emission processes
 - Extract singularities from integrals, integrate analytically
 - Integrate remainders numerically
- NNLO = two-loop diagrams, one-emission at one-loop, and two emissions
- But LHC events contain *hundreds* of additional particles...

Making predictions for hadron colliders

Cross Sections

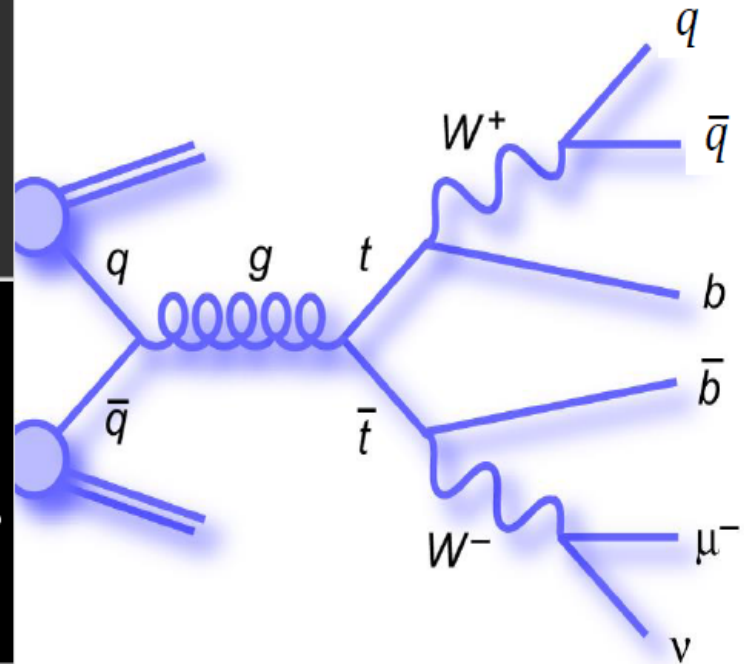
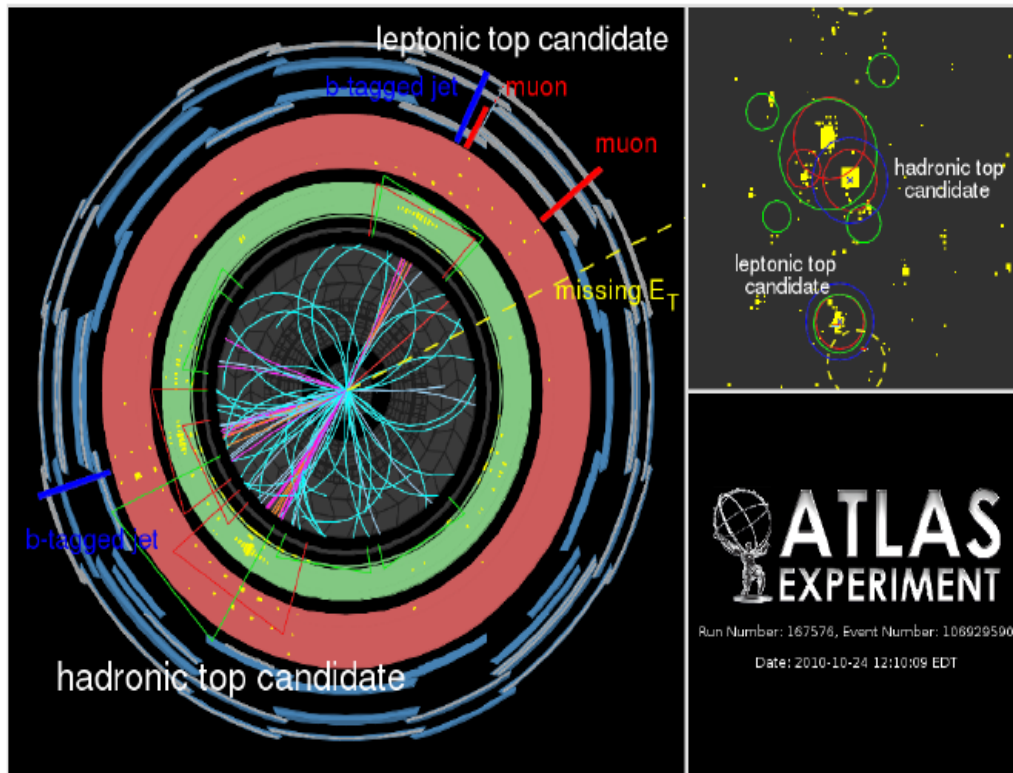
$$\sigma = \frac{1}{2s} \int |\mathcal{M}|^2 dLIPS$$

e.g. $pp \rightarrow t\bar{t}$
NNLO



Making predictions for hadron colliders

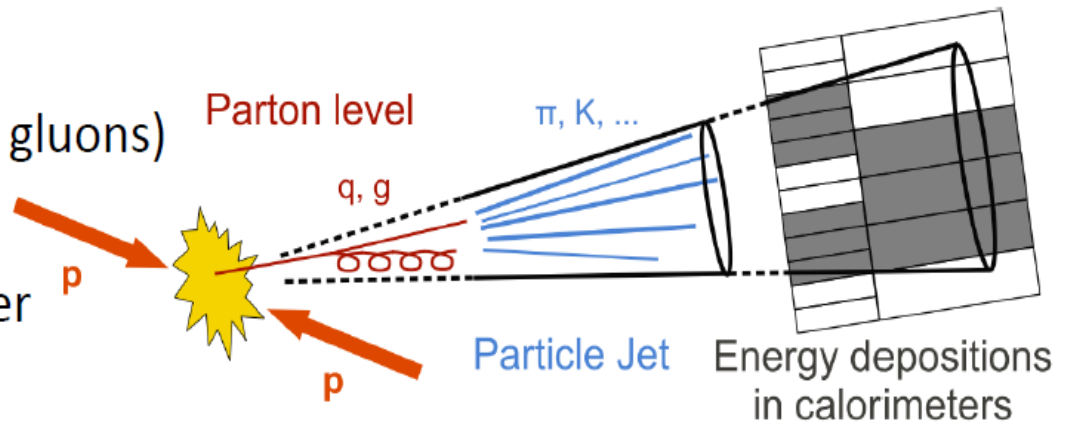
Cross Sections are not enough



Monte Carlo event structure

Need to describe *event structure*

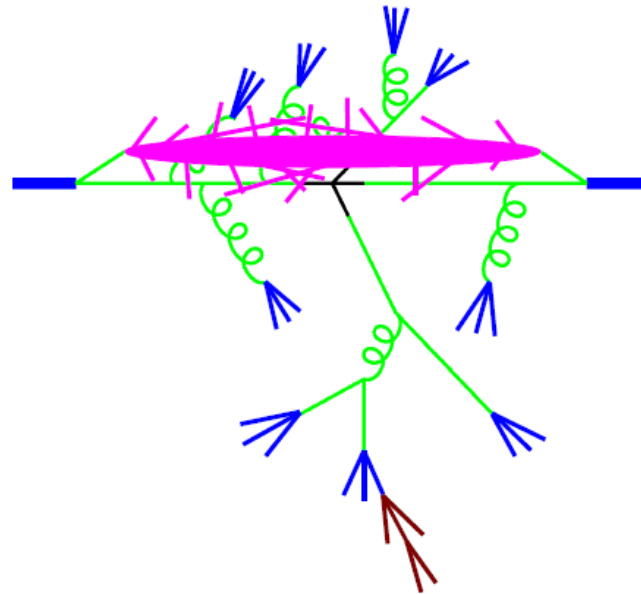
- Hadrons (not quarks and gluons)
- Jets of hadrons
- Remnants of protons after parton extracted
- Unstable particle decays



Monte Carlo event structure

Need Event Generators

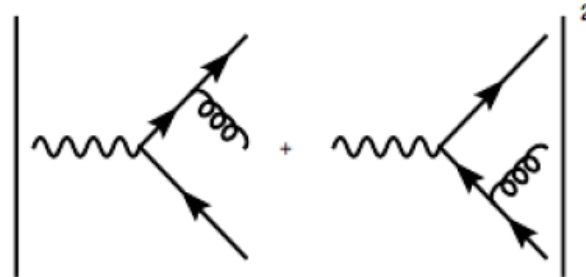
1. Hard process
2. Parton shower
3. Hadronization
4. Underlying event
5. Unstable particle decays



Parton showers

Gluon emission is universal

e.g. $e^+e^- \rightarrow 3$ partons:



$$\frac{d\sigma}{d \cos \theta dz_g} \sim \sigma_0 C_F \frac{\alpha_s}{2\pi} \frac{2}{\sin^2 \theta} \frac{1 + (1 - z_g)^2}{z_g}$$

$E_g/E_{g,\max}$ points to dz_g
 $e^+e^- \rightarrow 2$ partons points to σ_0
 "quark charge squared" points to C_F
 QCD running coupling ~ 0.1 points to α_s

Divergent in collinear limit $\theta \rightarrow 0, \pi$ (for massless quarks)
 and soft limit $z_g \rightarrow 0$

$$d\sigma = \sigma_0 \sum_{\text{jets}} C_F \frac{\alpha_s}{2\pi} \frac{d\theta^2}{\theta^2} dz \frac{1 + (1 - z)^2}{z}$$

Parton showers

Parton branching is universal

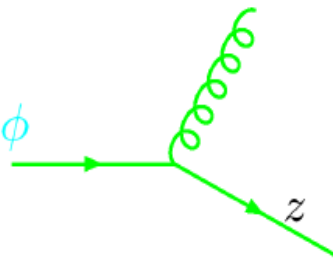
$$d\sigma = \sigma_0 \frac{\alpha_s}{2\pi} \frac{d\theta^2}{\theta^2} dz P(z, \phi) d\phi$$

$$P(z, \phi) =$$

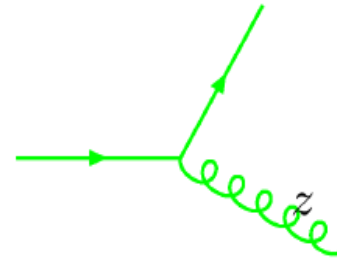
“Splitting function”:
 dependent on flavour and spin but not on how parton was produced

→ Probability distribution for parton branching

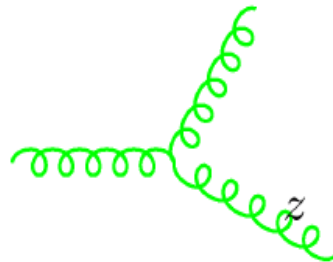
→ Simulation



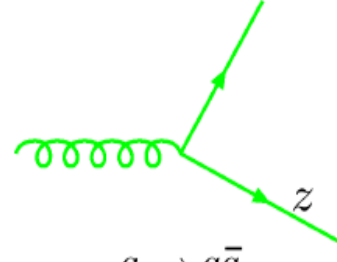
$$C_F \frac{1+z^2}{1-z}$$



$$C_F \frac{1+(1-z)^2}{z}$$

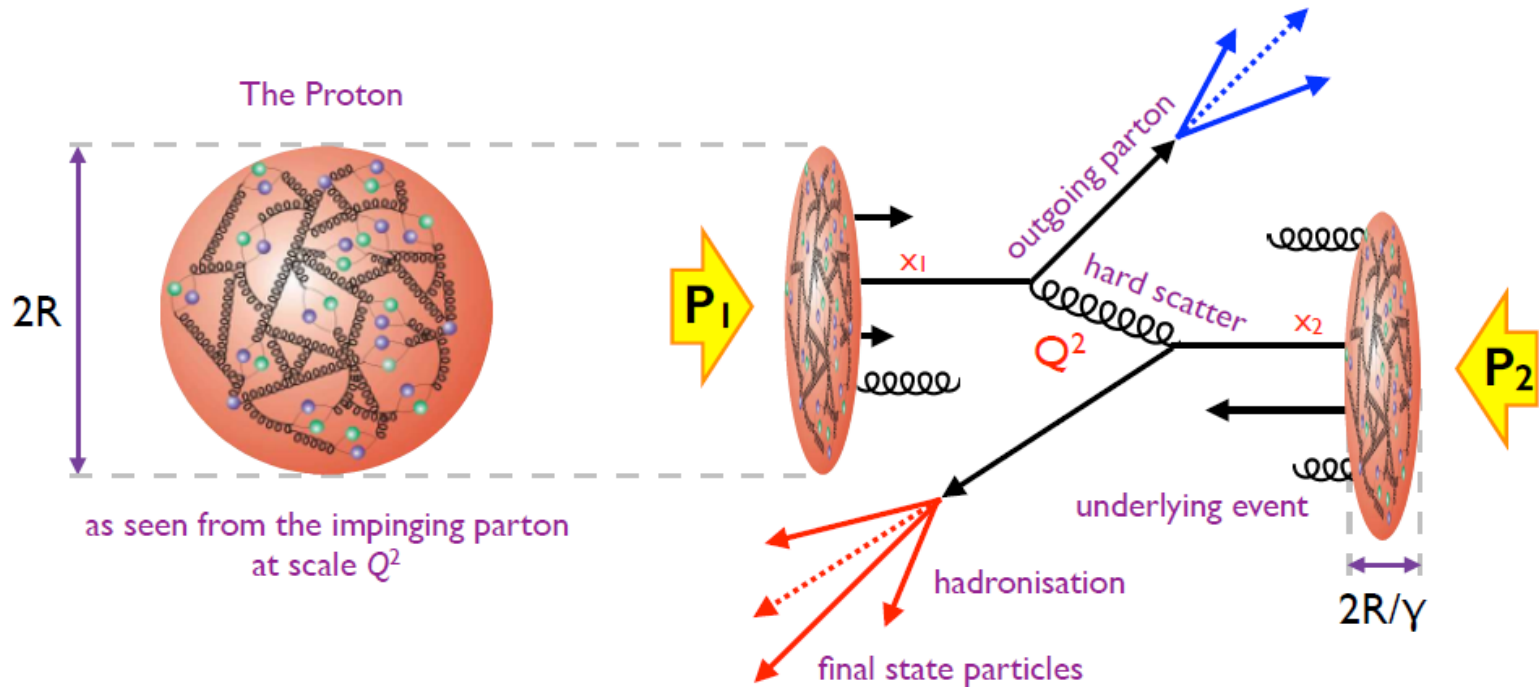


$$C_A \frac{z^4 + 1 + (1-z)^4}{z(1-z)}$$



$$T_R (z^2 + (1-z)^2)$$

Proton-(anti)proton collisions



Underlying event

- proton remnants from collective interaction of partons not involved in hard scatter
- description necessitate “tuning” of non-perturbative MC parameters based on data

Parton shower and hadronisation

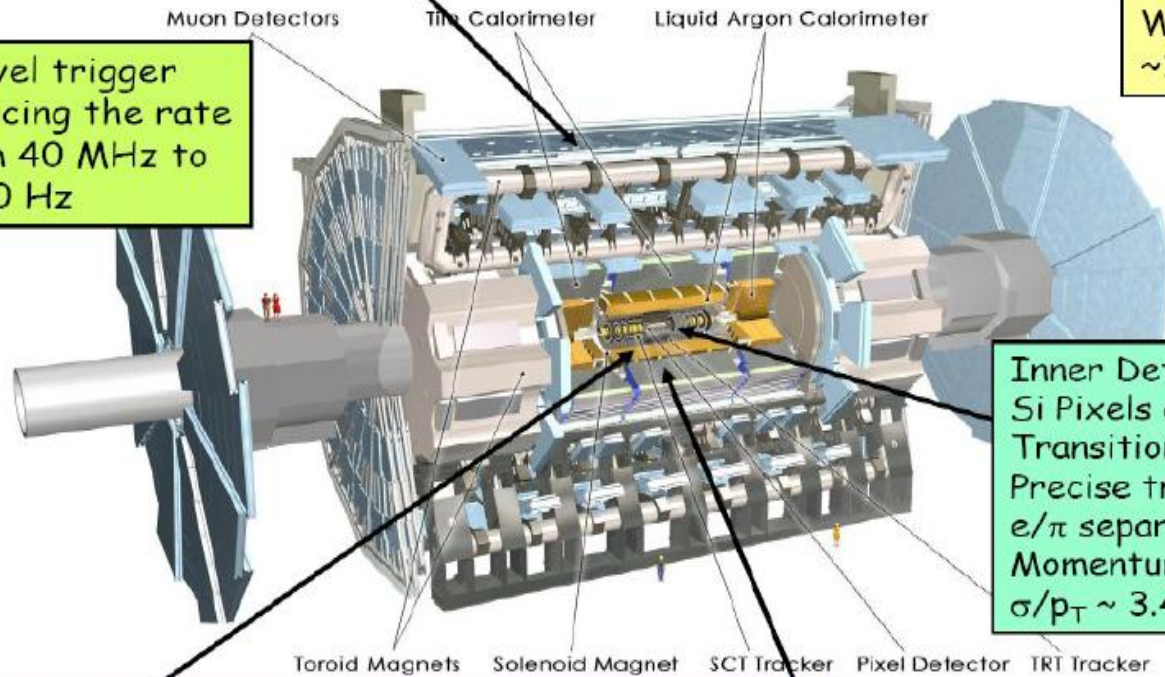
- ISR/FSR emission of gluons
- production of final states hadrons scale $< \Lambda_{\text{QCD}}$ (non-perturbative)
- MC models tuned on data

The ATLAS detector

Muon Spectrometer ($|\eta| < 2.7$): air-core toroids with gas-based chambers
 Muon trigger and measurement with momentum resolution $< 10\%$ up to $E_\mu \sim \text{TeV}$

Length : ~ 46 m
 Radius : ~ 12 m
 Weight : ~ 7000 tons
 $\sim 10^8$ electronic channels

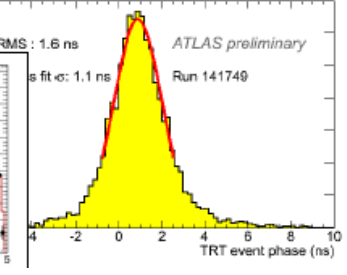
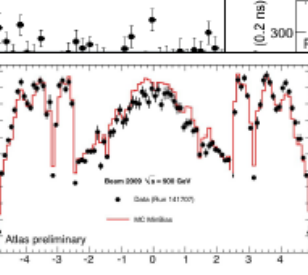
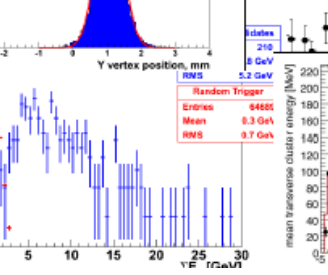
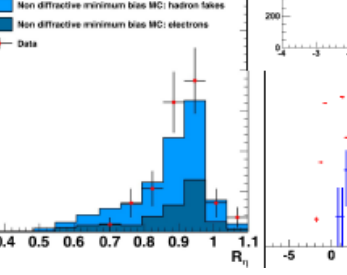
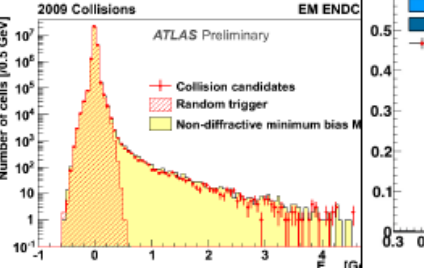
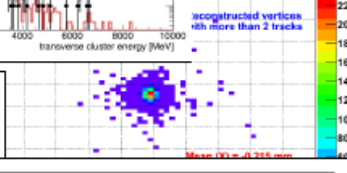
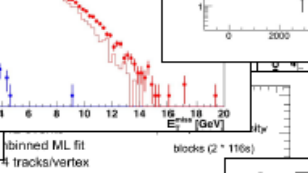
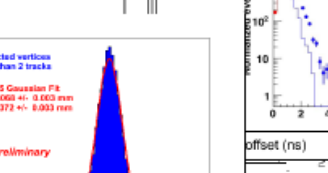
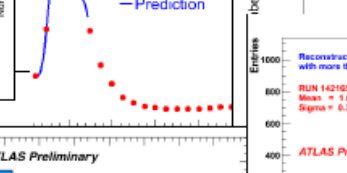
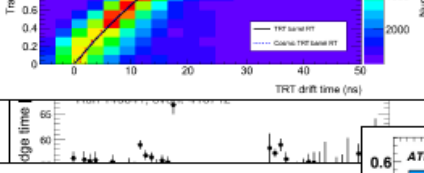
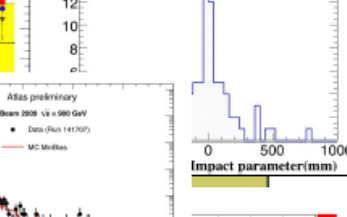
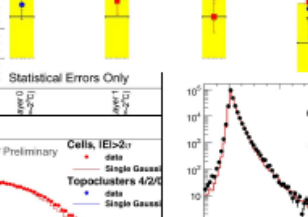
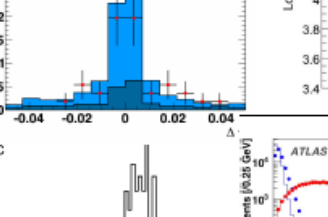
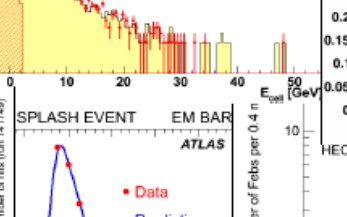
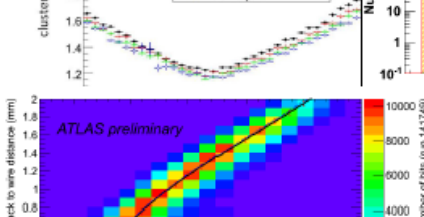
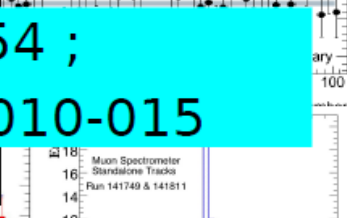
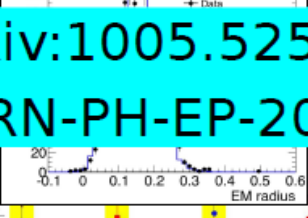
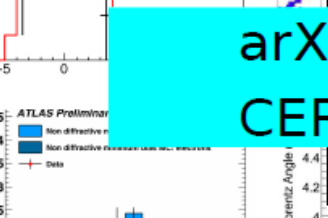
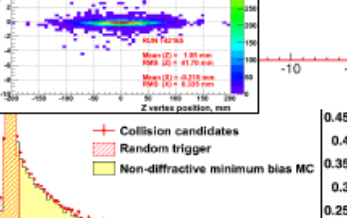
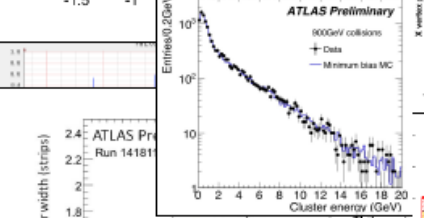
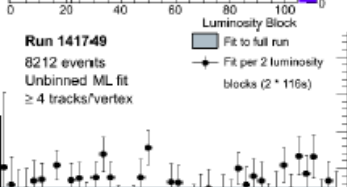
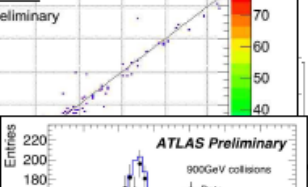
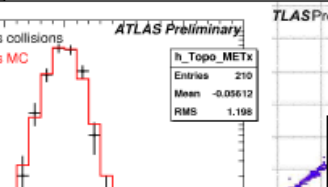
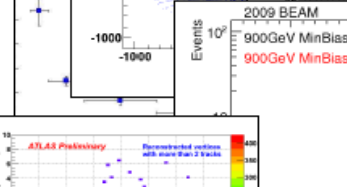
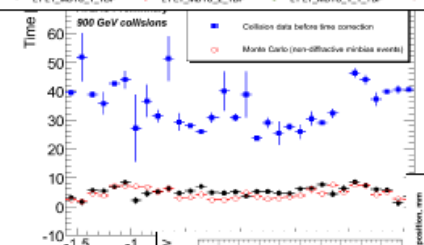
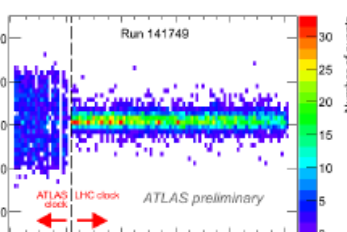
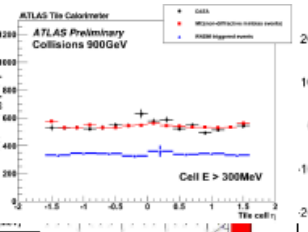
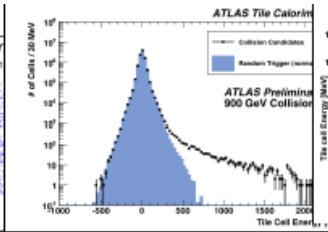
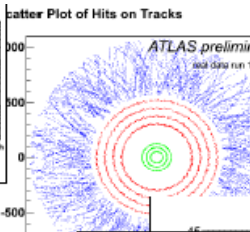
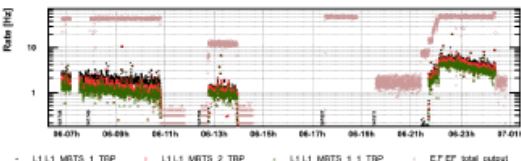
3-level trigger
 reducing the rate
 from 40 MHz to
 ~ 200 Hz



Inner Detector ($|\eta| < 2.5, B=2\text{T}$):
 Si Pixels and strips (SCT) +
 Transition Radiation straws
 Precise tracking and vertexing,
 e/π separation (TRT).
 Momentum resolution:
 $\sigma/p_T \sim 3.4 \times 10^{-4} p_T (\text{GeV}) \oplus 0.015$

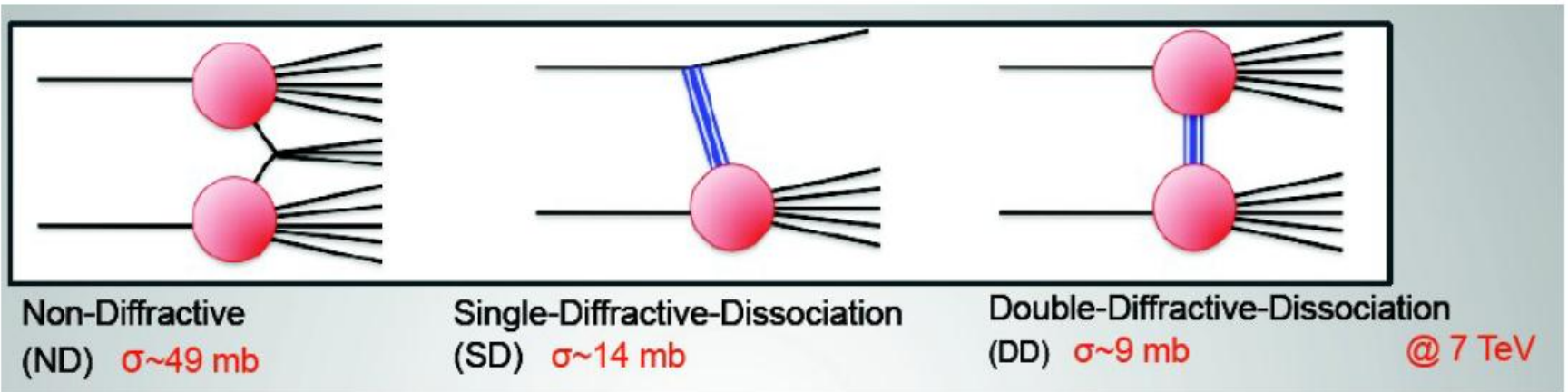
EM calorimeter: Pb-LAr Accordion
 e/γ trigger, identification and measurement
 E-resolution: $\sim 1\%$ at 100 GeV, 0.5% at 1 TeV

HAD calorimetry ($|\eta| < 5$): segmentation, hermeticity
 Tilecal Fe/scintillator (central), Cu/W-LAr (fwd)
 Trigger and measurement of jets and missing E_T
 E-resolution: $\sigma/E \sim 50\%/\sqrt{E} \oplus 0.03$

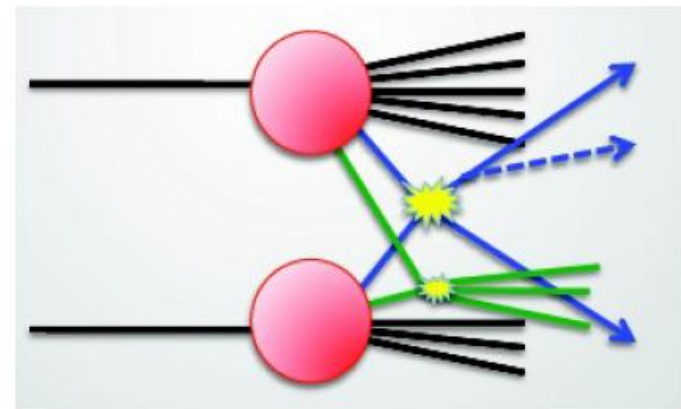


arXiv:1005.5254 ; CERN-PH-EP-2010-015

Dominant QCD processes



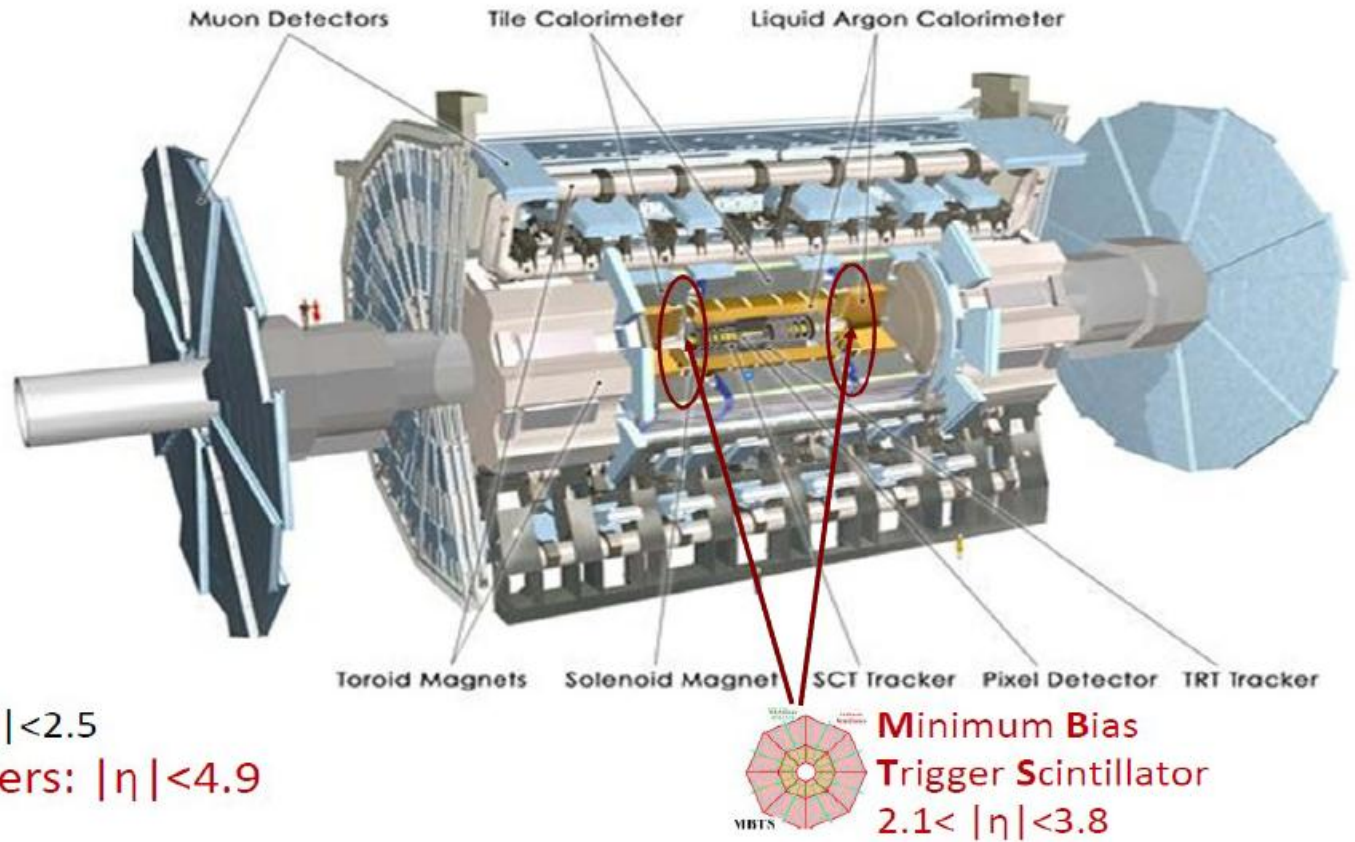
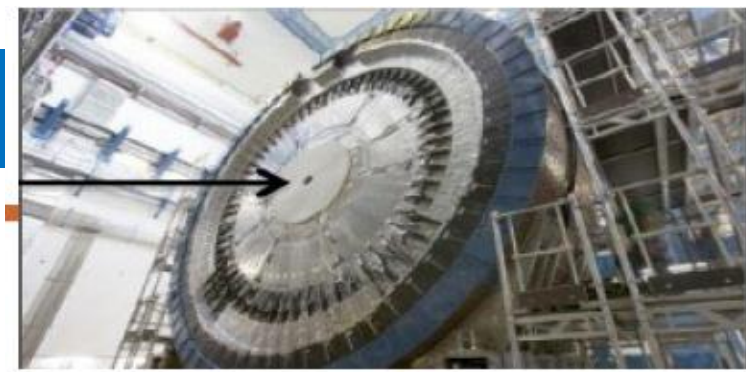
- Multi-parton interactions (**Underlying Event**)



Inelastic cross-sections

- Use only few runs: 7 TeV data ($190 \mu\text{b}^{-1}$) + 900 GeV data ($7 \mu\text{b}^{-1}$) and 2.36 TeV data ($0.1 \mu\text{b}^{-1}$)
 - We want to study **all** inelastic pp interactions
 - Instantaneous luminosity very low for these runs: on average ~ 0.007 interactions per bunch crossing \rightarrow **99.3% of crossings are empty.**
 - Need to **“trigger”** on inelastic interactions:
Minimum Bias Scintillator Trigger (MBTS)
 - \rightarrow sensitive to any charged particle $2.09 < |\eta| < 3.84$
 - \rightarrow 16 counters on each side of ATLAS
- Correct for detector inefficiencies and resolution, eg. present **spectrum of charge particles** not tracks
- **No extrapolation** to regions not seen by ATLAS

MBST Trigger



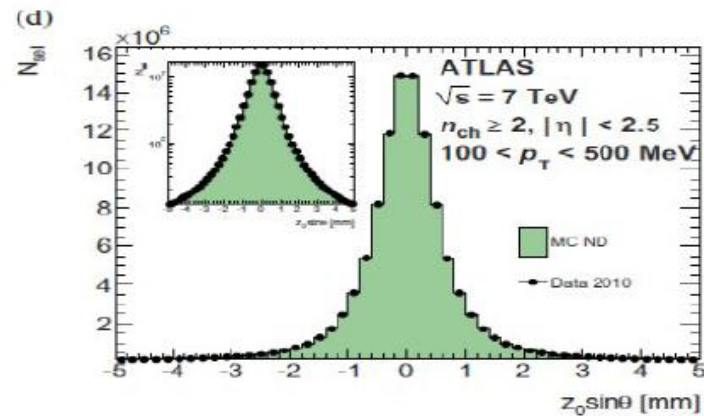
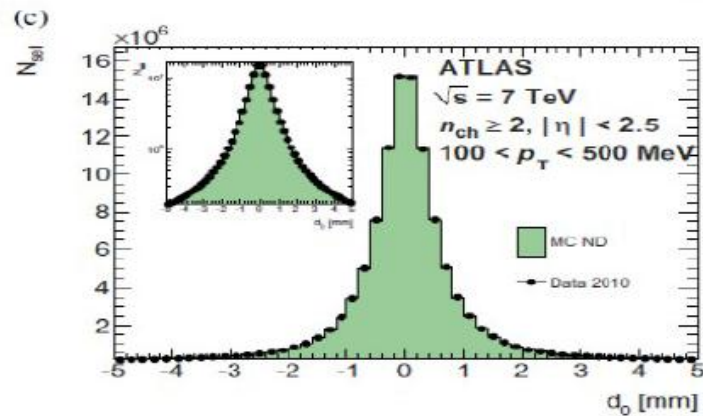
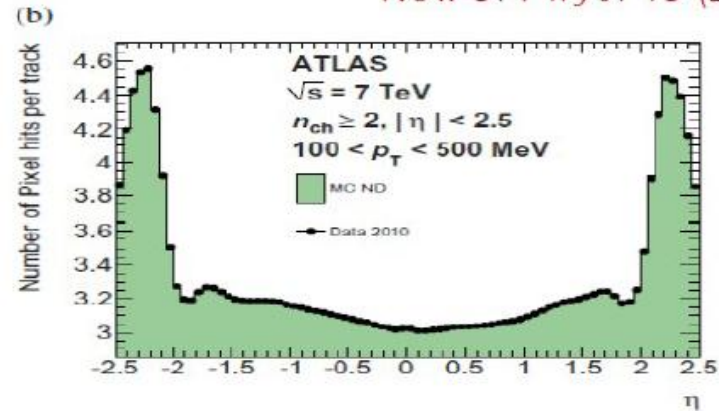
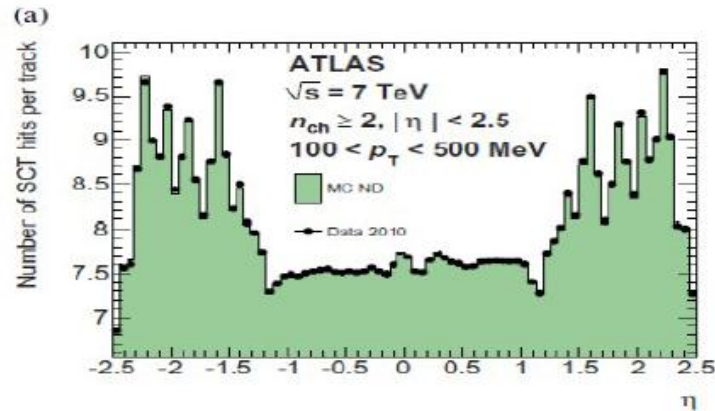
Trackers: $|\eta| < 2.5$

Calorimeters: $|\eta| < 4.9$

**Minimum Bias
Trigger Scintillator
 $2.1 < |\eta| < 3.8$**

How well we understood detector?

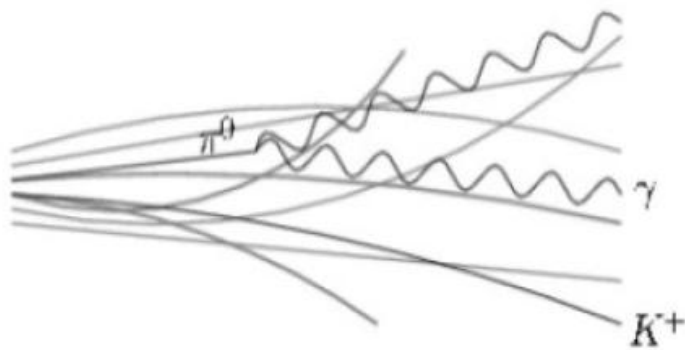
New J. Phys. 13 (2011) 053033



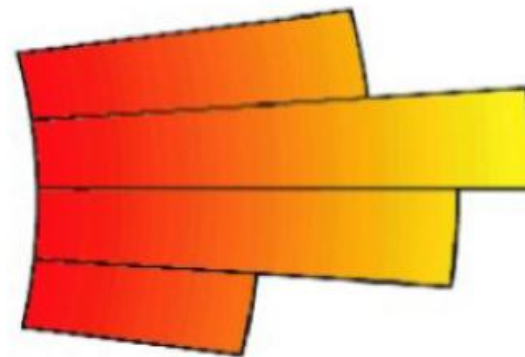
- Excellent agreement between data and MC: Pixel and Silicon hits per track

Unfolding to particle level

- Bayesian iterative unfolding used to correct tracks and clusters back to particle level.
 - Use mapping of truth particles on reconstructed objects (use Monte Carlo)

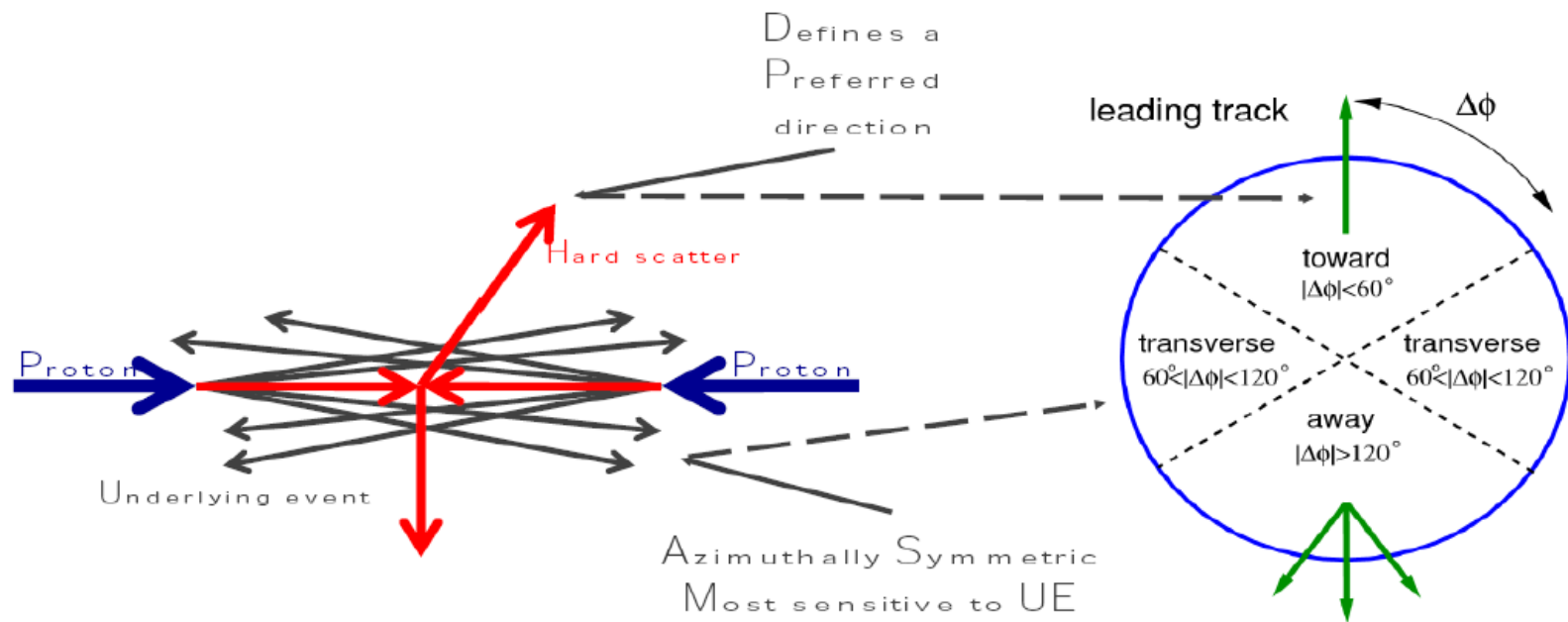


particle level



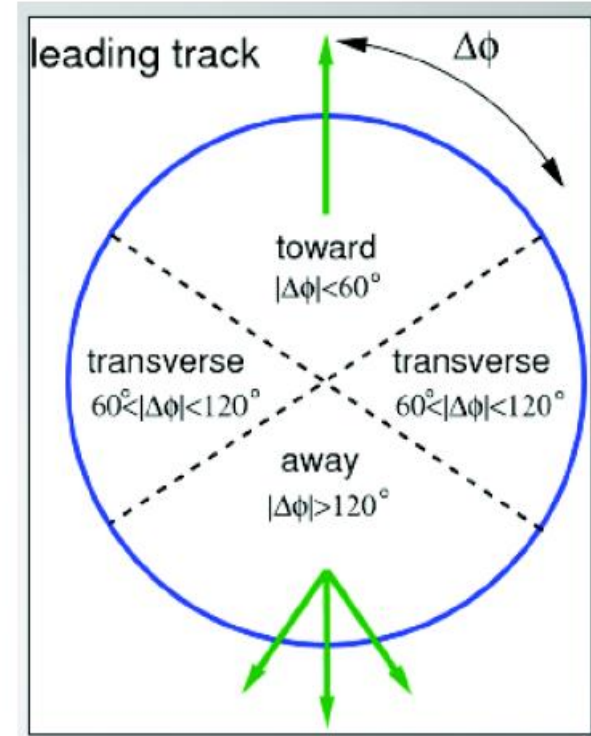
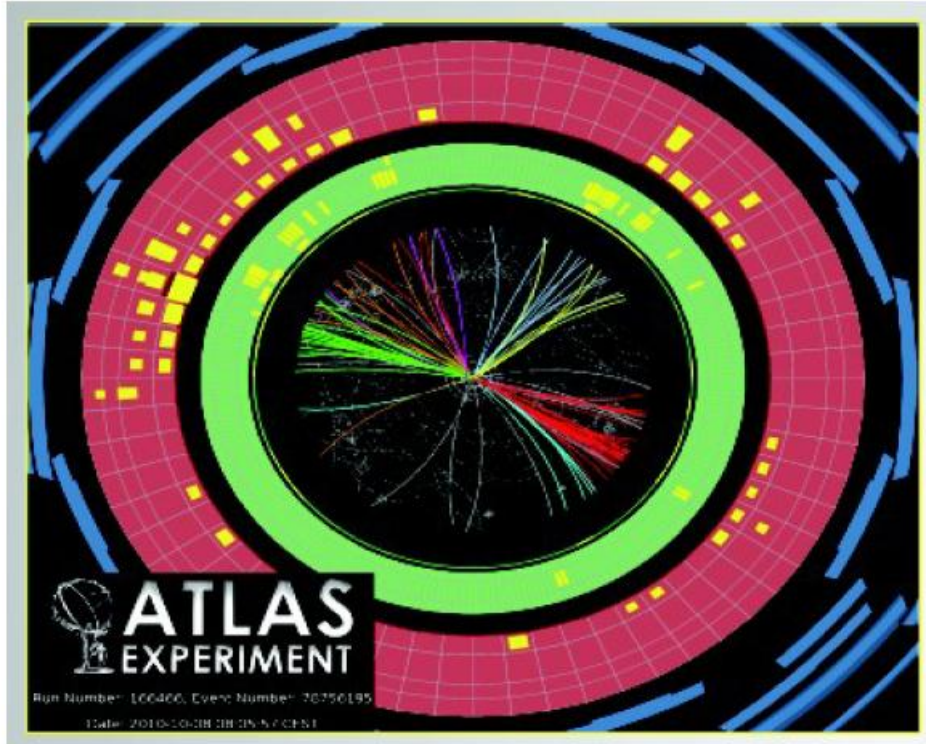
detector level

Underlying event



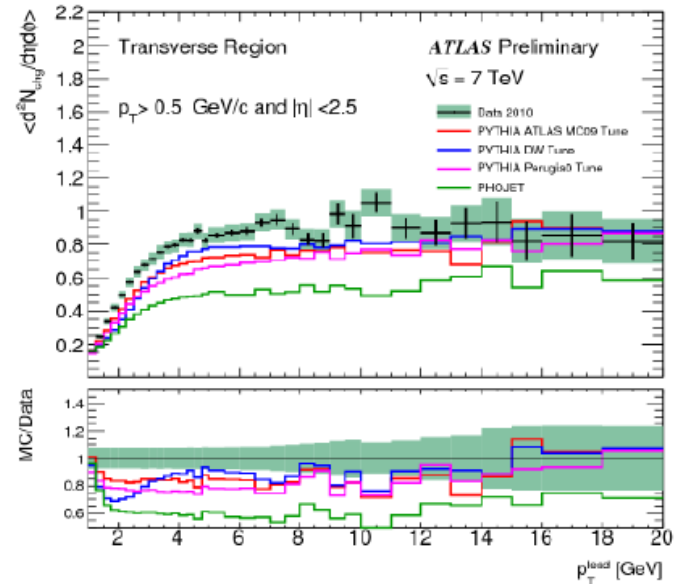
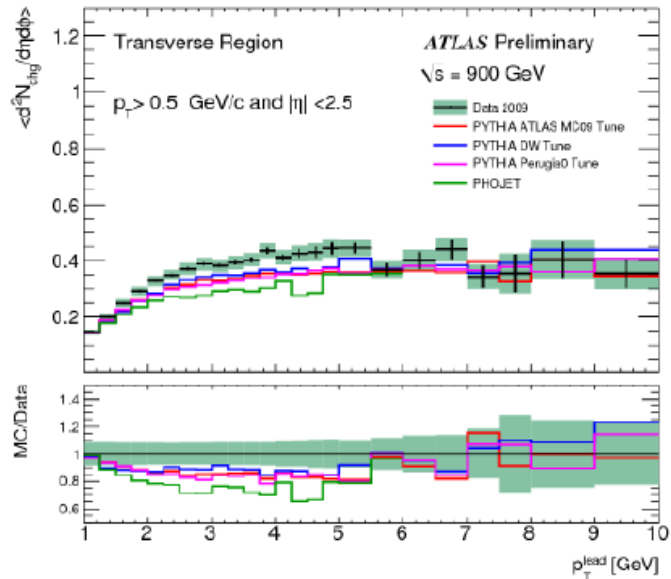
- UE = “everything” - “hard scatter” = beam-beam remnants, MPI, ISR
- Study: charged particle density, transverse momentum, average p_T . Transverse region considered most sensitive to UE

Underlying event



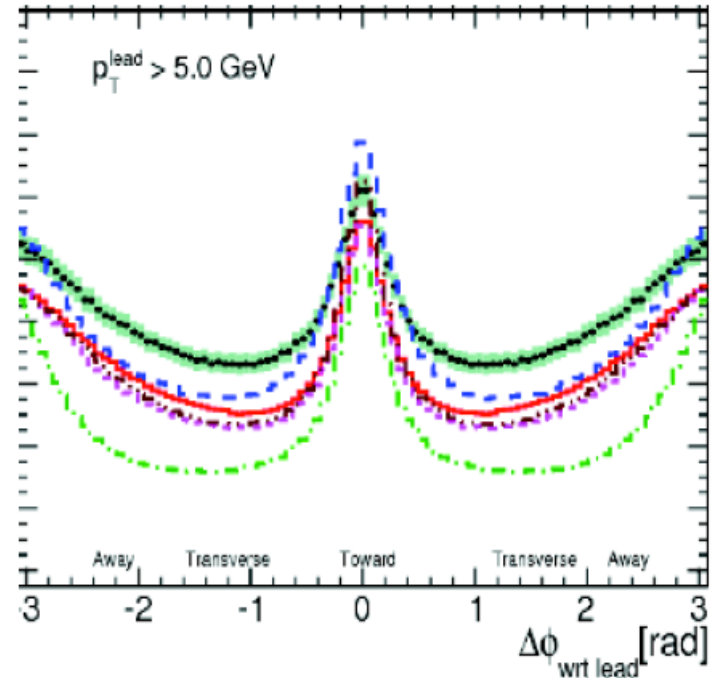
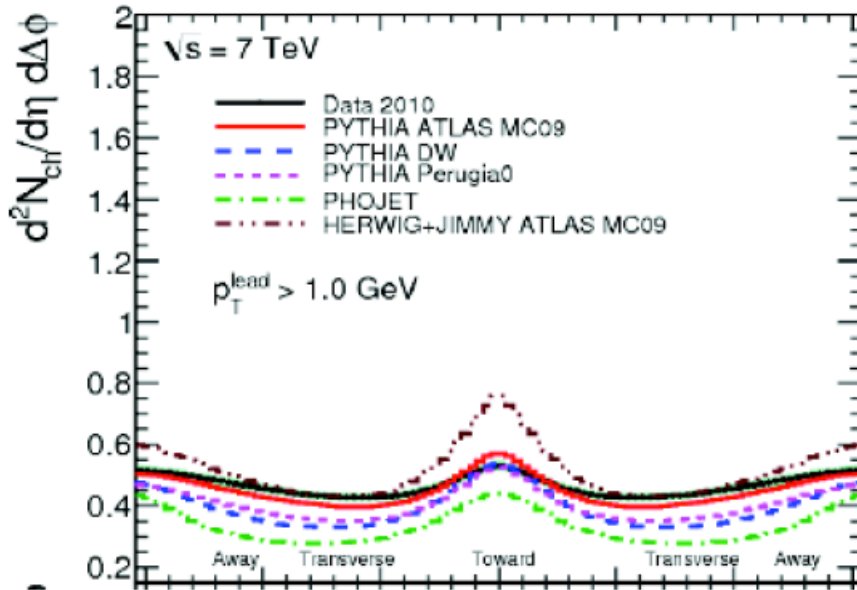
- Define the direction of “hard scatter” as the highest p_T particle
- Study the activity (# of particles) in the region “transverse” to the hard scatter.

Transverse region particle density



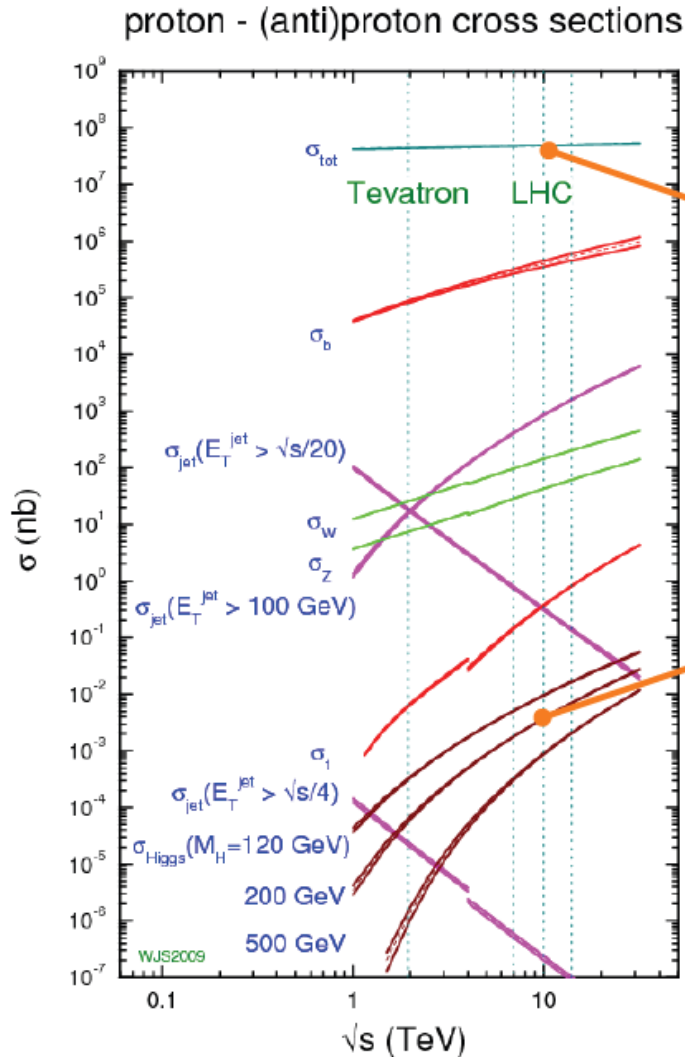
- All tunes underestimate particle density by 10%-15% in the plateau region
- There is factor of ~ 2 increase in activities between 900 GeV and 7 TeV
- In the plateau region the measured density corresponds to ~ 2.5 per unit η at 900 GeV and 5 particle at 7 TeV

Particle density angular correlations



- Define the event orientation by the azimuthal angle on the track with the highest p_T .
- MC tunes only reproduce the general features, disagreement in rates both in the transverse region (UE) and in the away region (MPI/Hard Core)

Cross-sections at LHC



10^8 events/s

$\sim 10^{10}$

10^{-2} events/s \sim

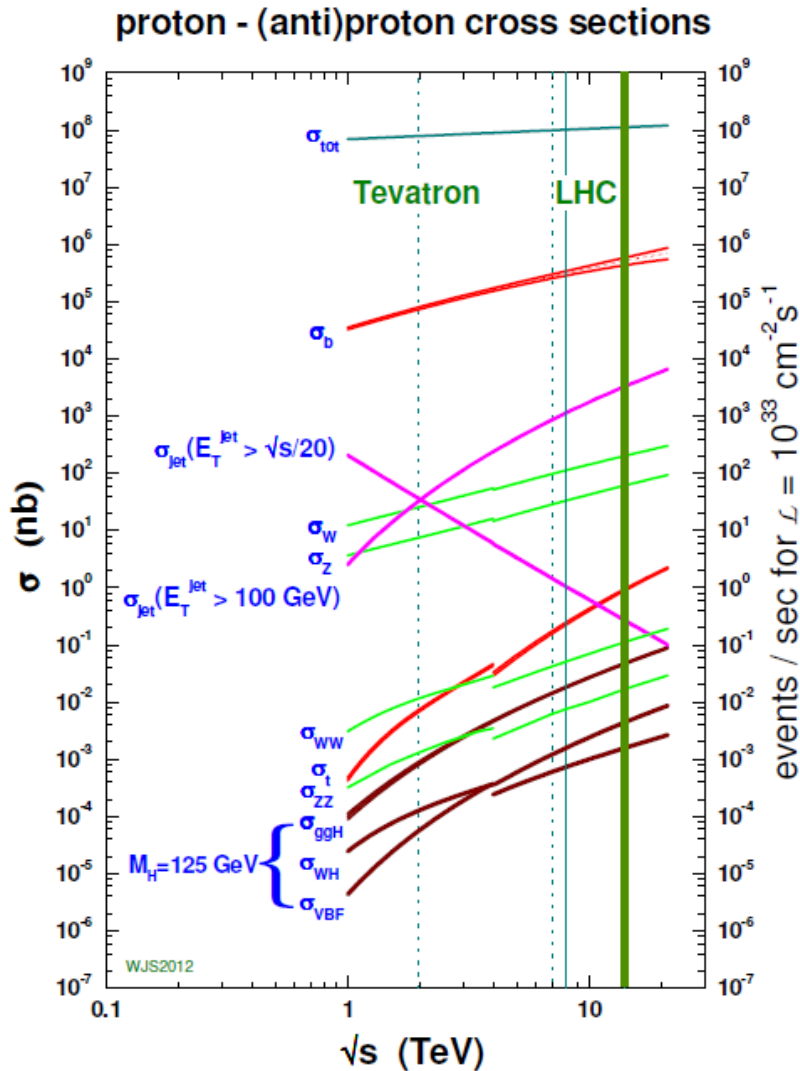
10 events/min

[$m_H \sim 120 \text{ GeV}$]

0.2% $H \rightarrow \gamma\gamma$

1.5% $H \rightarrow ZZ$

Cross-sections at LHC



- Cross sections in pp collisions at 13 TeV
 - total = 100 mb
 - inelastic = 80 mb (diffractive = 25 mb)
- b-quark pair production = 400 μb
- jet with $E_T > 100 \text{ GeV}$ = 3 μb
- W and Z bosons : 200 and 60 nb
- top quark pair = 1.0 nb
- WW = 100 pb
- H(125 GeV) = 60 pb
- ZZ = 20 pb

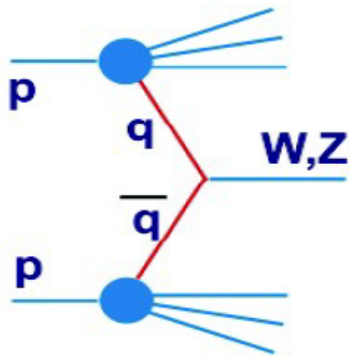
W & Z in leptonic modes

$$\sigma(pp \rightarrow W) \times (W \rightarrow \ell \nu) = 20 \text{ nb}$$

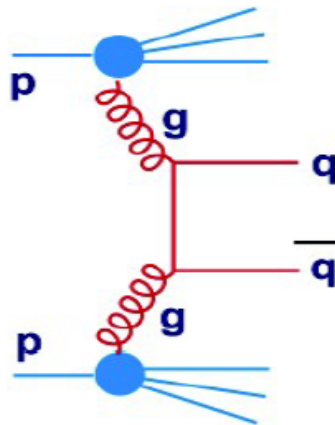
$$\sigma(pp \rightarrow Z) \times (Z \rightarrow \ell \ell) = 2 \text{ nb}$$

QCD hard scattering processes

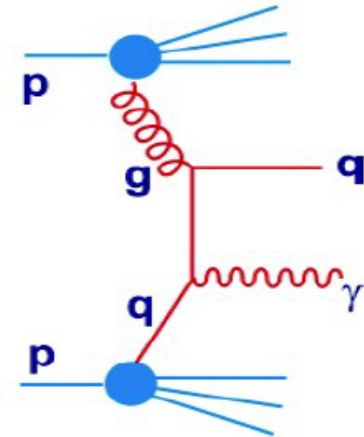
- EW gauge bosons



- Di-jets



- Direct photons



- Measuring those processes test our understanding of:

- Partonic structure of protons
- QCD scattering via calculations of N(NLO)
- Hadronisation/underlying event
- What makes a good jet algorithm
- Data driven background estimates for rare processes

Parton kinematics

Example of the **Drell-Yan** process

- lepton pair production via **quark-antiquark annihilation**

4-momentum of lepton pair (LO)

$$\begin{cases} E = (x_1 + x_2)\sqrt{s}/2 \\ p_z = (x_1 - x_2)\sqrt{s}/2 \end{cases}$$

$$Q^2 = E^2 - p_z^2 = x_1 x_2 s$$

Define “**rapidity**” y such that

$$\frac{x_1}{x_2} = \frac{E + p_z}{E - p_z} \equiv e^{2y}$$

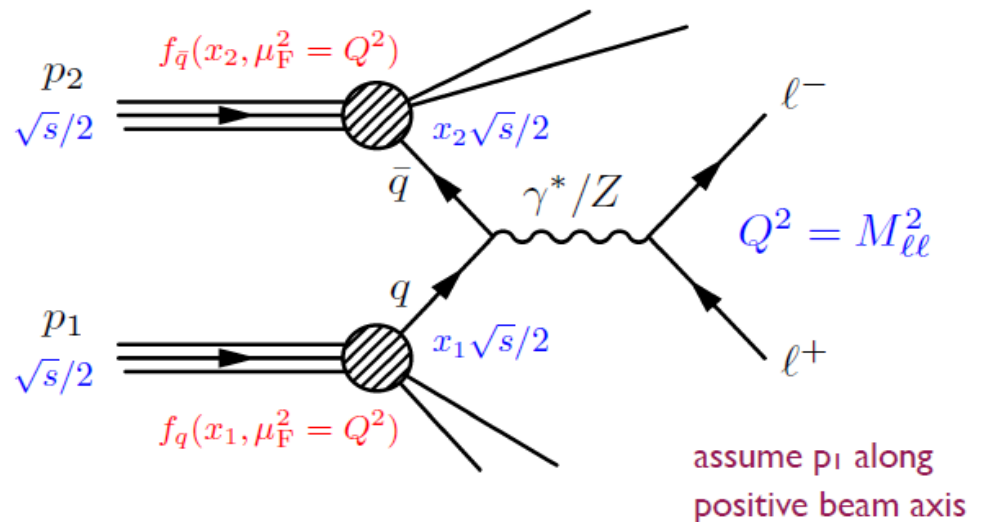
$$\begin{aligned} x_1 x_2 &= Q^2/s \\ x_1/x_2 &= e^{2y} \end{aligned}$$



$$x_{1,2} = \frac{Q}{\sqrt{s}} e^{\pm y}$$

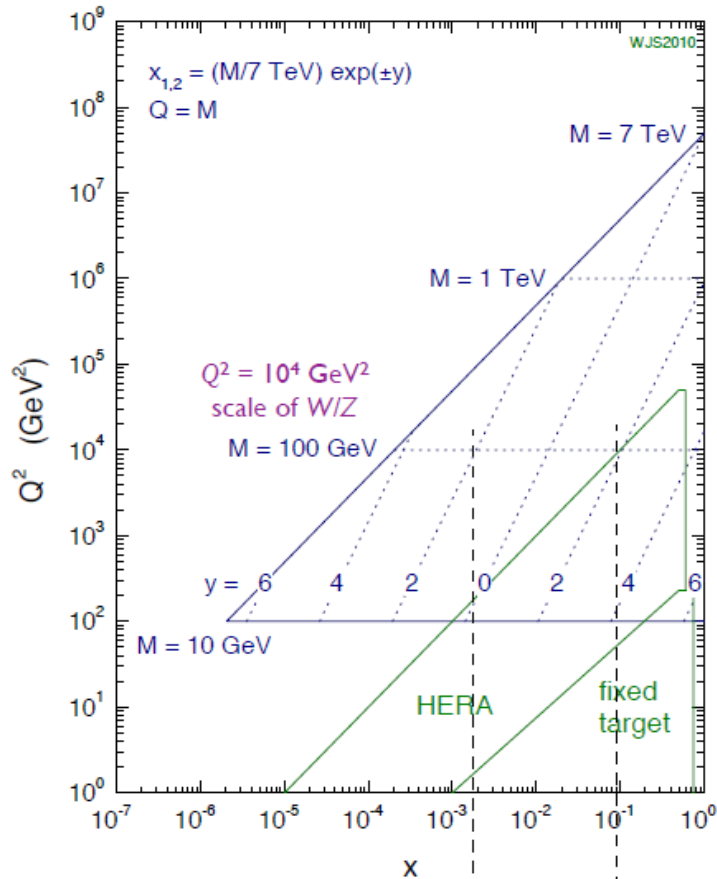
for a given Q^2 ,
the **rapidity** y relates
the x_1 and x_2 of the two partons

$$q(x_1) + \bar{q}(x_2) \rightarrow \gamma^*/Z \rightarrow \ell^+ \ell^-$$

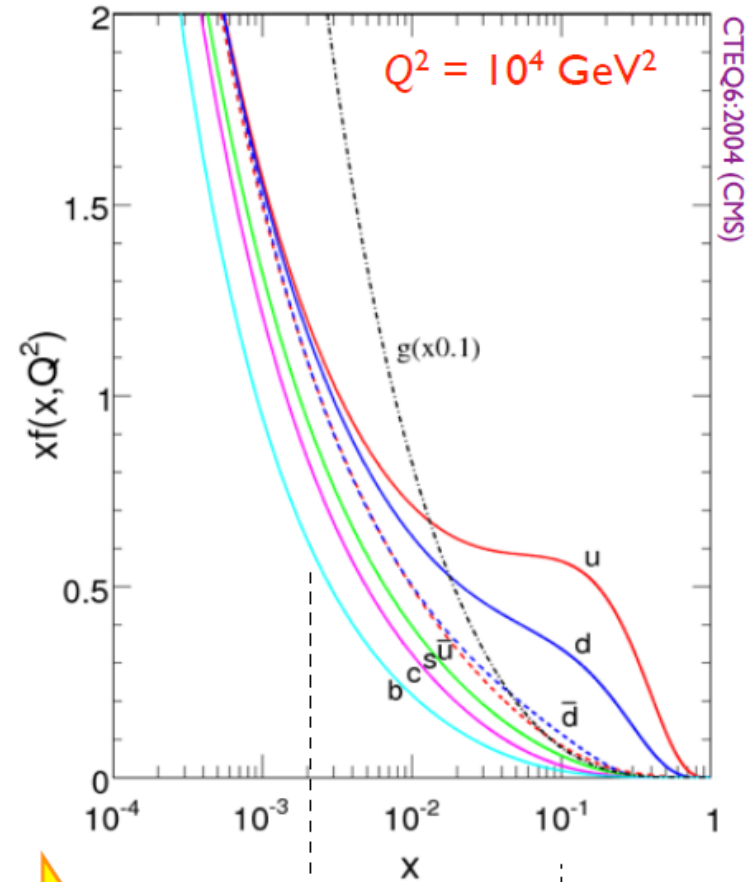


Parton kinematics

7 TeV LHC parton kinematics



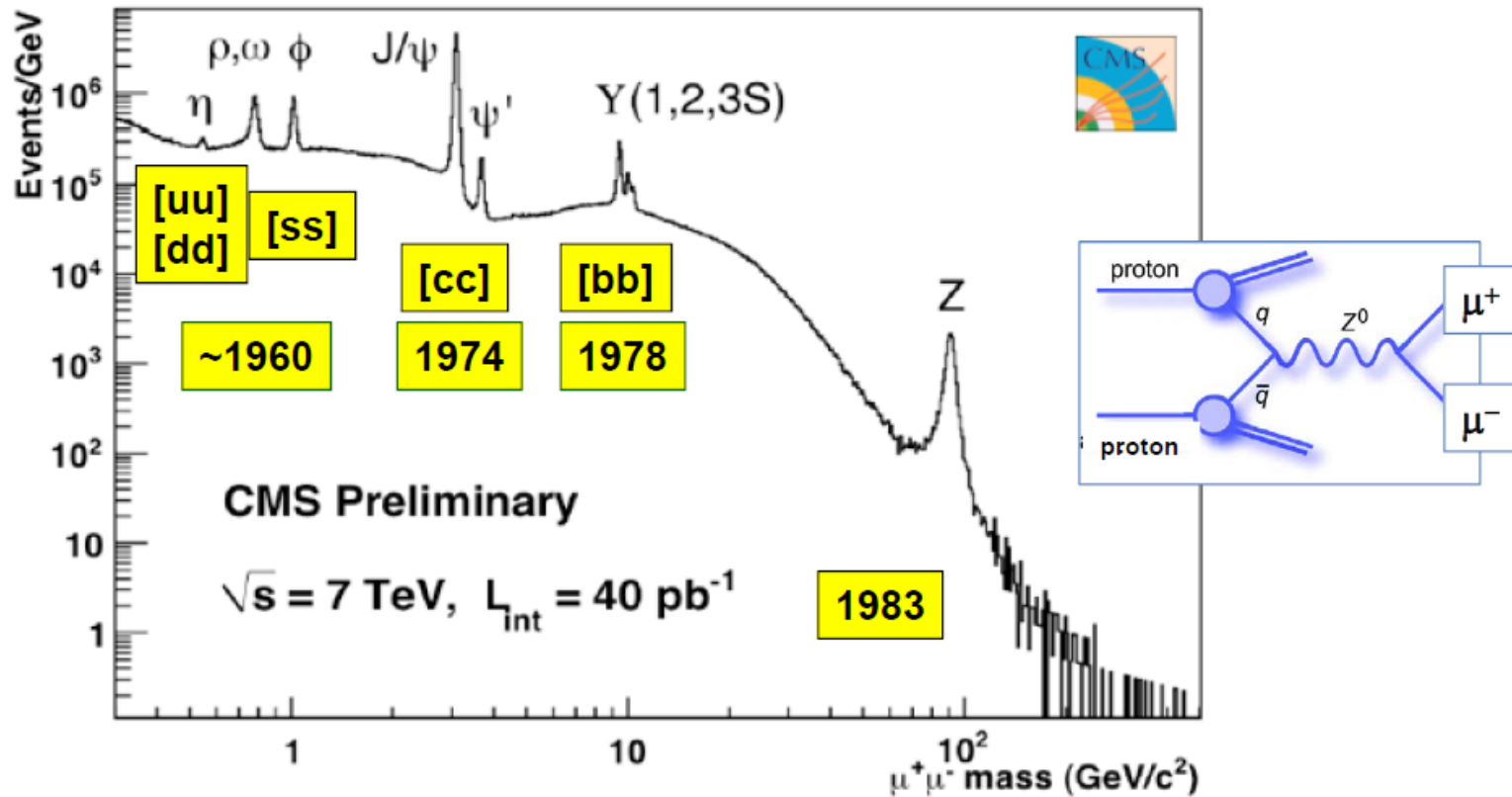
range in x for the central production ($|y| < 2$) of W/Z boson



Year 2010: Retracing history of particle physics

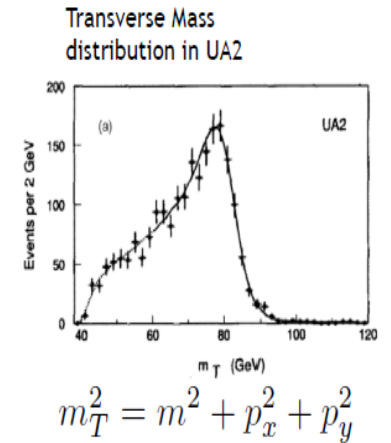
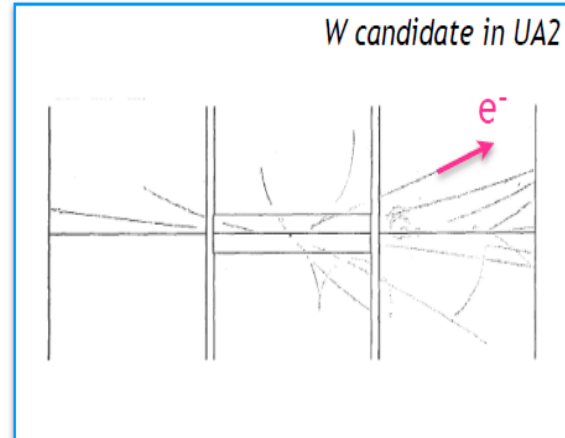
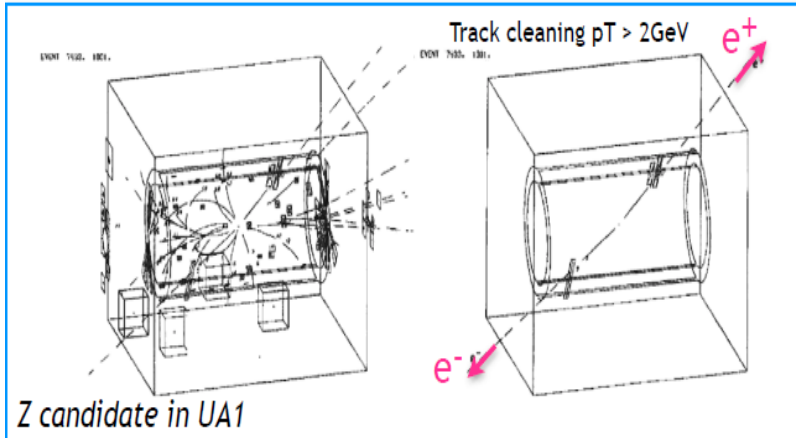
2010

Data corresponding to $\sim 40 \text{ pb}^{-1}$ collected
→ re-discovery of the Standard Model



The di-muon spectrum recalls a long period of particle physics:
Well known quark-antiquark resonances (bound states) appear “online”

The discovery of the W and Z bosons at CERN SppS



Altogether $O(100)$ Z events.

Already important measurements (examples):

$$M_Z = 91.5 \pm 1.2 \pm 1.7 \text{ (GeV)} \quad \text{(UA1)}$$

$$M_W = 81.0 \pm 0.8 \pm 1.3 \text{ (GeV)} \quad \text{(UA2)}$$

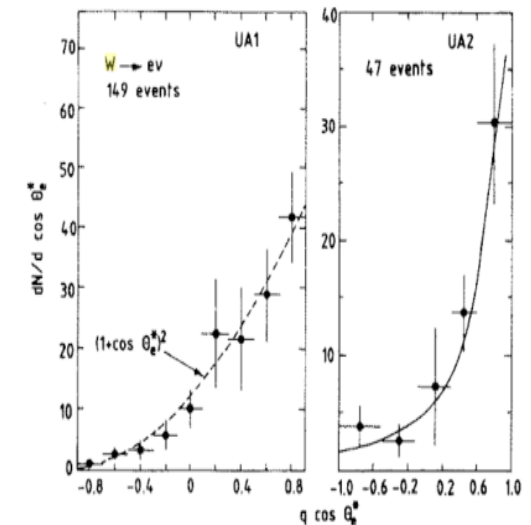
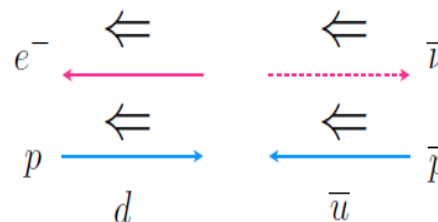
$$\rho = 1.004 \pm 0.052 \quad \text{(UA1)}$$

$$\sin^2 \theta_W = 0.226 \pm 0.014 \quad \text{(UA1)}$$

Altogether $O(1000)$ W events

At SppS W production dominated by valence quarks

W polarised in the anti-proton direction.

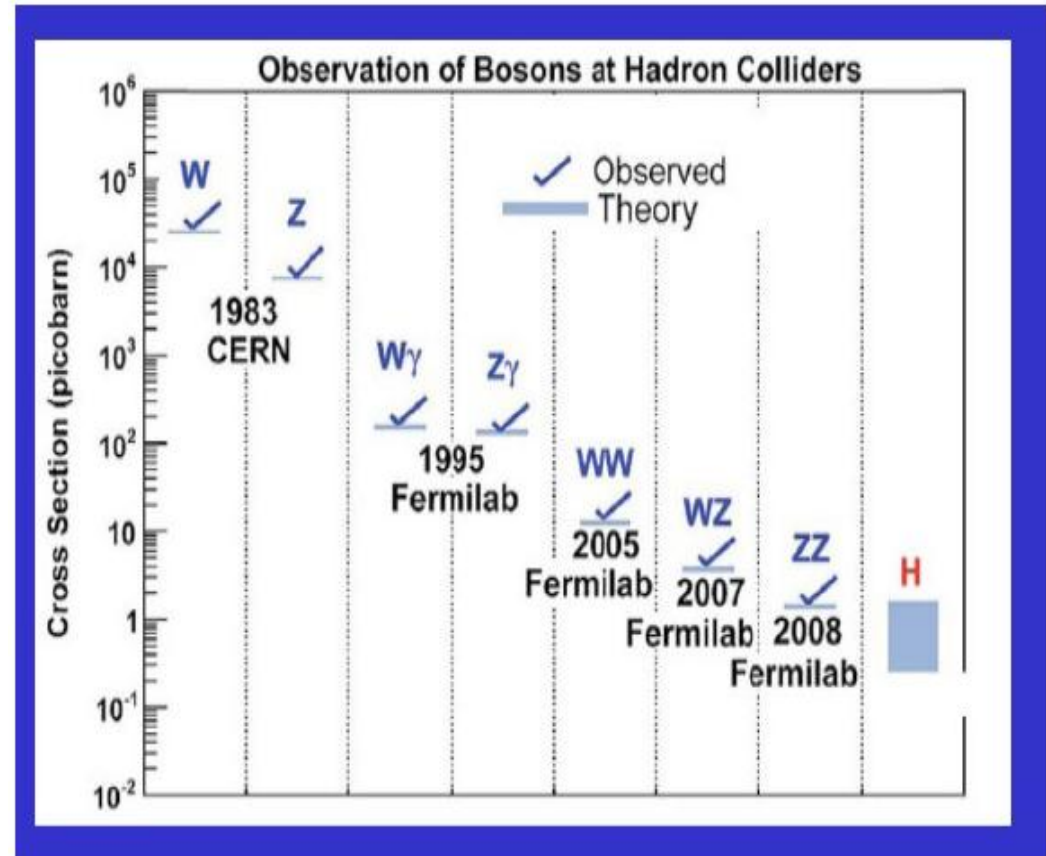


Bosons at hadron colliders

2010

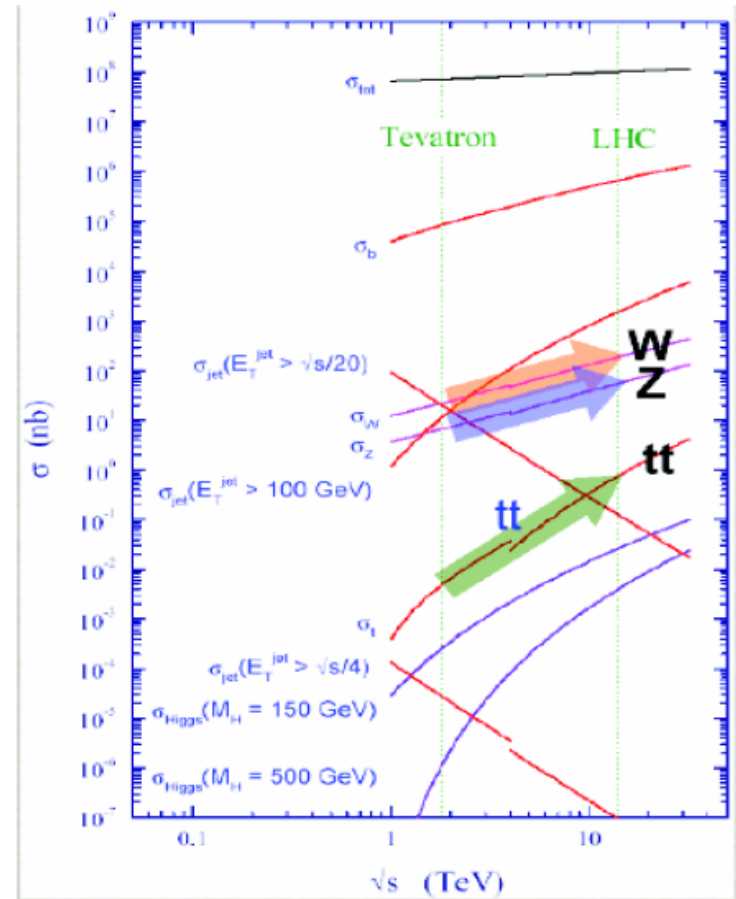
The primary decay channel is through leptonic decays:

- $BR(W \rightarrow e \nu) \sim 10\%$
- $BR(Z \rightarrow ee) \sim 3\%$
- It means that we are probing $\sigma \times BR$ values orders of magnitude smaller
- At LHC cross-section 5-10 x higher than at Tevatron at Fermilab.

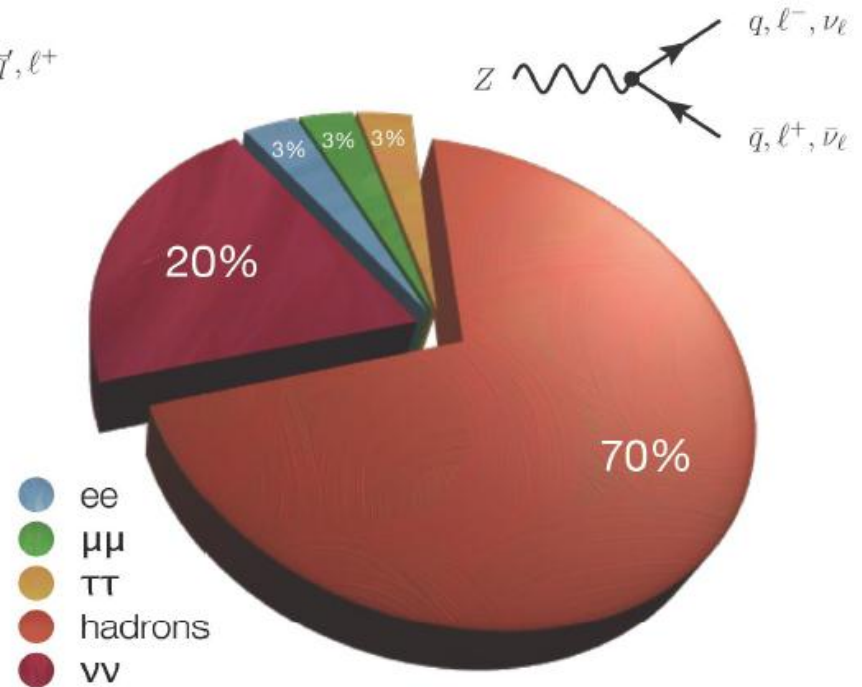
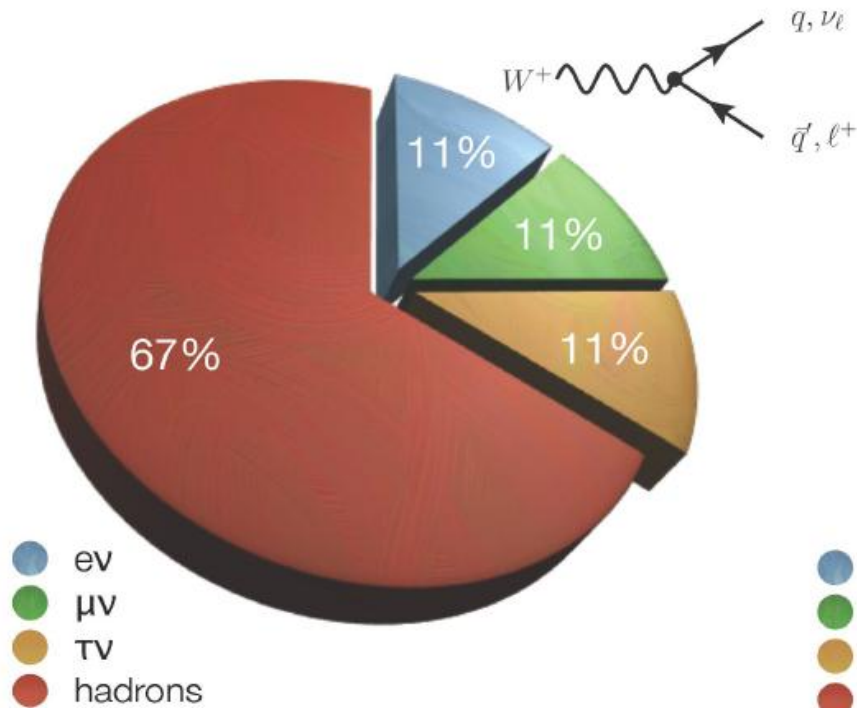


Bosons and top quark at LHC

- Well measured by previous experiments
- Still educational at LHC
 - Cross-sections
 - New PDF constraints
- „Standard candles” for high p_T analyses
 - Calibration, alignment
 - Independent luminosity measurements

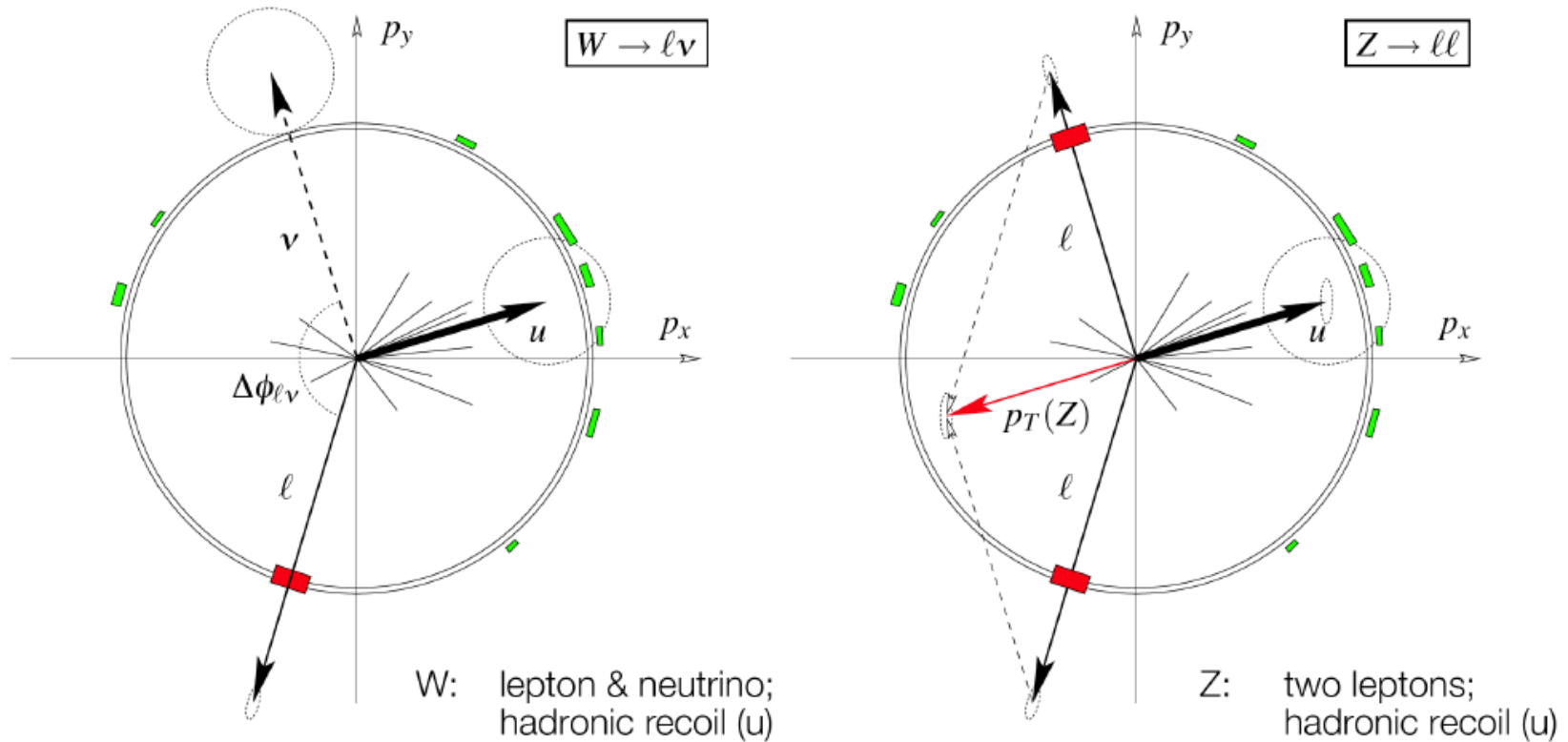


W and Z boson decays



Leptonic decays (e/μ): very clean, but small(ish) branching fractions
 Hadronic decays: two-jet final states; large QCD dijet background
 Tau decays: somewhere in between...

W and Z boson signatures



Additional hadronic activity \rightarrow recoil, not as clean as e^+e^-
Precision measurements: only leptonic decays

Lepton identification

- **Electron:**

- Compact electromagnetic cluster in calorimeter
- Matched to track

- **Muons:**

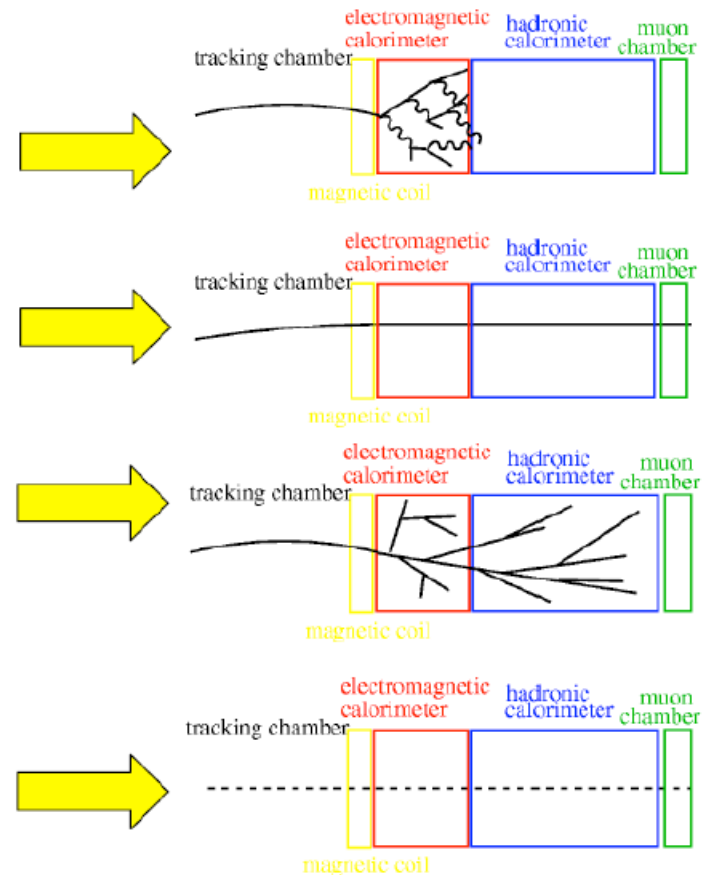
- Track in the muon chambers
- Matched to track

- **Taus:**

- Narrow jet
- Matched to one or three tracks

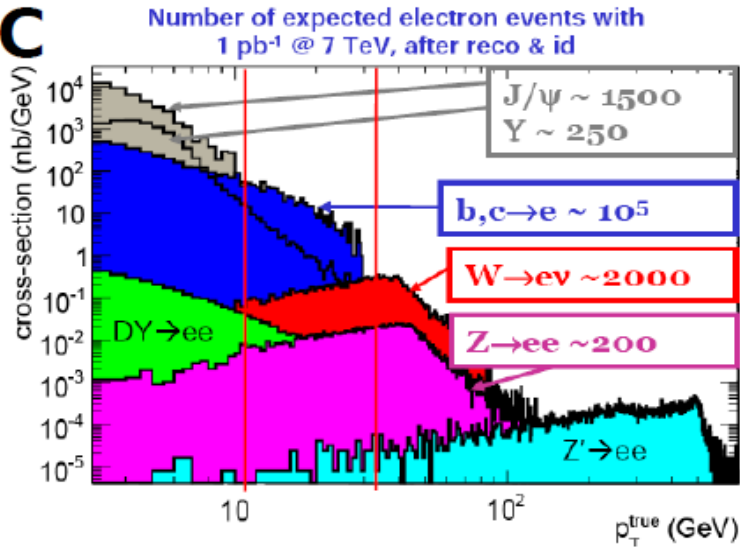
- **Neutrinos**

- Imbalance in transverse momentum
- Inferred from total transverse energy in detector



Electrons and jets

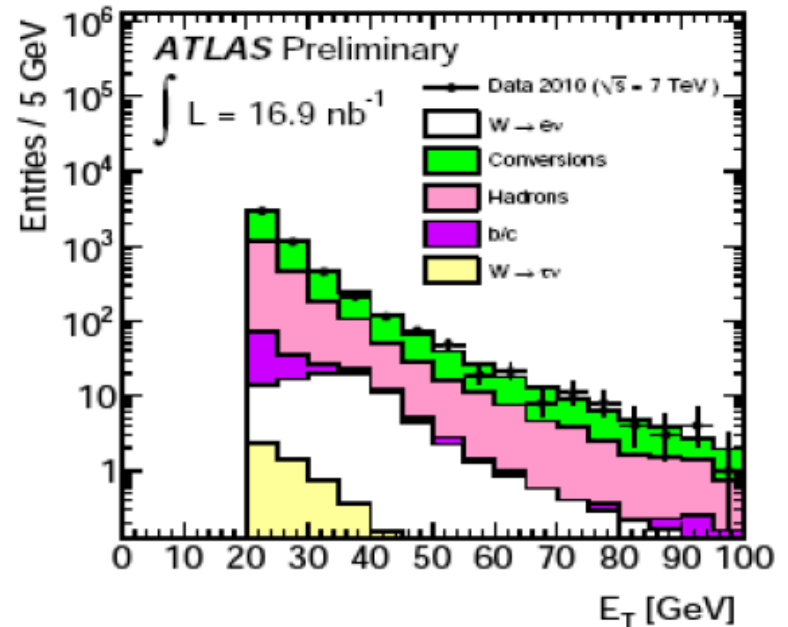
MC



- There is also lot of true electrons from semileptonic decays inside jets

- Jets can look like electrons
 - Photon conversion from π^0 's
 - Early showering charged pions
- And there is lot of jets
- Difficult to model in Monte Carlo
 - Detailed simulation in tracking and calorimeter volume

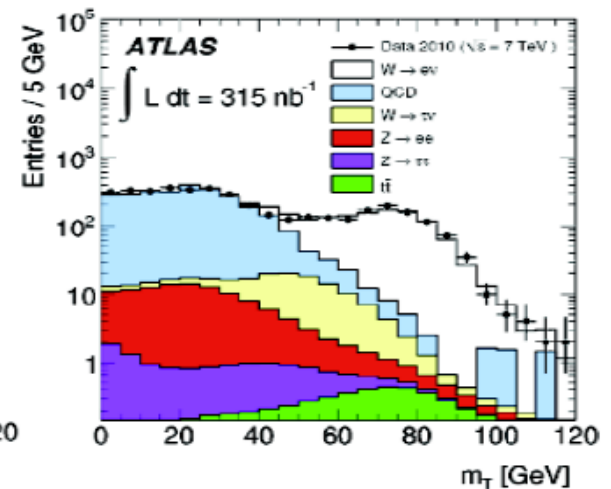
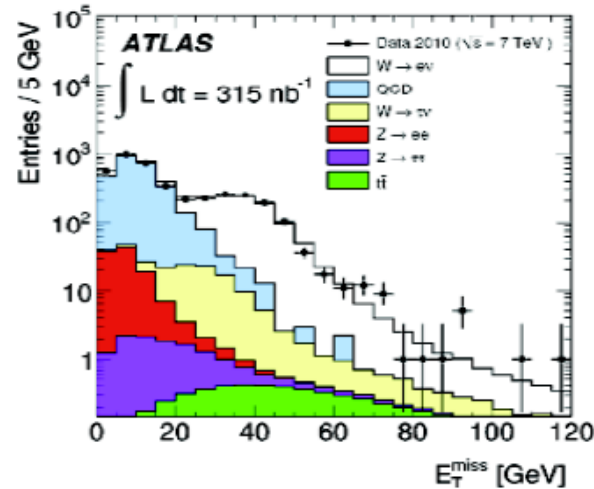
DATA: loose electron ID



W selection (2010)

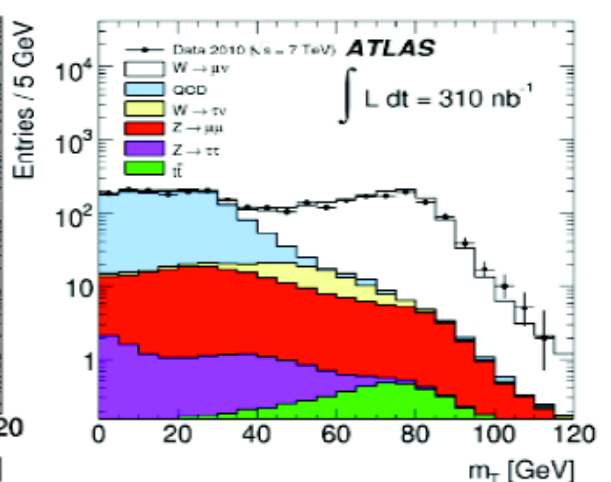
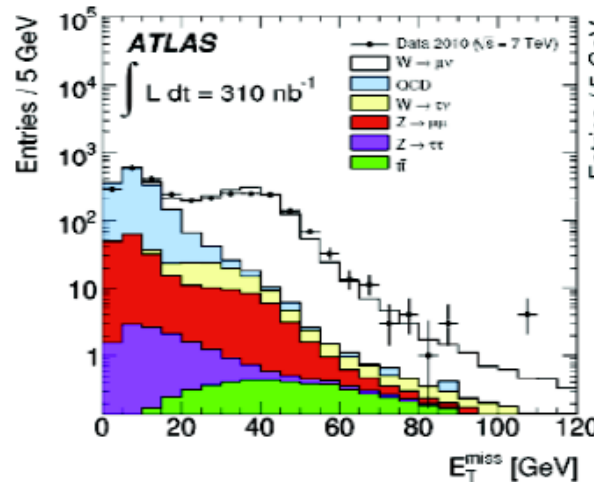
Electrons:

- $E_T > 20 \text{ GeV}$
- Tight ID
- Missing $E_T > 25 \text{ GeV}$
- $m_T > 40 \text{ GeV}$
- 1069 Candidates



Muons:

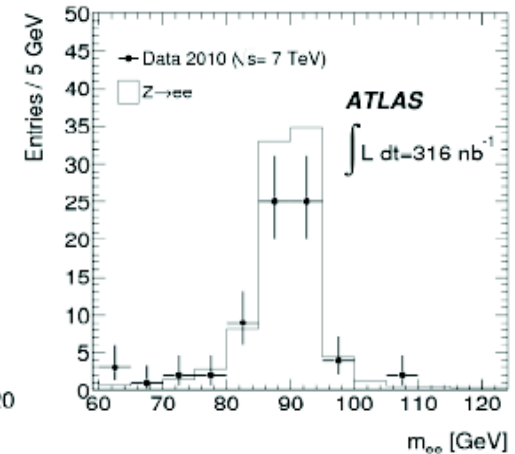
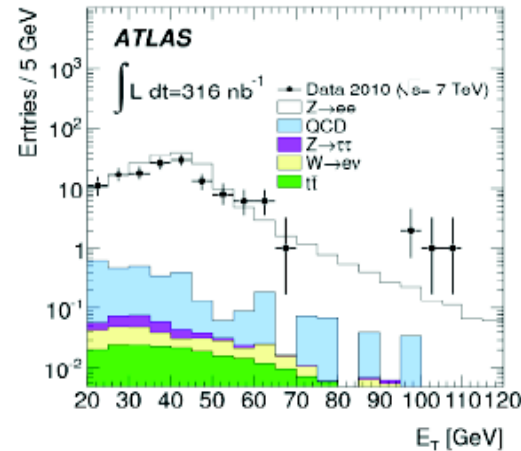
- $p_T > 20 \text{ GeV}$
- Track isolation
- Missing $E_T > 25 \text{ GeV}$
- $m_T > 40 \text{ GeV}$
- 1181 Candidates



Z selection (2010)

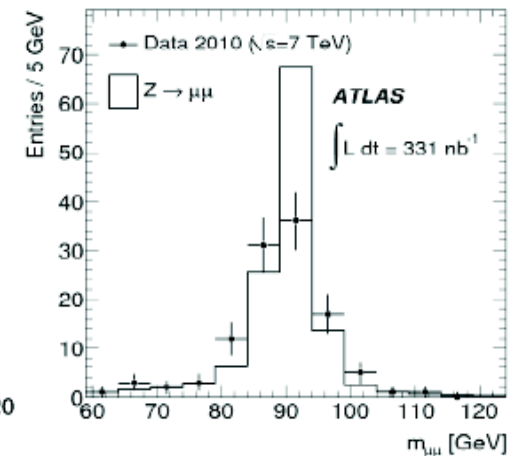
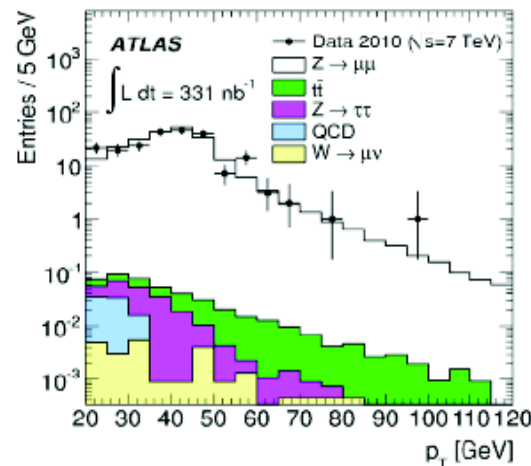
2 Electrons :

- $E_T > 20 \text{ GeV}$
- *Opposite charge*
- *Medium ID*
- $66 < m_{ee} < 116 \text{ GeV}$
- *70 Candidates*



2 Muons :

- $p_T > 20 \text{ GeV}$
- *Track isolation*
- *Opposite charge*
- $66 < m_{\mu\mu} < 116 \text{ GeV}$
- *109 Candidates*



W backgrounds

Electrons:

- EW + top background: $W \rightarrow \tau \nu + Z \rightarrow e^+e^- + t\bar{t}$

$$N_{EW+TOP} = 33.5 \pm 0.2(\text{stat}) \pm 3.0(\text{syst})$$

- QCD background is estimated with the template method using the missing energy distribution.

$$N_{QCD} = 28.0 \pm 3.0(\text{stat}) \pm 10.0(\text{syst})$$

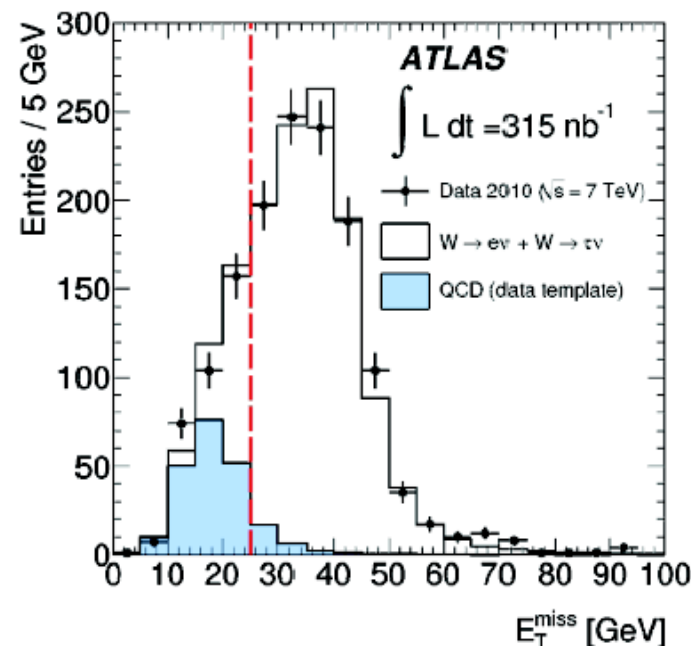
Muons:

- EW + top background: $Z \rightarrow \mu^+\mu^- + W \rightarrow \tau \nu + t\bar{t}$

$$N_{EW+TOP} = 77.6 \pm 0.3(\text{stat}) \pm 5.4(\text{syst})$$

- QCD background estimated from comparison of events seen in data after the full selection to number of events observed if the isolation is not applied.

$$N_{QCD} = 22.8 \pm 4.6(\text{stat}) \pm 8.7(\text{syst})$$



$$N_{loose} = N_{nonQCD} + N_{QCD}$$
$$N_{iso} = \epsilon_{nonQCD}^{iso} N_{nonQCD} + \epsilon_{QCD}^{iso} N_{QCD}$$

Cross-section & Luminosity

Number of observed events

just count ...

Background

measured from data or
calculated from theory

$$\sigma = \frac{N^{\text{obs}} - N^{\text{bkg}}}{\int \mathcal{L} dt \cdot \epsilon}$$

Luminosity

determined by accelerator,
triggers, ...

Efficiency

many factors, optimized
by experimentalist

W cross-section measurement

The total cross section for each lepton channel can be obtained by:

$$\sigma_W \times BR(W \rightarrow l\nu) = \frac{N_W^{obs} - N^{bkg}}{A_W C_W L_{int}}$$

A_W is the geometrical acceptance calculated at generator level:

$$A_W = \left(\frac{N^{acc}}{N^{all}} \right)_{gen}$$

MC	A_W $W^+ \rightarrow e^+\nu$	A_W $W^- \rightarrow e^-\nu$	A_W $W \rightarrow e\nu$	A_W $W^+ \rightarrow \mu^+\nu$	A_W $W^- \rightarrow \mu^-\nu$	A_W $W \rightarrow \mu\nu$
PYTHIA MRST LO*	0.466	0.457	0.462	0.484	0.475	0.480
PYTHIA CTEQ6.6	0.479	0.458	0.471	0.499	0.477	0.490
PYTHIA HERAPDF1.0	0.477	0.461	0.470	0.496	0.479	0.489
MC@NLO HERAPDF1.0	0.475	0.454	0.465	0.494	0.472	0.483
MC@NLO CTEQ6.6	0.478	0.452	0.465	0.496	0.470	0.483

W cross-section measurement

The total cross section for each lepton channel can be obtained by:

$$\sigma_W \times BR(W \rightarrow l\nu) = \frac{N_W^{obs} - N^{bkg}}{A_W C_W L_{int}}$$

A_W is the geometrical acceptance calculated at generator level:

$$A_W = \left(\frac{N^{acc}}{N^{all}} \right)_{gen}$$

MC	A_W $W^+ \rightarrow e^+\nu$	A_W $W^- \rightarrow e^-\nu$	A_W $W \rightarrow e\nu$	A_W $W^+ \rightarrow \mu^+\nu$	A_W $W^- \rightarrow \mu^-\nu$	A_W $W \rightarrow \mu\nu$
PYTHIA MRST LO*	0.466	0.457	0.462	0.484	0.475	0.480
PYTHIA CTEQ6.6	0.479	0.458	0.471	0.499	0.477	0.490
PYTHIA HERAPDF1.0	0.477	0.461	0.470	0.496	0.479	0.489
MC@NLO HERAPDF1.0	0.475	0.454	0.465	0.494	0.472	0.483
MC@NLO CTEQ6.6	0.478	0.452	0.465	0.496	0.470	0.483

C_W correction factor and uncertainties

$$\sigma_W \times BR(W \rightarrow l\nu) = \frac{N_W^{obs} - N^{bkg}}{A_W C_W L_{int}}$$

- C_W is a factor correcting for reconstruction, identification and trigger efficiencies of the lepton.

	$W \rightarrow e\nu$	$W \rightarrow \mu\nu$
C_W	0.66	0.76

- Components to systematic uncertainties, are summarized below:

Parameter	$\delta C_W / C_W (\%)$
Trigger efficiency	<0.2
Material effects, reconstruction and identification	5.6
Energy scale and resolution	3.3
E_T^{miss} scale and resolution	2.0
Problematic regions in the calorimeter	1.4
Pile-up	0.5
Charge misidentification	0.5
FSR modelling	0.3
Theoretical uncertainty (PDFs)	0.3
Total uncertainty	7.0

Electrons

Parameter	$\delta C_W / C_W (\%)$
Trigger efficiency	1.9
Reconstruction efficiency	2.5
Momentum scale	1.2
Momentum resolution	0.2
E_T^{miss} scale and resolution	2.0
Isolation efficiency	1.0
Theoretical uncertainty (PDFs)	0.3
Total uncertainty	4.0

Muons

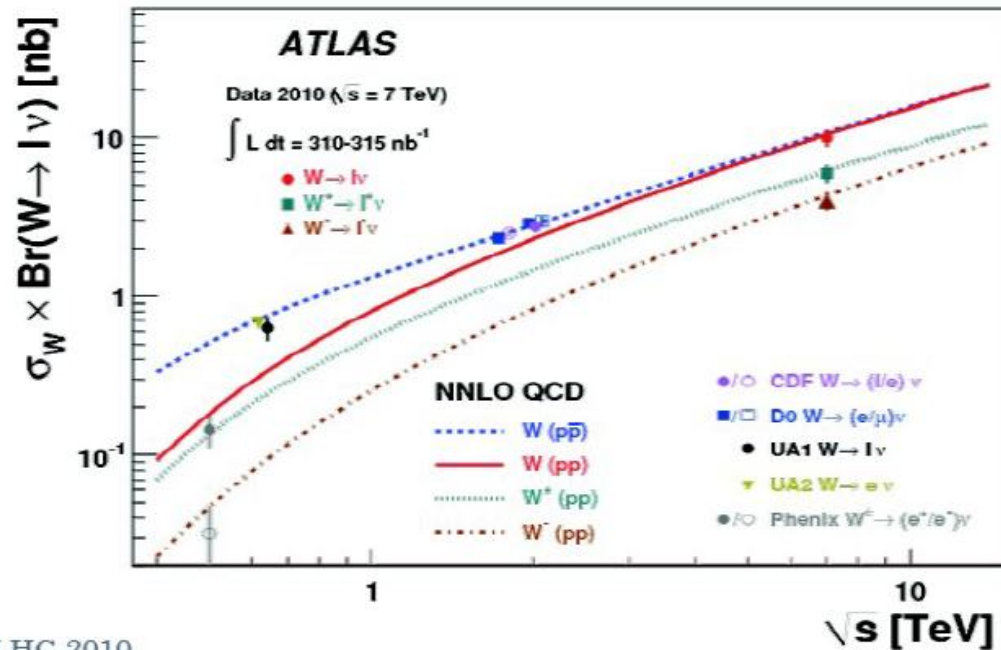
W cross-section measurement

$$L \approx 310 - 315 \text{ nb}^{-1}$$

Theory prediction : $10.46 \pm 0.42 \text{ nb}$

$$\sigma_W \times BR(W \rightarrow e\nu) = [10.51 \pm 0.34(\text{stat}) \pm 0.81(\text{sys}) \pm 1.16(\text{lumi})] \text{ nb}$$

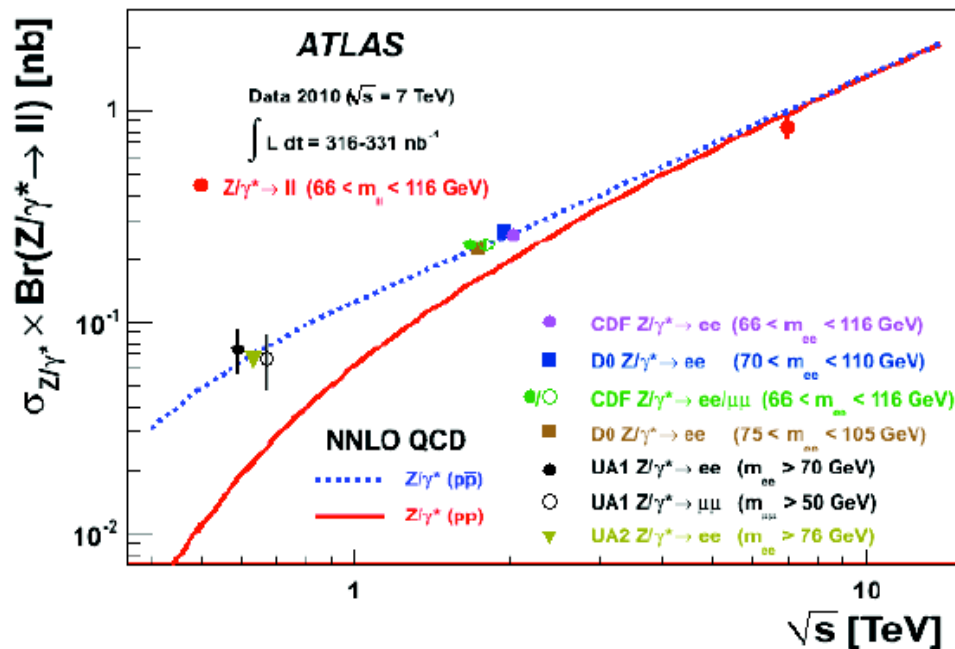
$$\sigma_W \times BR(W \rightarrow \mu\nu) = [9.58 \pm 0.30(\text{stat}) \pm 0.50(\text{sys}) \pm 1.05(\text{lumi})] \text{ nb}$$



Z cross-section measurement

$$L \approx 310 - 315 \text{ nb}^{-1}$$

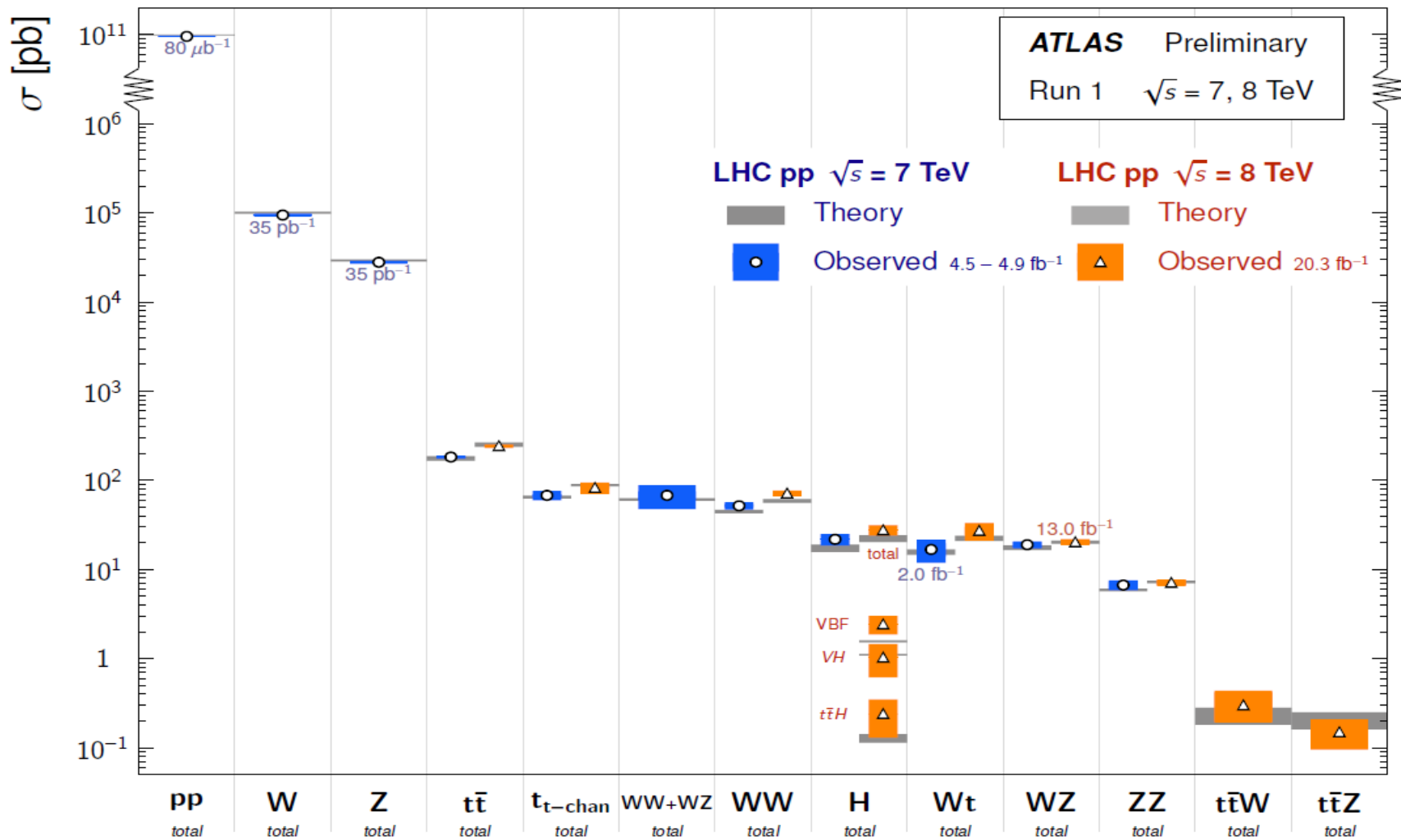
Theory prediction : $0.96 \pm 0.04 \text{ nb}$ for $[66 - 116] \text{ GeV}$ mass window
 $\sigma_Z \times BR(Z \rightarrow e^+e^-) = [0.75 \pm 0.09(\text{stat}) \pm 0.08(\text{sys}) \pm 0.08(\text{lumi})] \text{ nb}$
 $\sigma_Z \times BR(Z \rightarrow \mu^+\mu^-) = [0.87 \pm 0.08(\text{stat}) \pm 0.06(\text{sys}) \pm 0.10(\text{lumi})] \text{ nb}$



Production cross-sections

Standard Model Total Production Cross Section Measurements

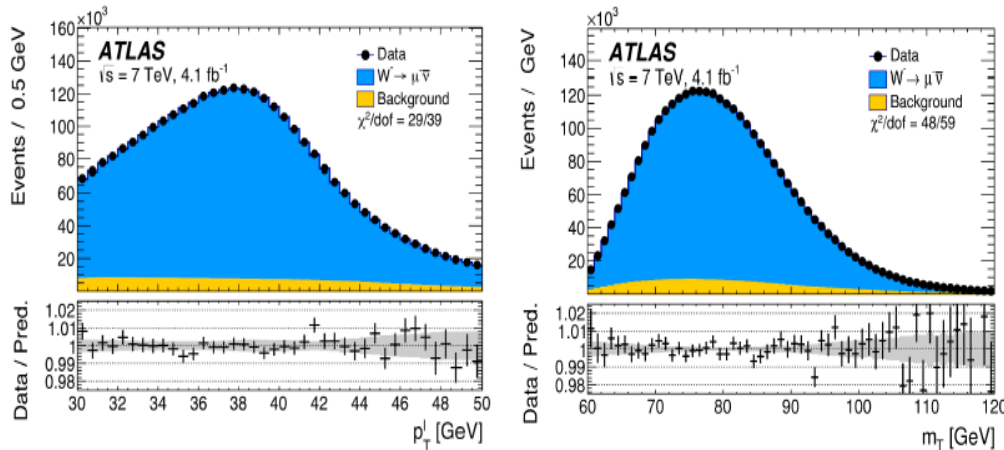
Status: March 2015



Measurement of the M_W at the LHC

A Milestone measurement!

Analysis strategy based on two kinematic distributions fitted in several categories



$$p_T^\ell$$

Clean energy measurement, but more sensitive to the modelling of the W transverse momentum

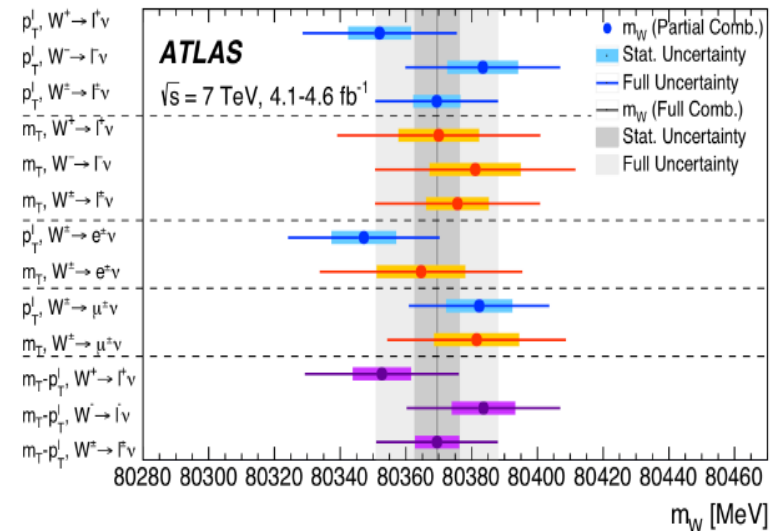
$$m_T$$

Less sensitive to modelling but more difficult from to reconstruct (based on the missing transverse energy).

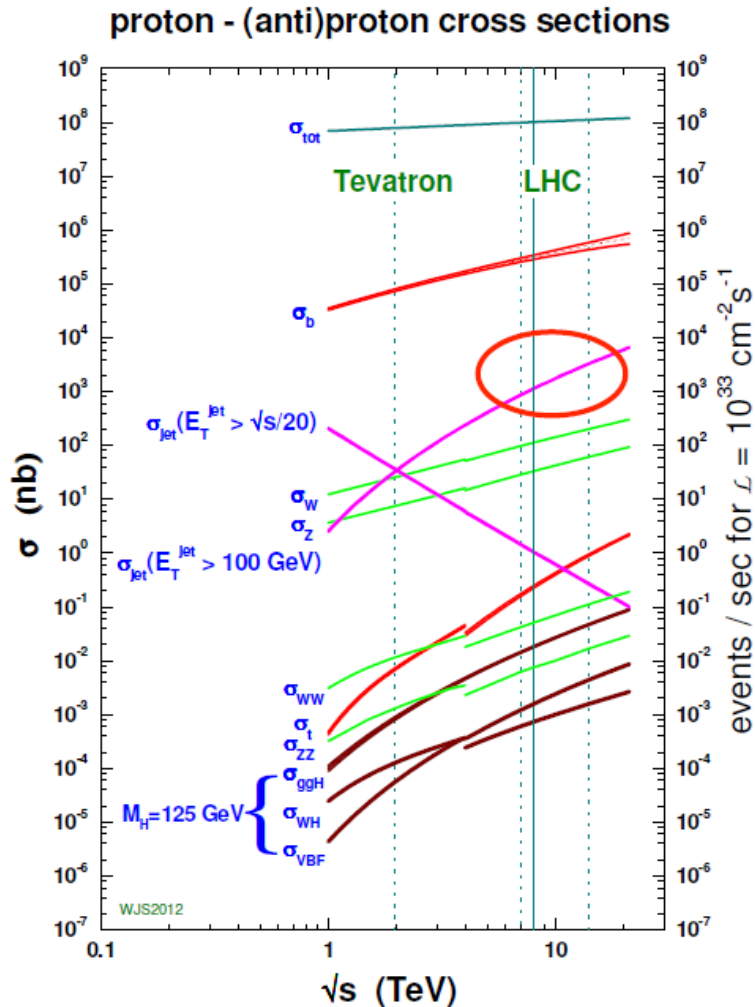
$$m_T = \sqrt{2p_T^\ell p_T^{miss} (1 - \cos\Delta\phi)}$$

Categories are defined by the charge of the reconstructed lepton, its flavor (electron or muon) and its pseudo rapidity.

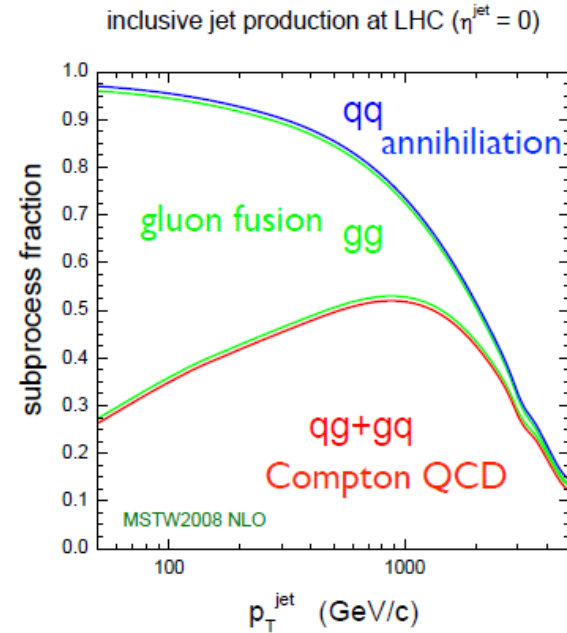
$$m_W = 80369.5 \pm 18.5 \text{ MeV} \\ (\pm 6.8 \text{ (Stat)}) \\ \pm 10.6 \text{ (Exp. Sys.)} \\ \pm 13.6 \text{ (Mod. Sys.) MeV}$$



Jet physics



99% of events at the LHC contain at least one jet with $E_T^{\text{jet}} > 20 \text{ GeV}$



- Understand quark-gluon content of proton up to highest energies
- Perform Rutherford analysis at quark level and constrain quark compositeness

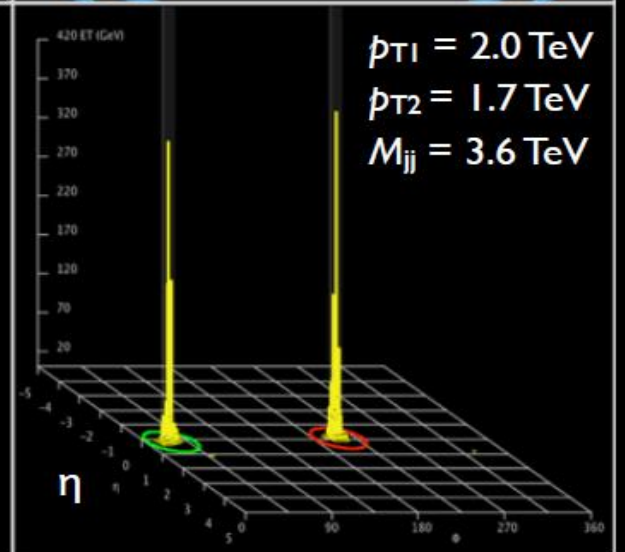
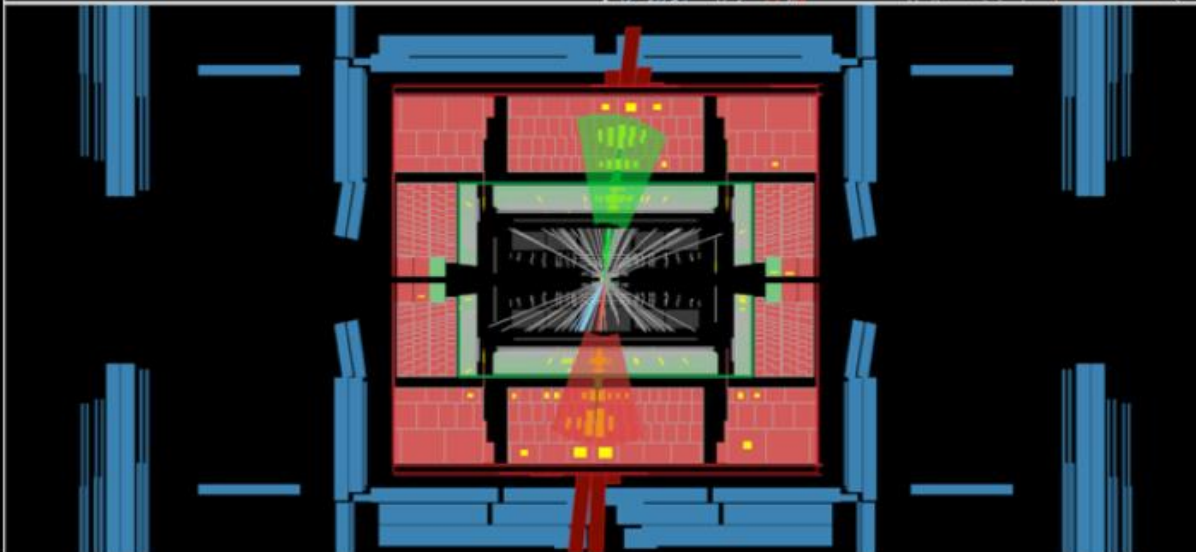
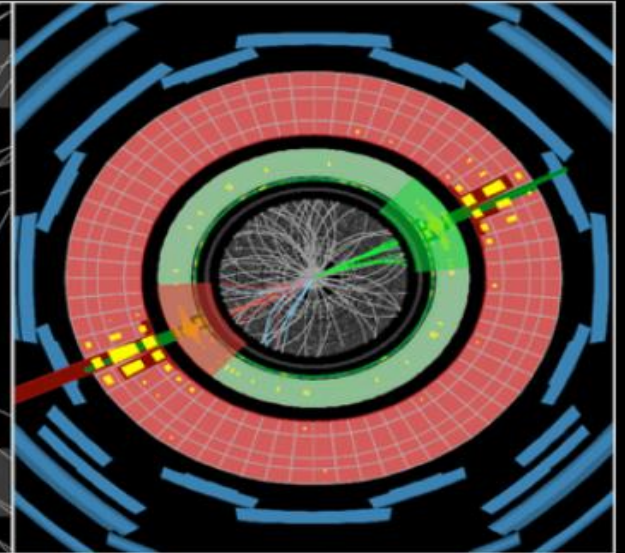
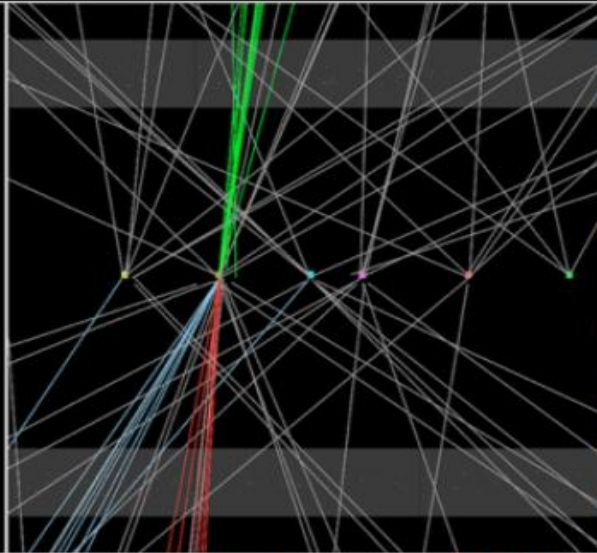
Confinement, hadronisation, jets...



ATLAS
EXPERIMENT

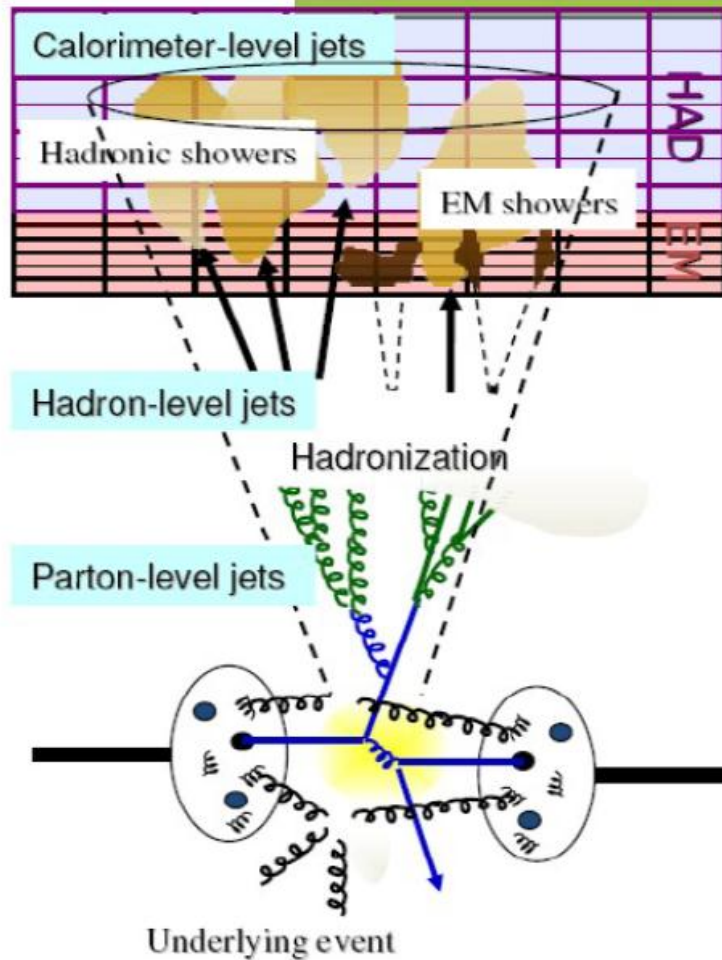
Run Number: 201006, Event Number: 55422459

Date: 2012-04-09 14:07:47 UTC



ϕ

Inclusive jet production



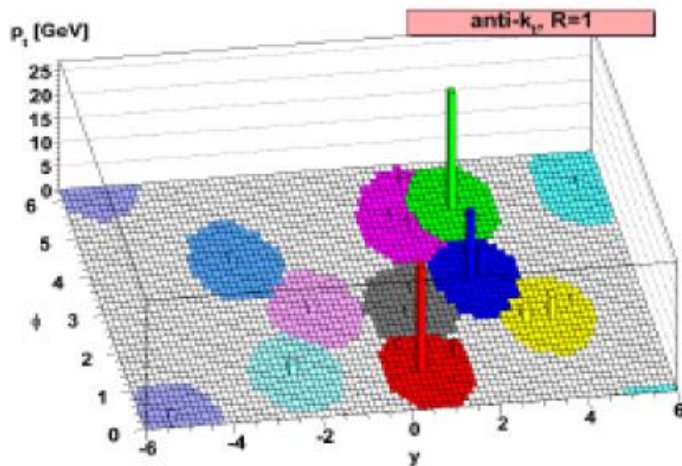
Unfold measurements to the hadron (particle) level

Correct parton-level theory for non-perturbative effects (hadronization & underlying event)

Jets are collimated spray of particles originating from parton fragmentation.
→ To be defined by an algorithm

Jet reconstruction

- Jet finding: from partons/particles/energy deposits to jet

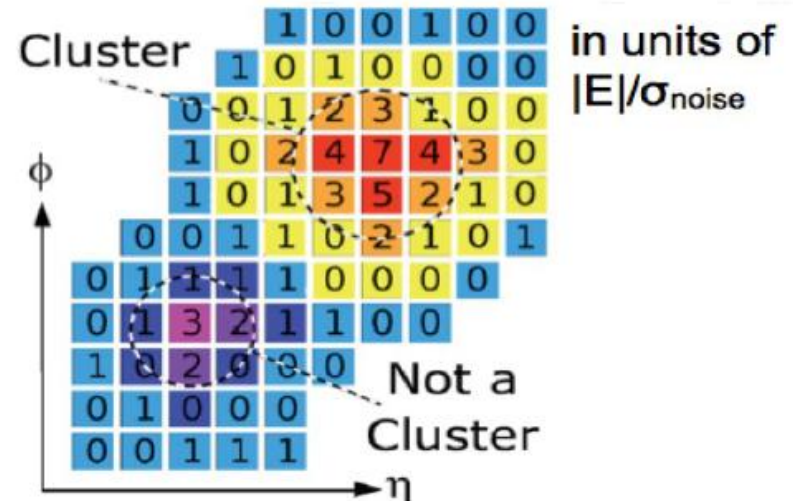


[Cacciari, Salam, Soyez
JHEP 0804:063,2008]

Energy deposits \rightarrow noise-suppressed **3D clusters**:
exploit transverse and longitudinal calorimeter segmentation

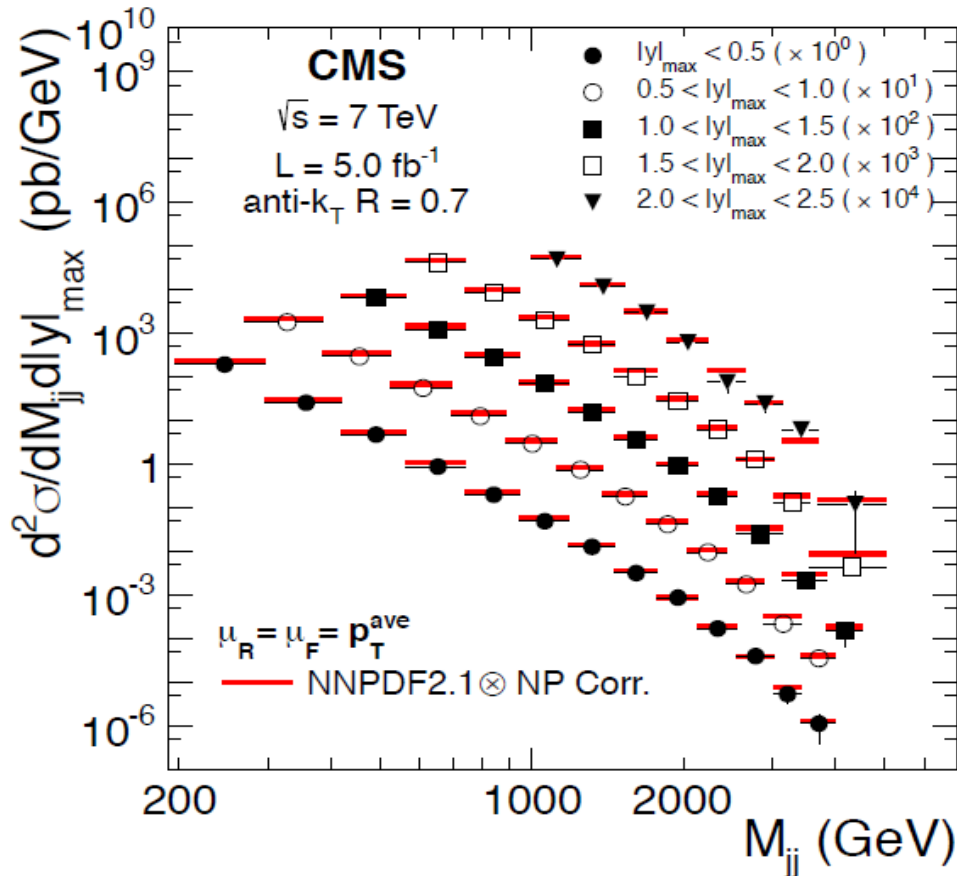
Jet inputs clustered with **anti- k_T** algorithm:

- Infrared safe, collinear safe (\Rightarrow NLO comparisons)
- Regular, cone-like jets in calorimeters
- Distance parameter 0.4, 0.6



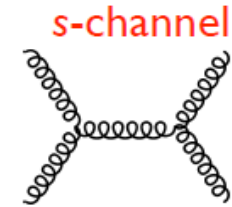
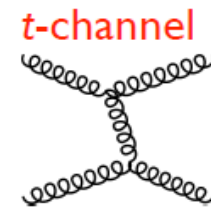
Di-jet cross-section

As a function of di-jet invariant mass
in bins of rapidity (up to $y_{\max} = 2.5$)

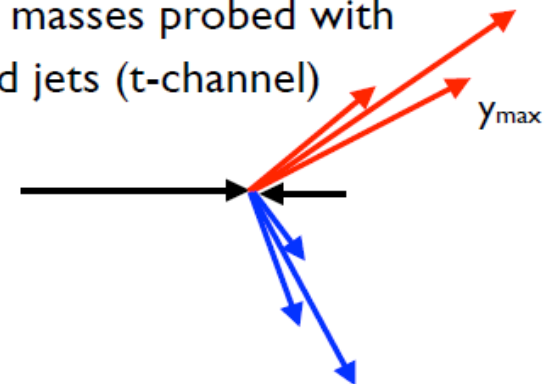


Excellent agreement
between NLO theory
prediction and data over
eight orders of magnitude

Probing di-jet masses up to 4 TeV



Higher masses probed with
forward jets (*t*-channel)



2 → 2 process

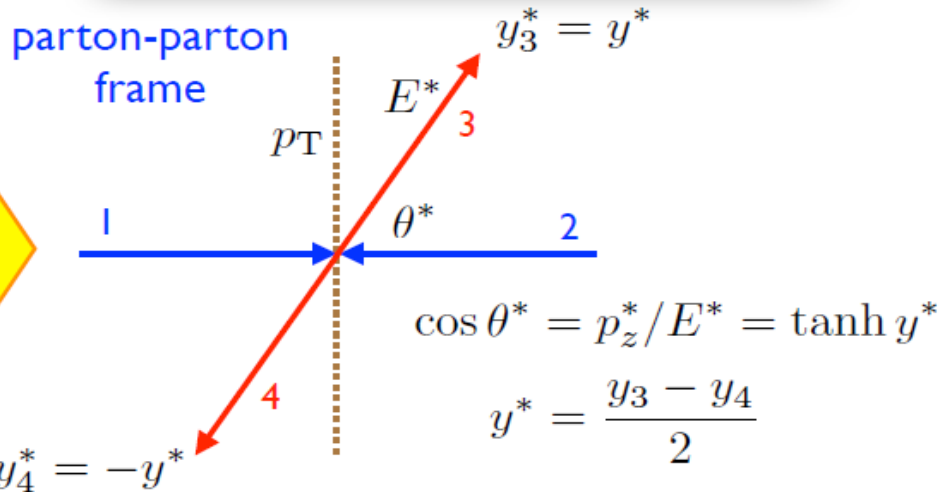
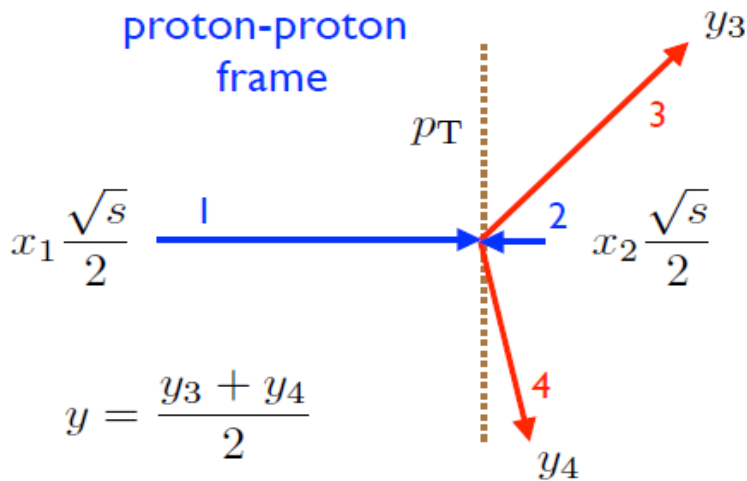
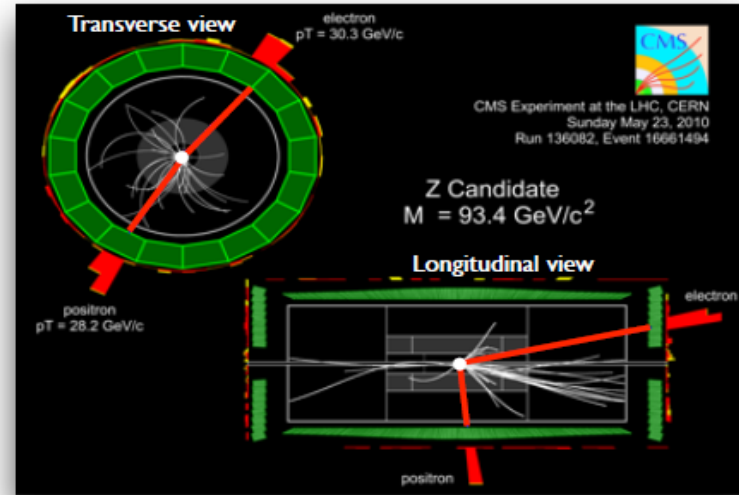
$$p_1 + p_2 \rightarrow p_3 + p_4$$

incoming partons
(along beam axis)

outgoing particles
(assumed massless)

From p_T, y_3 and y_4 extract:

- mass and rapidity of the 3+4 pair
- (hence x_1 and x_2)
- CoM scattering angle



$$M = 2p_T \cosh \frac{y_3 - y_4}{2}$$

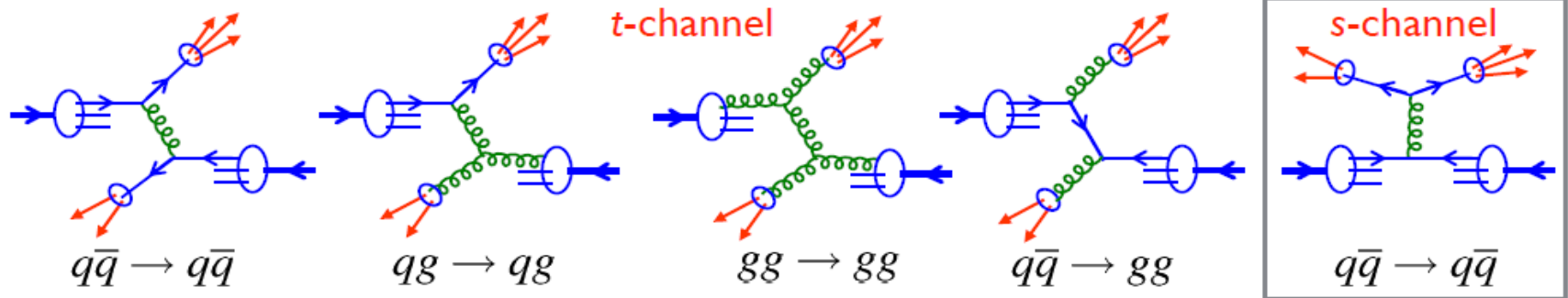
$$x_{1,2} = \frac{M}{\sqrt{s}} e^{\pm y}$$

$$\cos \theta^* = \tanh \frac{y_3 - y_4}{2}$$

The difference in rapidity determines the centre of mass scattering angle

Quark Compositeness?

Most important subprocesses via exchange of a massless vector boson in the t -channel



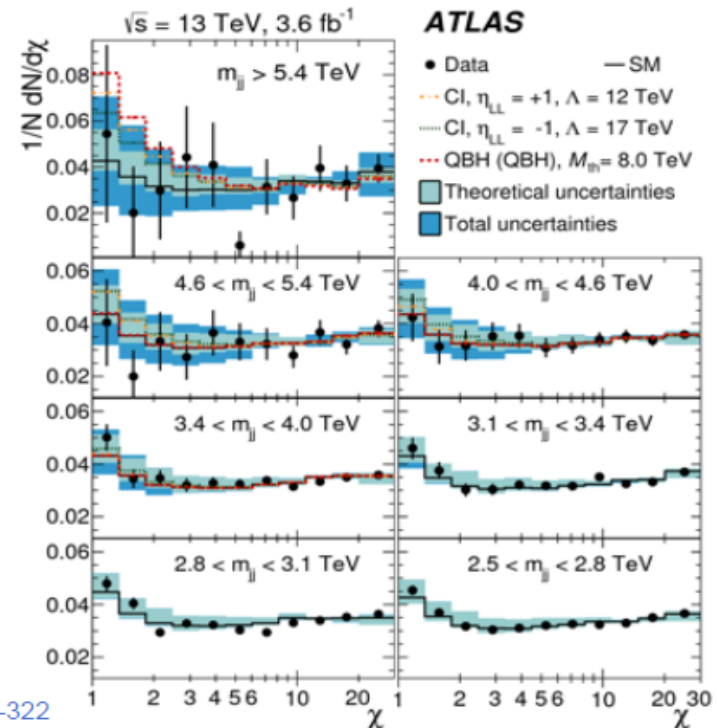
Rutherford
at quark level

$$\frac{d\hat{\sigma}}{d\cos\theta^*} \sim \frac{1}{\sin^4(\theta^*/2)}$$

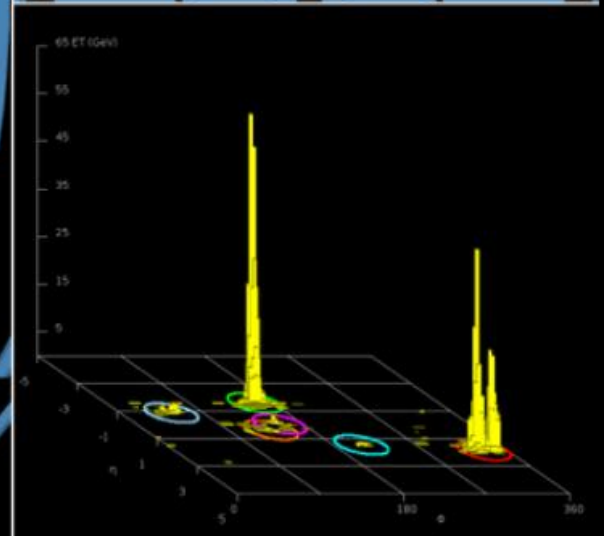
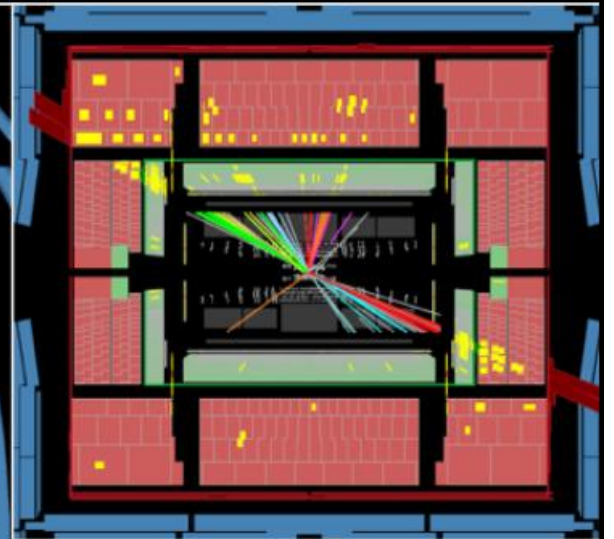
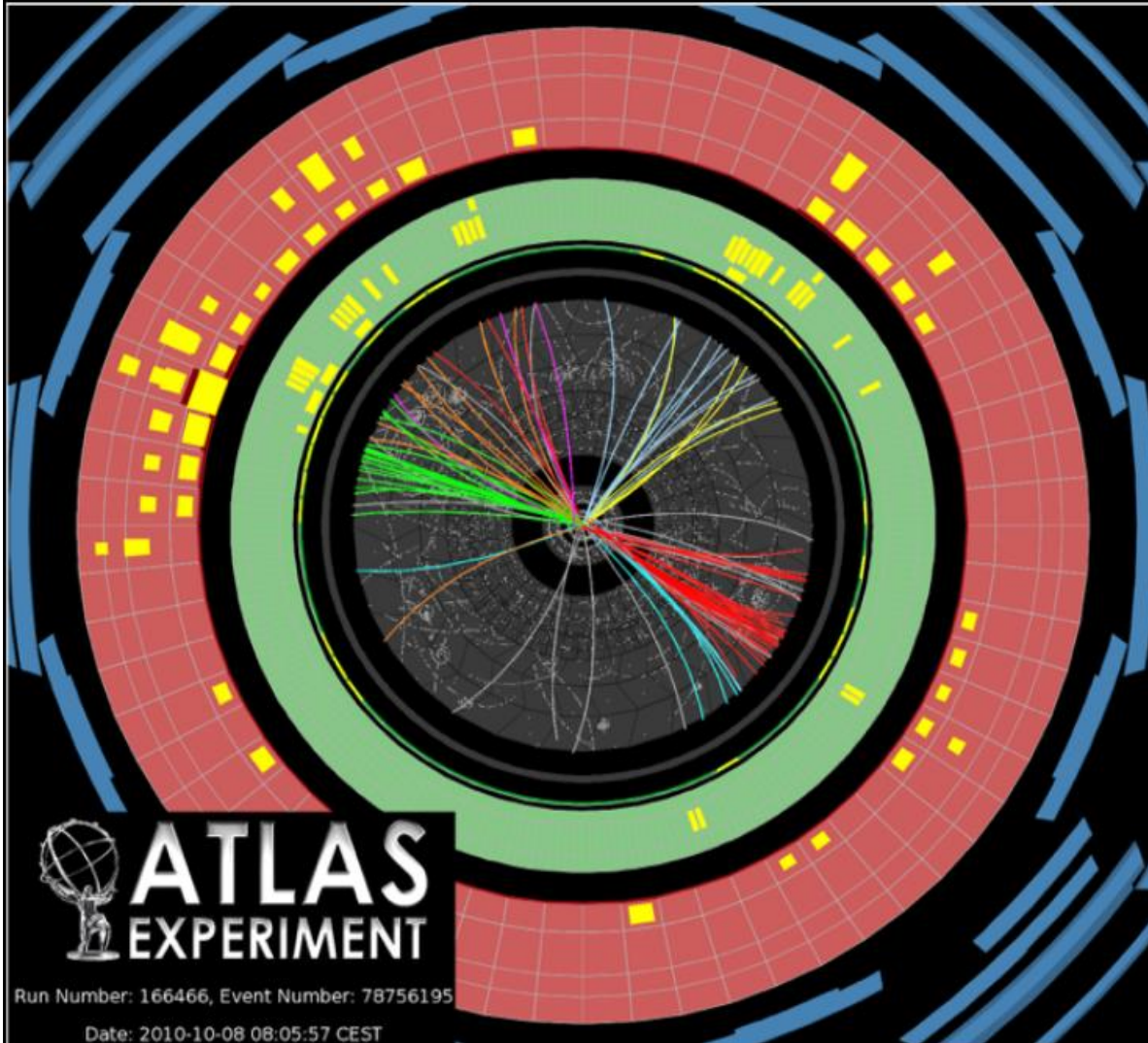
Variable
$$\chi = \frac{1 + \cos\theta^*}{1 - \cos\theta^*} = e^{|y_3 - y_4|}$$

For pointlike quark: $\frac{d\hat{\sigma}}{d\chi} \sim \text{cst}$ at small angle

No evidence for quark/gluon compositeness
from angular distributions



Three jets

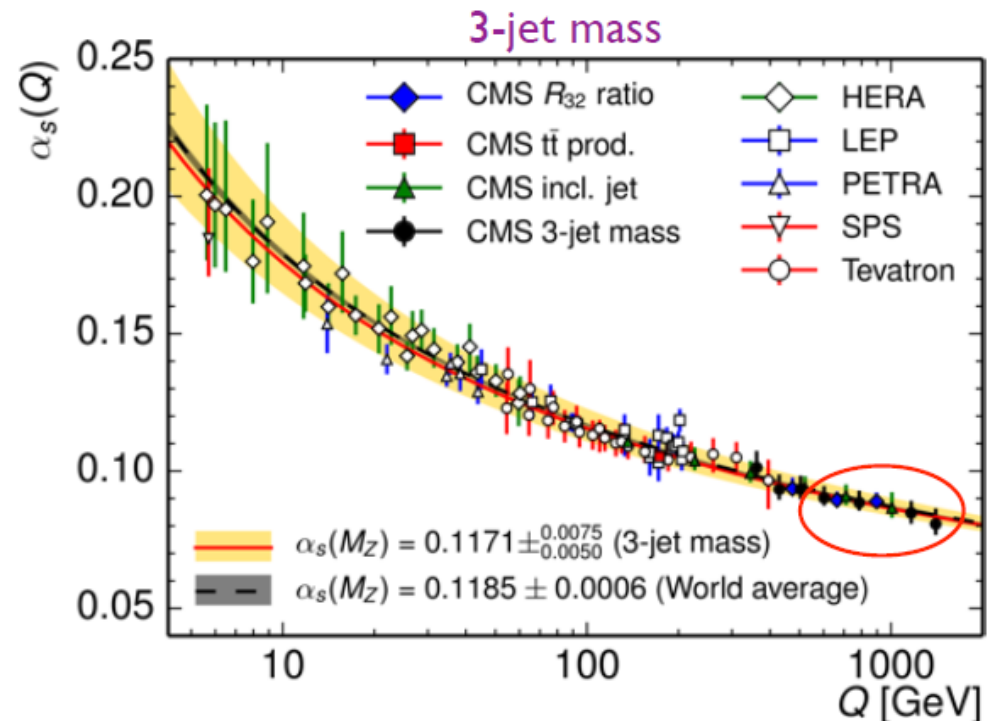
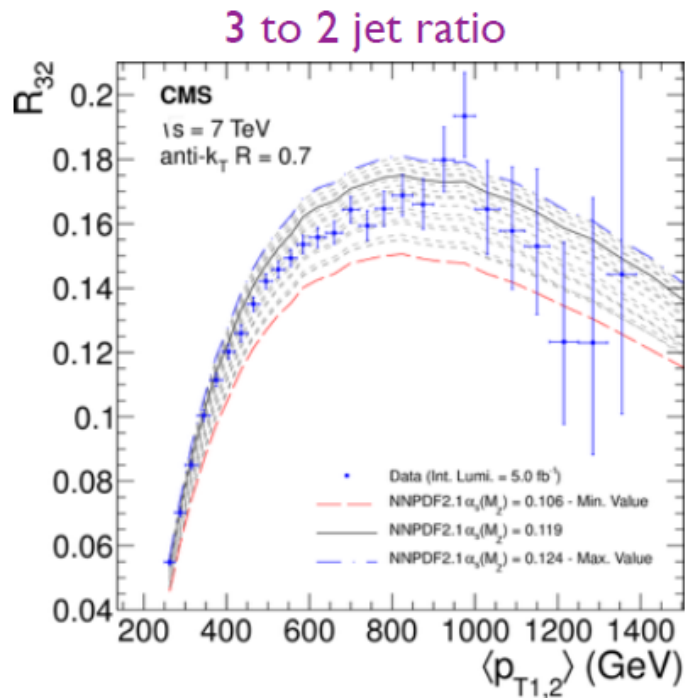


Constraints on Strong Coupling

Constraints on α_s from several jet analyses

- inclusive jet production
- ratio 3-jets to 2-jets
- 3-jet mass spectrum

Uncertainties usually dominated by theory (PDFs and scales)

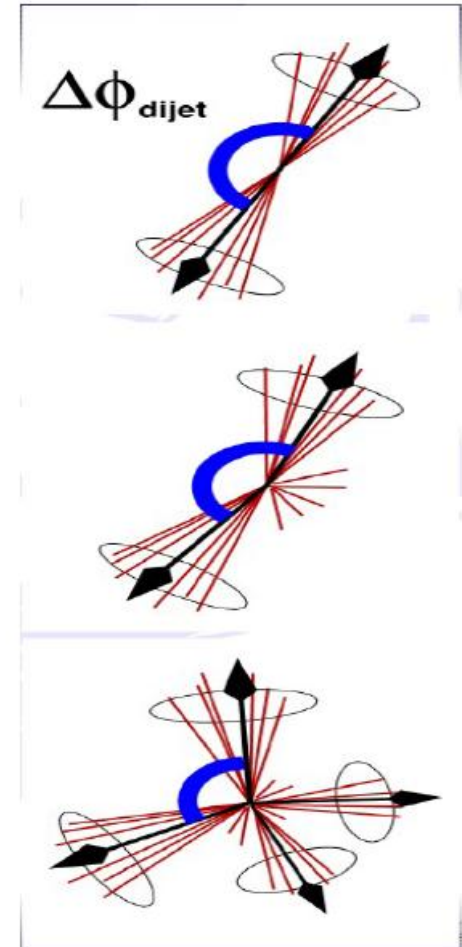


Not competitive with most precise measurements at the **Z** boson

- but in unprecedented range in energy (two orders of magnitude in Q !)

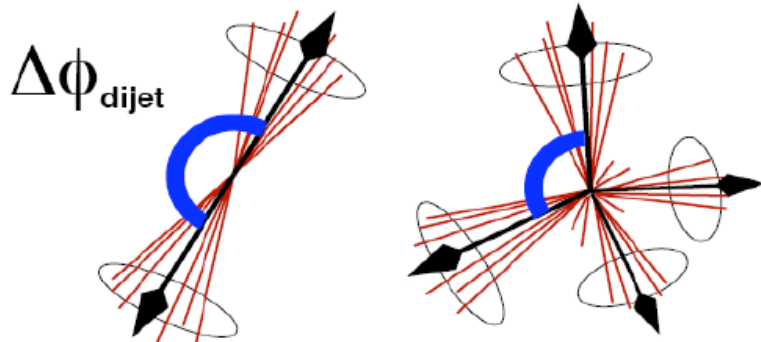
Multi-jet events

- Azimuthal decorrelations in dijet events and distribution of energy within jets sensitive to QCD radiation structures
 - Probing higher order QCD radiation
 - Main systematics: cluster energy scale (separate from JES) and unfolding

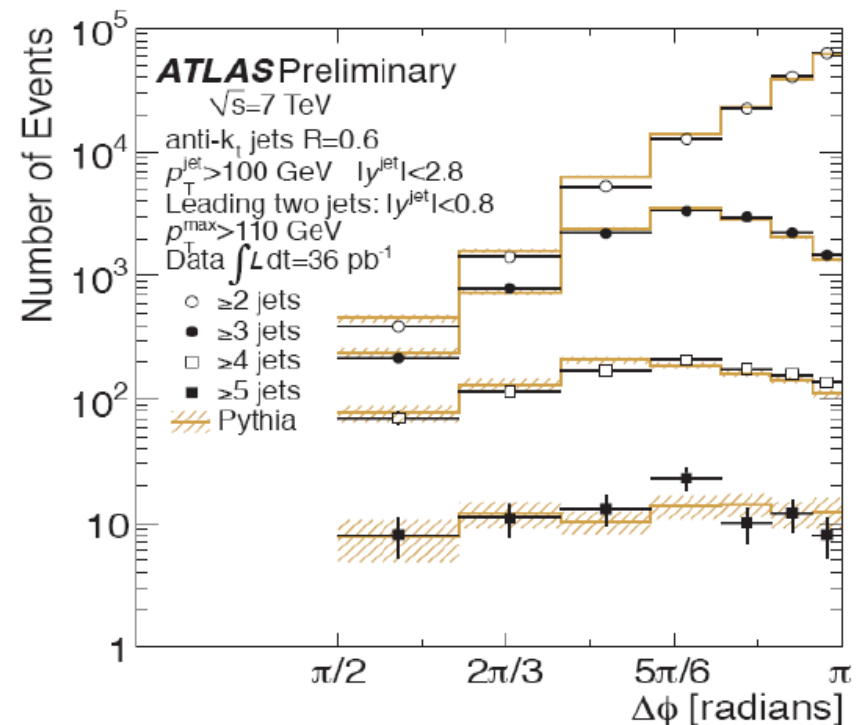


Azimuthal decorrelations

- Complementary to multi-jet cross section measurement.
- Pure di-jets have azimuthal angle Φ between jets equal to π .
- With additional hard radiation, i.e. extra jets, phi becomes smaller.



- Requiring additional jets flattens distribution.

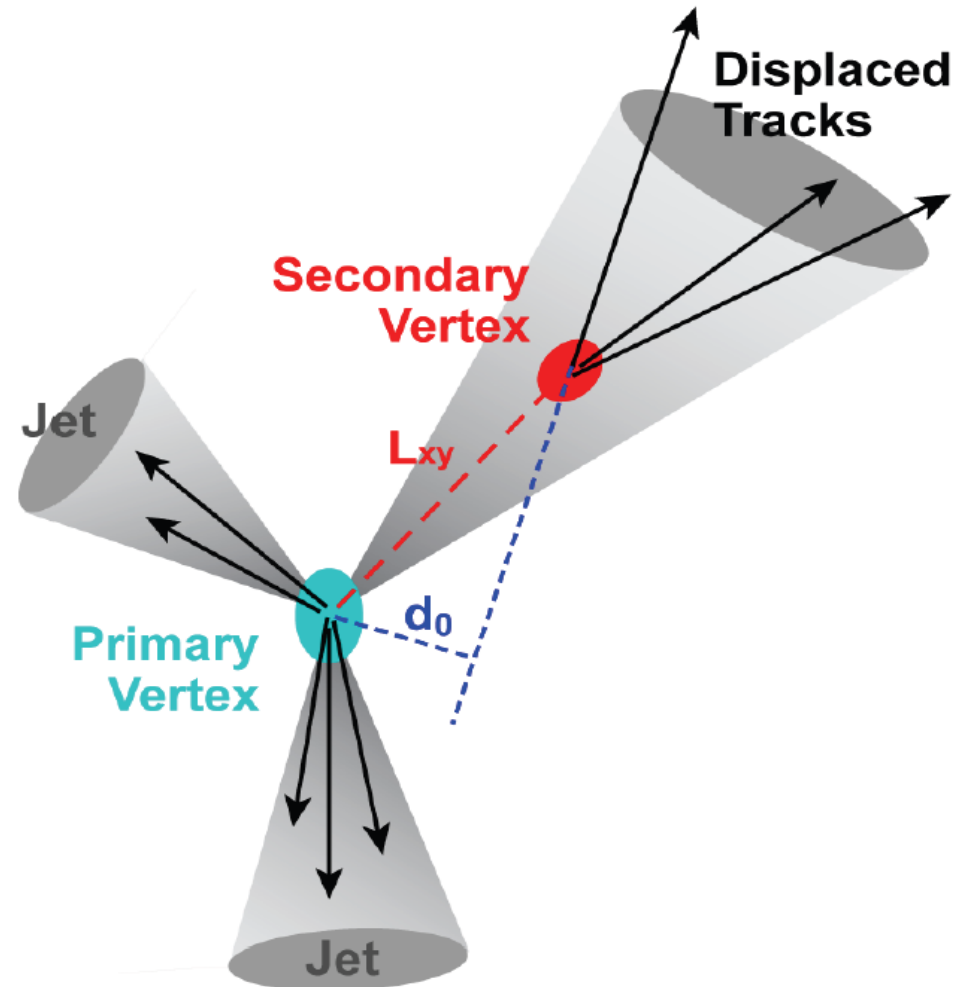


Confinement, hadronisation, jets....

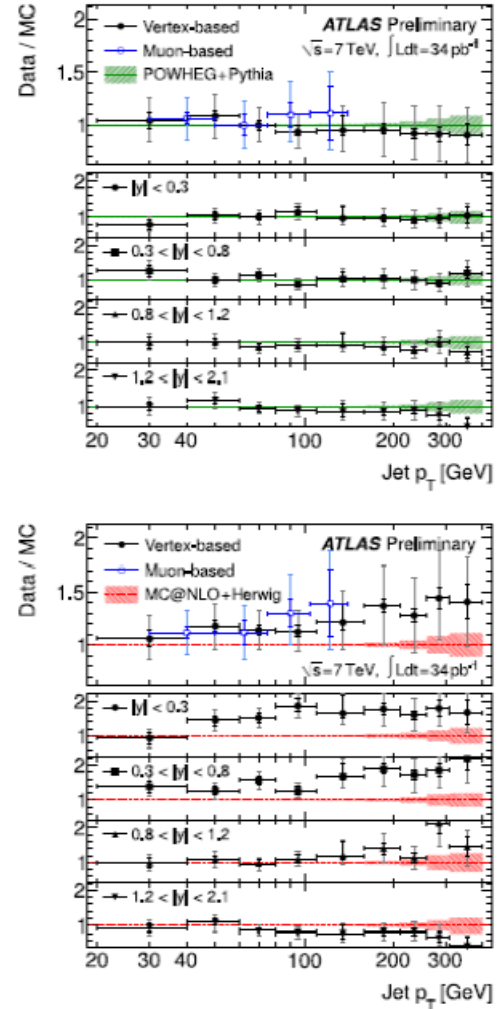
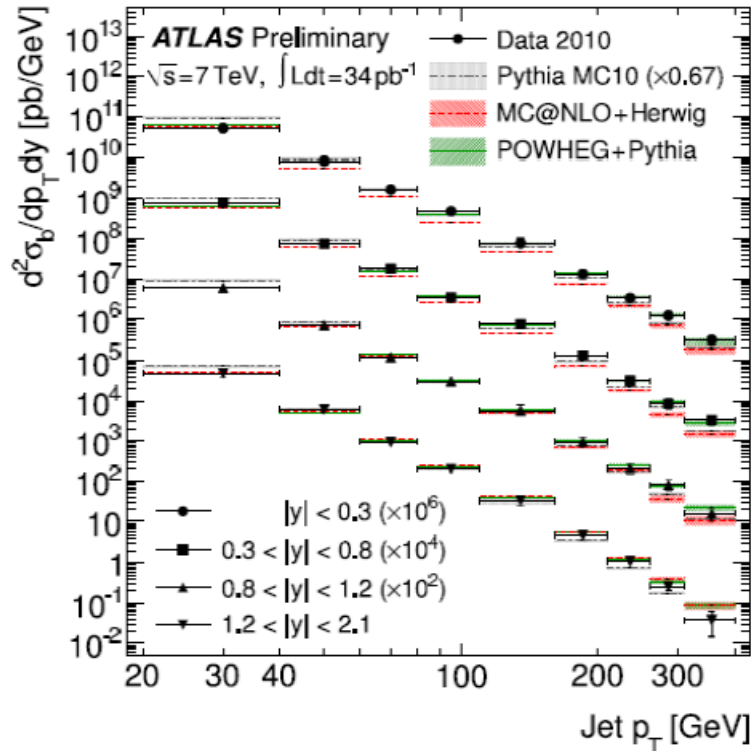
B-tagging



- When a b quark is produced, the associated jet will very likely contain at least one B meson or hadron
- B mesons/hadrons have relatively long lifetime
 - ✓ They will travel away from collision point before decaying
- Identifying a secondary decay vertex in a jet allow to tag its quark content
- Similar procedure for c quark...

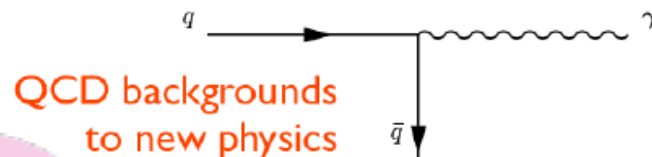
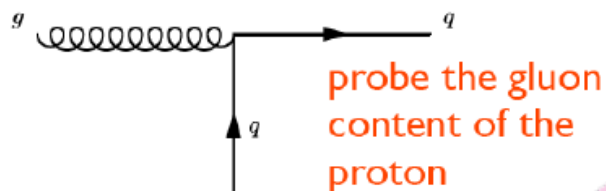


b-jet cross-sections

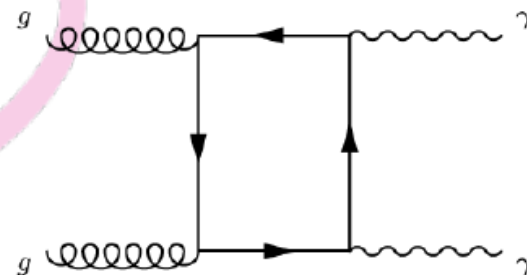
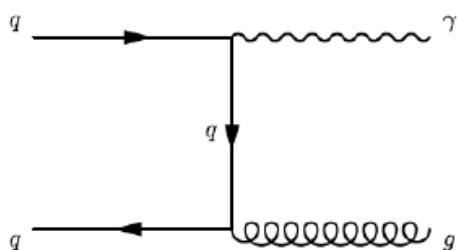


- Good agreement with Powheg+PYTHIA
- MC@NLO+Herwig predicts too few central jets, too many forward jets

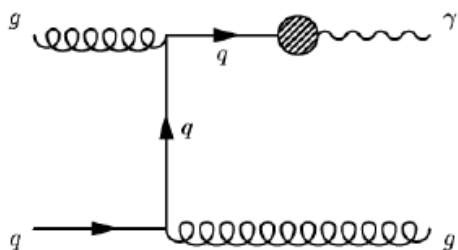
Why measure prompt photons



test
NLO pQCD
 predictions using
 a measurement
 without jets

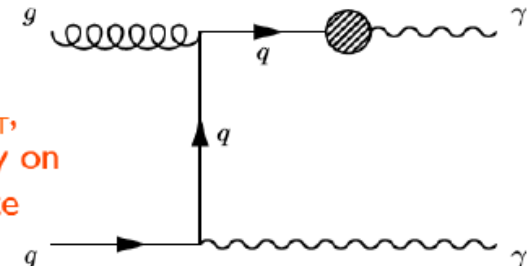


resummation



k_T factorisation

fragmentation important at low E_T ,
 suppressed by isolation cut. MCs rely on
 fragmentation function to compute



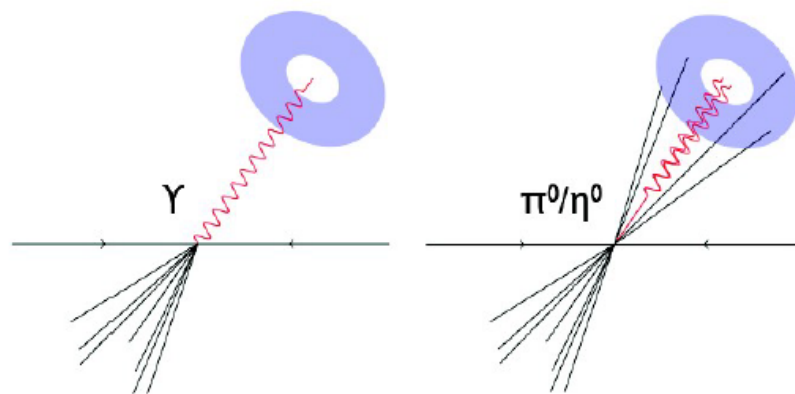
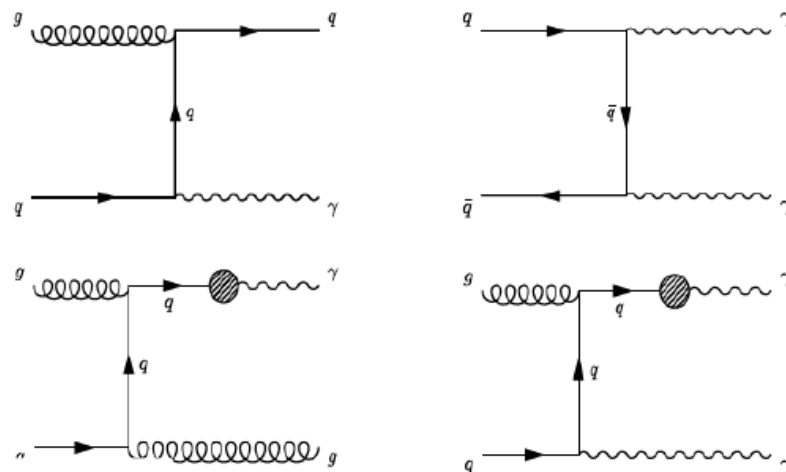
Prompt and isolated photons

■ Prompt:

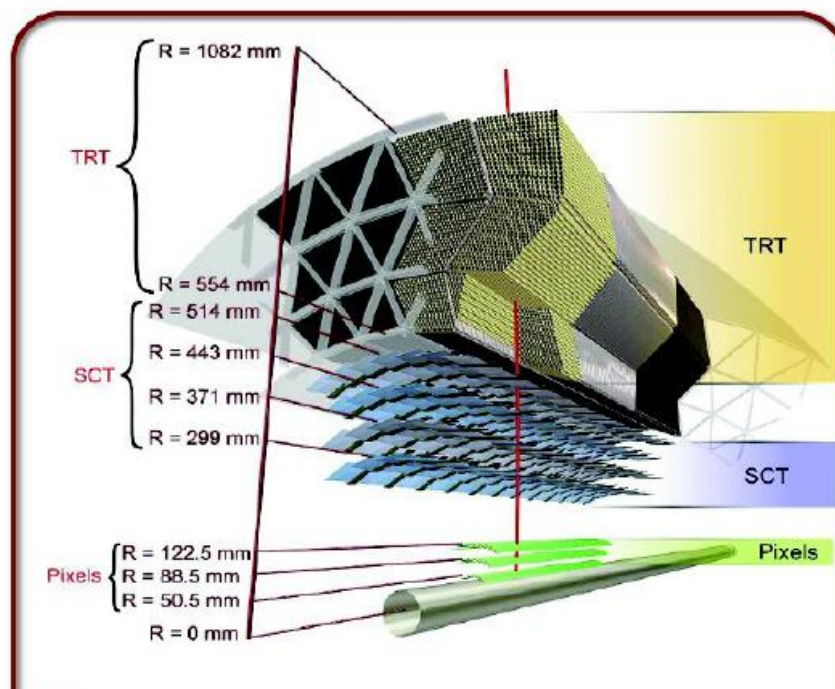
- Direct from the hard scattering
- Parton fragmentation more important at low E_T

■ Isolated:

- Isolation criteria to reduce bgd from QCD jets
 - Photons from neutral meson decay in jets
- Reduced fragmentation component:
 - $\sim 30\%$ reduction at 15 GeV
 - $<10\%$ above 35 GeV

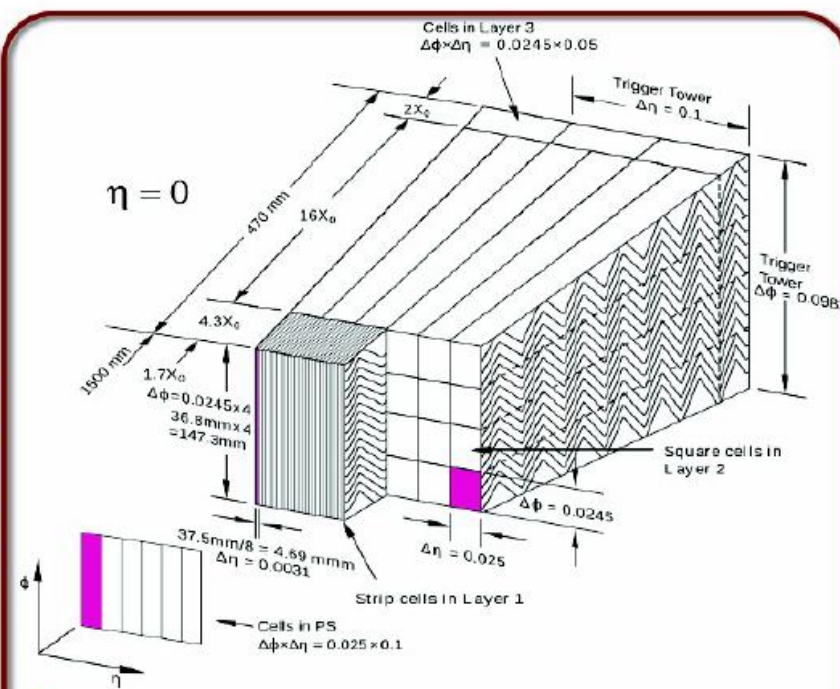


Measuring photons with ATLAS



- Inner detector

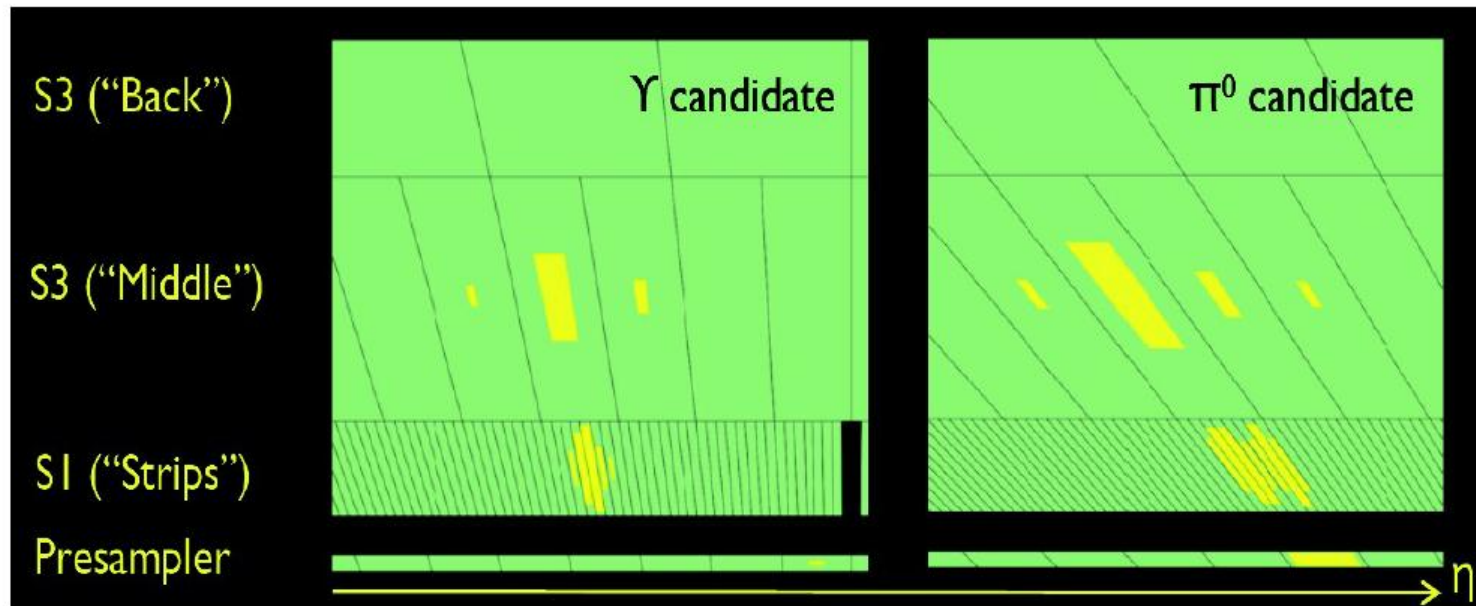
- ✓ track charged particles
- ✓ measure transition radiation
- ✓ e/γ discrimination
- ✓ γ conversion reconstruction



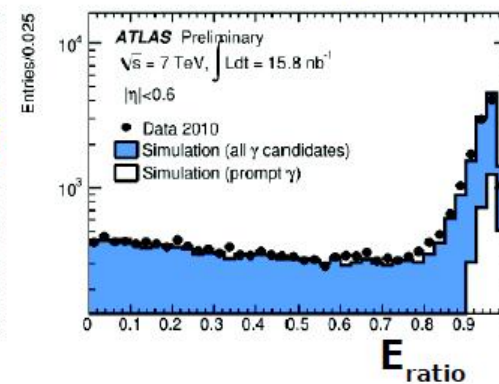
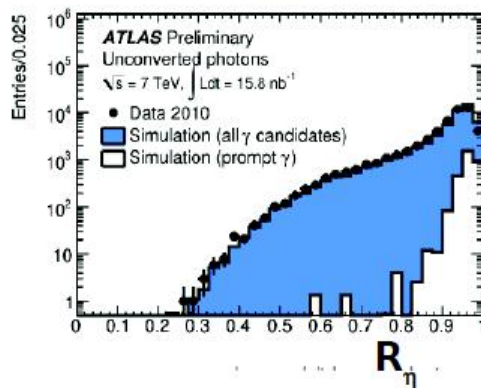
- Pb-LAr EM calorimeter

- ✓ η/φ/longitudinal segmentation
- ✓ fine granularity in 1st layer up to η < 2.37
- ✓ γ energy and direction
- ✓ γ/π⁰ separation (EM shower moments)

Photon identification

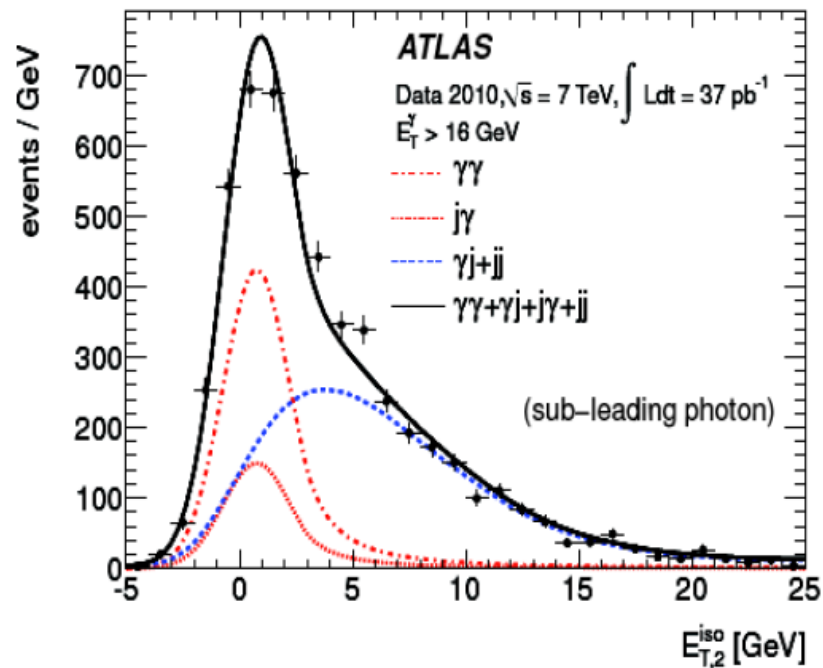
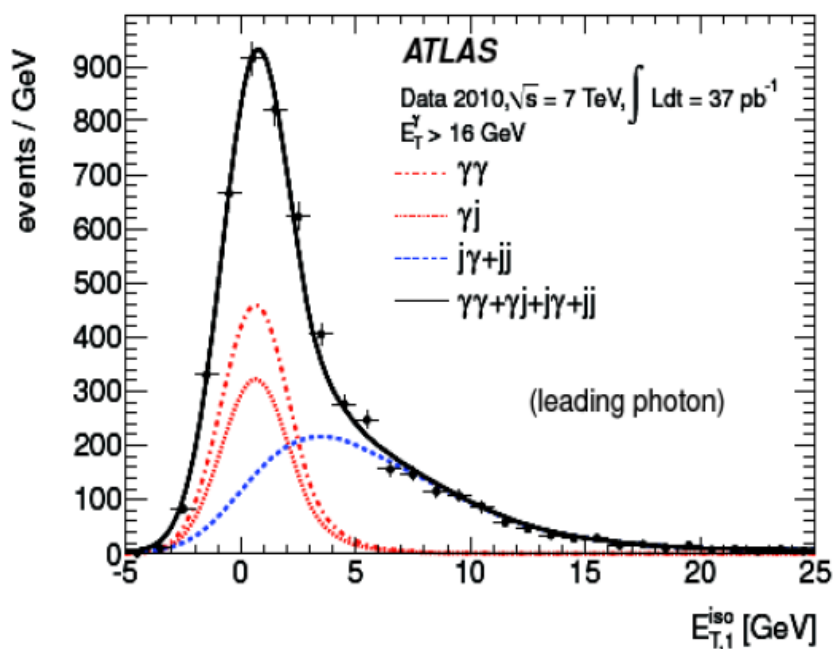


- loose and tight selection
- optimised separately for unconverted and converted photons

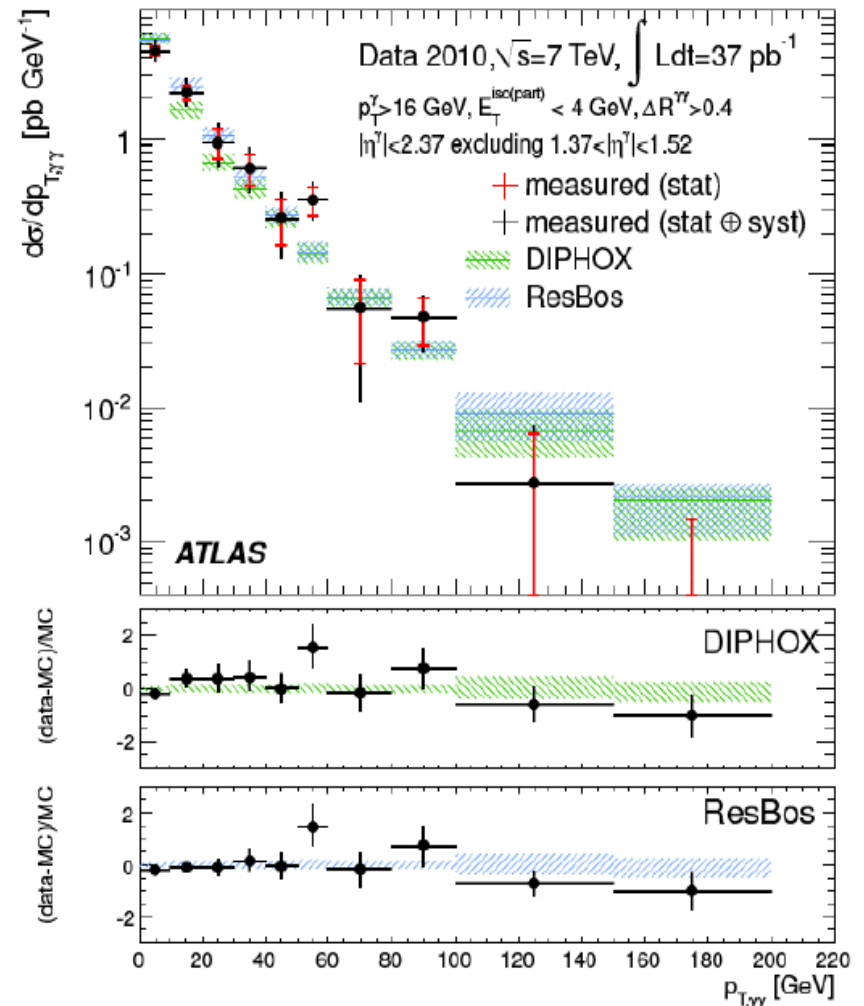
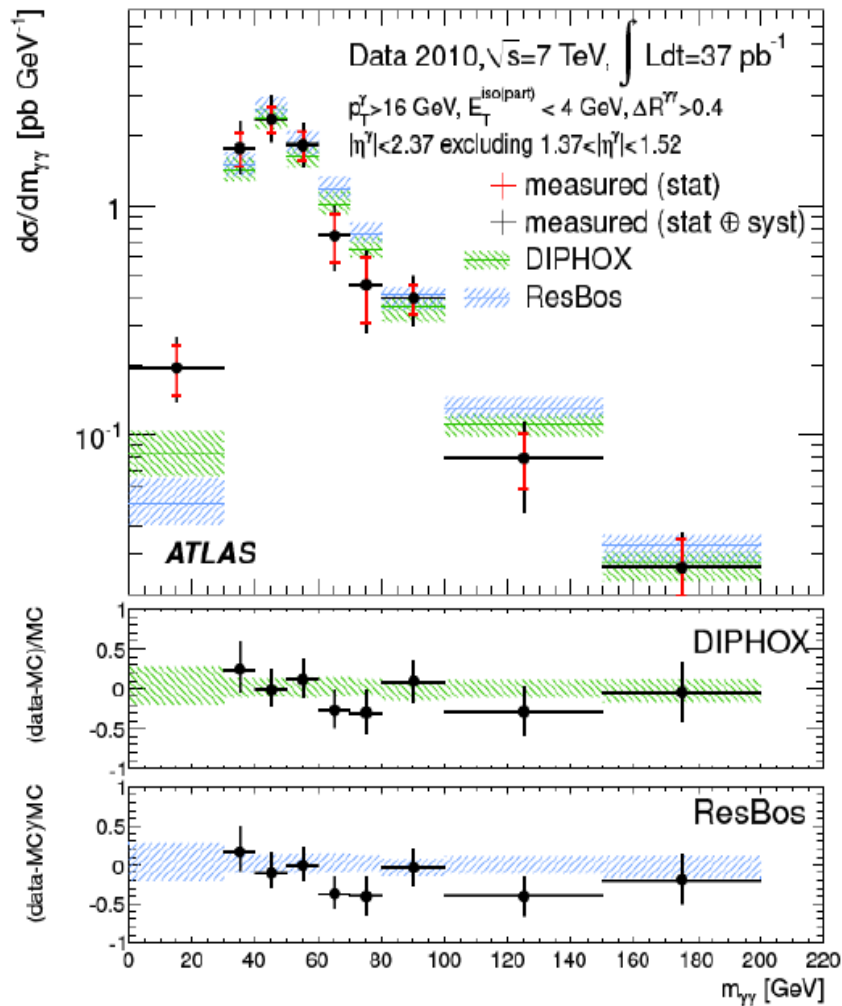


Photon isolation and background estimate

- Background estimated with two methods:
 - ABCD method: extrapolate from the bgd enriched control regions
 - here shown example of 2D template fit



Isolated di-photon cross-section

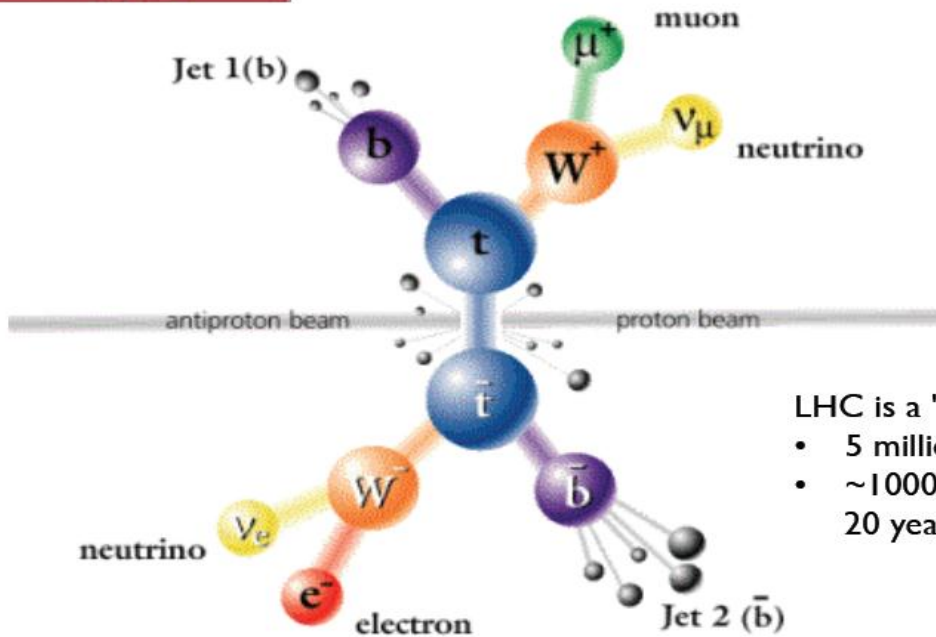
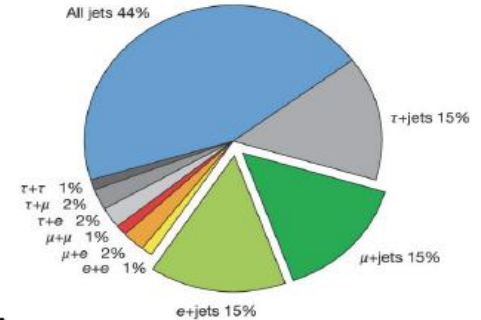


Complicated topologies....

top quark

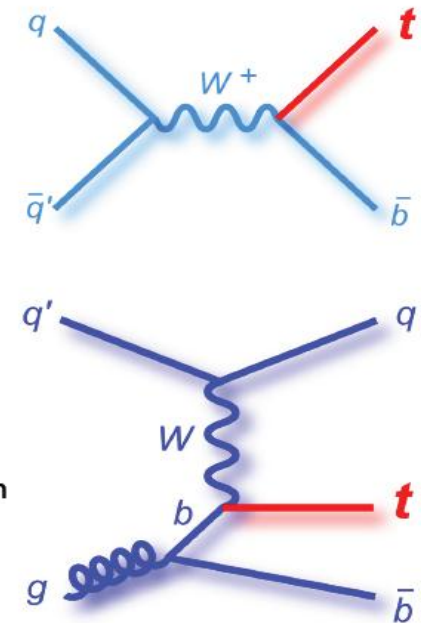


- Top quark has a mean lifetime of 5×10^{-25} s, shorter than time scale at which QCD acts: no time to hadronize!
 - ✓ It decays as $t \rightarrow Wb$
- Events with top quarks are very rich in (b) jets...



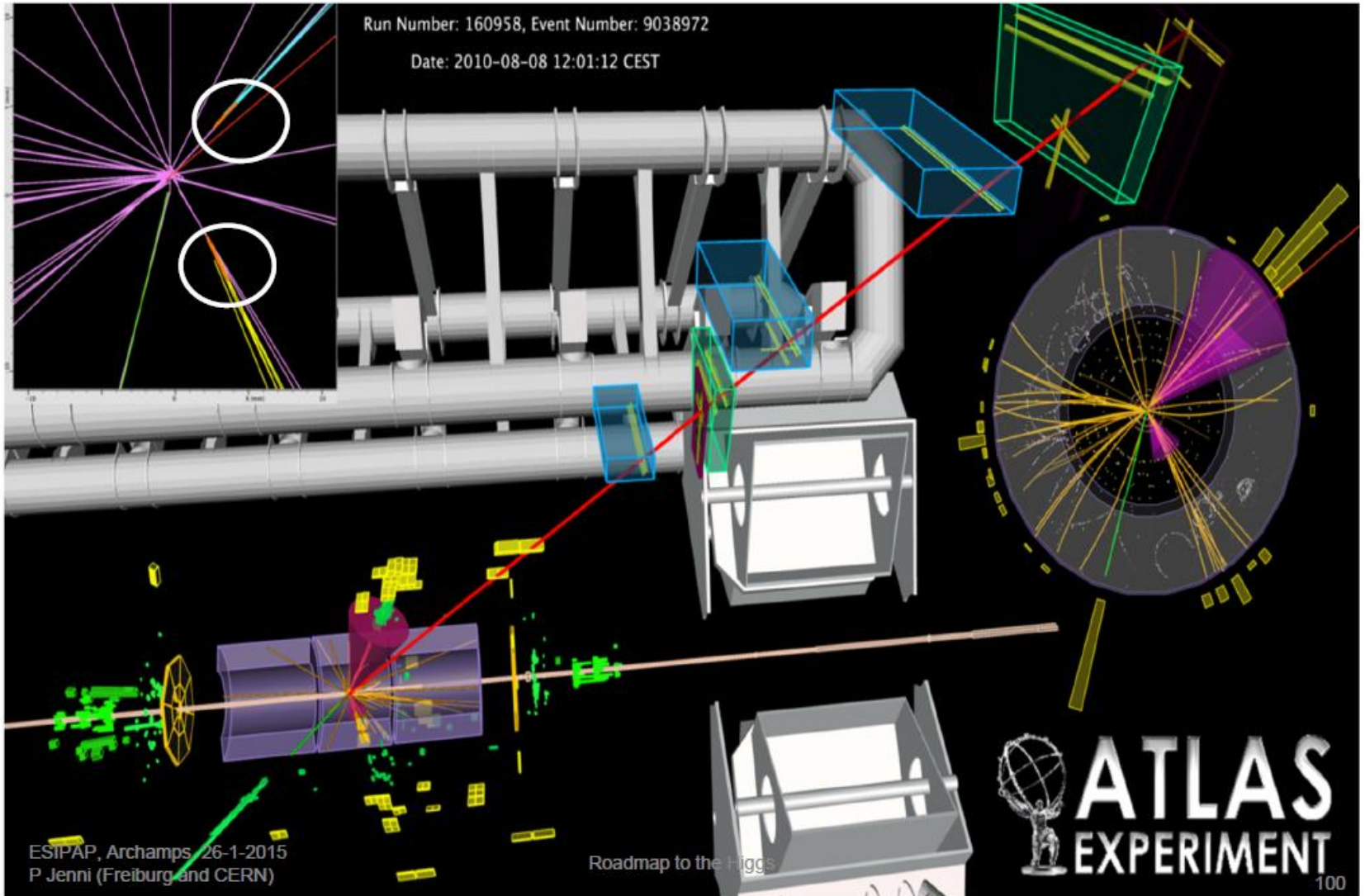
LHC is a "top factory"!

- 5 millions of $t\bar{t}$ pairs
- ~ 100000 in Tevatron in 20 years



$t\bar{t}$ candidate event

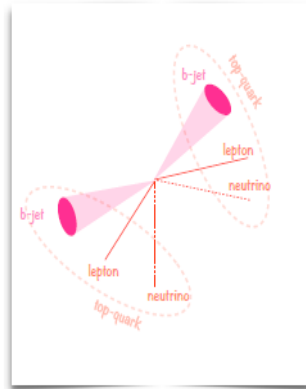
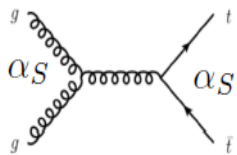
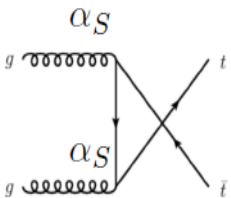
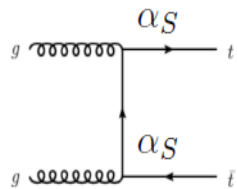
$e + \mu + 2 \text{ jets (b-tagged)} + E\text{T}_{\text{miss}}$



Top pair production cross-section

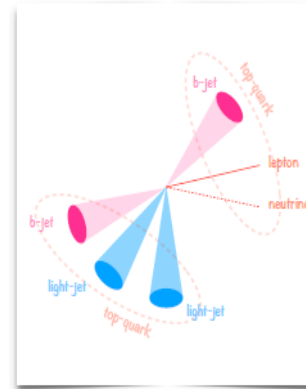
Main production diagrams
At tree level leading order

$$O(\alpha_S^2)$$



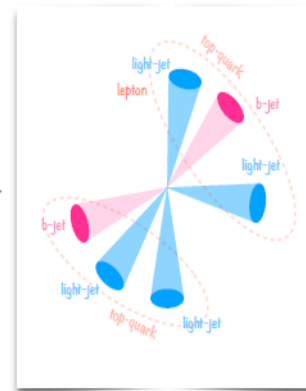
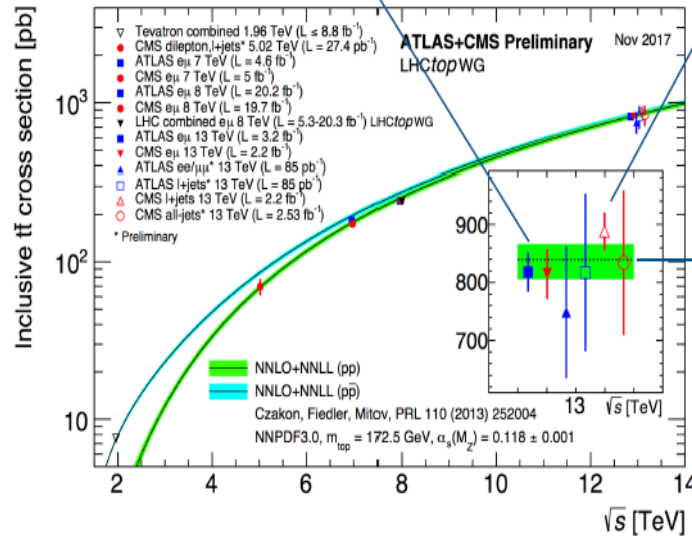
Di-lepton topology:

Precise determination of cross section in the different flavour electron-muon channel in particular. Excellent signal to background ratio. Lower stats (4%).



Semi-leptonic topology:

Best compromise between statistics (30%) and signal to background ratio.

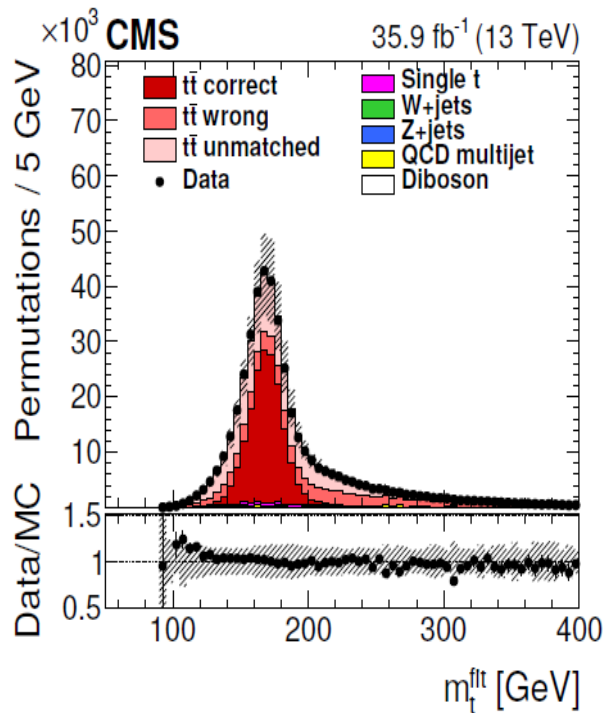


Full hadronic topology:

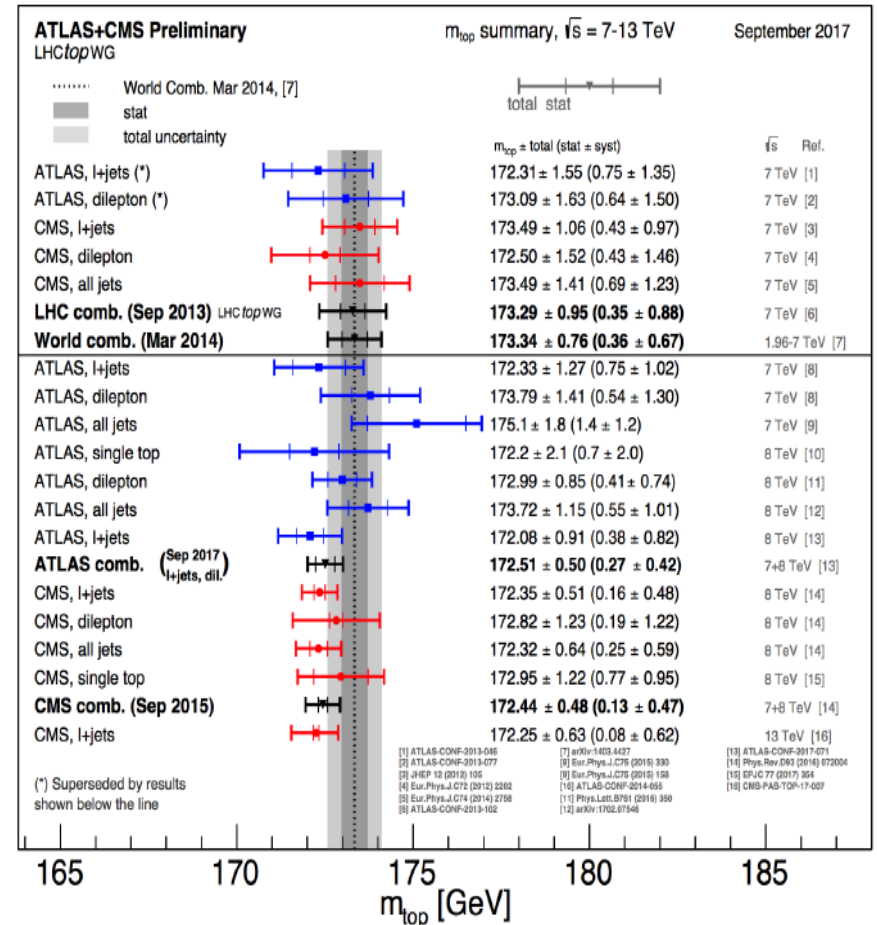
Largest stats (50%) but larger multi-jet background and large combinatorial.

Top quark mass from events kinematics

Direct measurements made using template fit to the reconstructed mass spectrum.



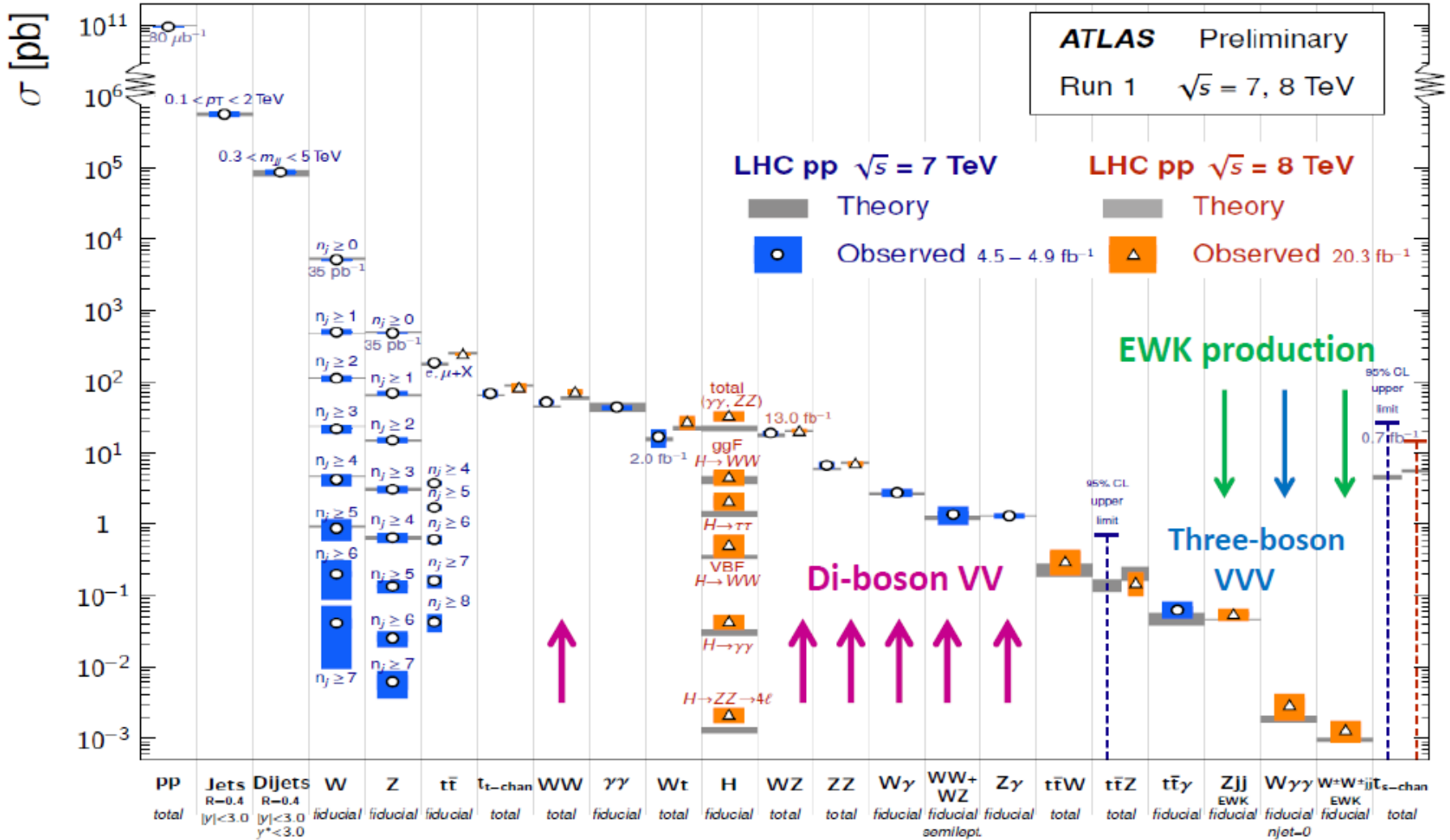
172.34 ± 0.20 (stat + JSF) ± 0.76 (syst) GeV



Electroweak measurements (2015)

Standard Model Production Cross Section Measurements

Status: March 2015



Electroweak measurements (2021)

Standard Model Production Cross Section Measurements

Status: March 2021

